The Term Structure of Interest Rates in a Heterogeneous Monetary Union*

James Costain, Galo Nuño, and Carlos Thomas
Banco de España

December 2023

Abstract

We build an arbitrage-based model of the yield curves in a heterogeneous monetary union with sovereign default risk, which can account for the asymmetric shifts in euro area yields during the Covid-19 pandemic. We derive an affine term structure solution, and decompose yields into term premium and credit risk components. In an extension, we endogenize the peripheral default probability, showing that it decreases with central bank bond-holdings. Calibrating the model to Germany and Italy, we show that a "default risk extraction" channel is the main driver of Italian yields, and that flexibility makes asset purchases more effective.

Keywords: sovereign default, quantitative easing, yield curve, affine model, Covid-19 crisis, ECB, pandemic emergency purchase programme.

JEL classification: E5, G12, F45.

*The views expressed in this manuscript are those of the authors and do not necessarily represent the views of Banco de España or the Eurosystem. The authors are grateful for helpful comments from Marcin Bielecki, Valery Charnavoki, Ricardo Gimeno, Ruggero Jappelli, Iryna Kaminska, Thomas King, Wolfgang Lemke, Bartosz Mackowiak, Dimitros Malliaropulos, Stephen Millard, Paolo Santos Monteiro, Ken Nyholm, Olaf Posch, Walker Ray, Ricardo Reis, Jean-Paul Renne, Dominik Thaler, Dmitry Vayanos, Andrea Vladu, and several anonymous referees, and also from participants in many seminars and workshops. We thank Ana Arencibia and Rubén Fernández Fuertes for substantial assistance with data, computations, and graphics. All remaining errors are ours.

Disclosure statements

Disclosure statement of James Costain.
I have no conflicts of interest to disclose.

Disclosure statement of Galo Nuño.
I have no conflicts of interest to disclose.

Disclosure statement of Carlos Thomas.
I have no conflicts of interest to disclose.

1 Introduction

The sovereign yield curve – also known as the "term structure of interest rates" – is a crucial indicator of financing conditions for any given country. Central banks pay great attention to the yield curve(s) under their jurisdiction, since they constitute a key channel of monetary policy transmission, and also provide relevant information about the shocks hitting the economy. The importance of yield curves for monetary policy analysis has only increased since the Great Financial Crisis of 2008-09: as (short-term) policy rates in advanced economies approached their effective lower bounds, central banks resorted to unconventional tools, such as large-scale asset purchases and forward guidance about future short rates, in order to flatten the yield curve and thus provide further policy stimulus.

In this context, term structure models have become important analytical tools, both for central bankers and for scholars of monetary policy. In particular, they underlie the prevailing view of the effects of asset purchase programmes, which revolves around the "duration risk extraction" channel (*e.g.* Greenwood and Vayanos, 2014; Hamilton and Wu, 2012; or Krishnamurthy, 2022). Under this mechanism, net purchases of long-maturity bonds flatten the yield curve by reducing the term premium that private markets demand to compensate for duration risk, while the short end of the curve is anchored by the risk-free short rate. However, the movements of euro area yield curves (see Figure 1) in response to the pandemic outbreak in early 2020 and to the ECB's subsequent monetary policy response challenge this view. While duration extraction might explain the flattening of the German yield curve after the pandemic emergency purchase programme (PEPP) announcement on March 18, 2020, it offers no explanation of the much larger movements in the Italian and Spanish yield curves. A key feature of these movements is the large shift in the short end of the peripheral curves, which cannot be explained by term premium considerations. The same is true for the large upward shift in peripheral yield curves as the pandemic shock unfolded (before PEPP was announced), which cannot be explained by invoking the pandemic's impact on the expected amount of duration risk to be absorbed by the market.

It is not hard to see why the mainstream view of term structure dynamics fails to explain yields in southern Europe, when we consider that today's workhorse models, such as the influential Vayanos and Vila (2021) framework, abstract from sovereign default risk. While it may be reasonable to assume that there is no nominal default

Figure 1: Effects of the pandemic and the PEPP announcement on German, Spanish, and Italian yields

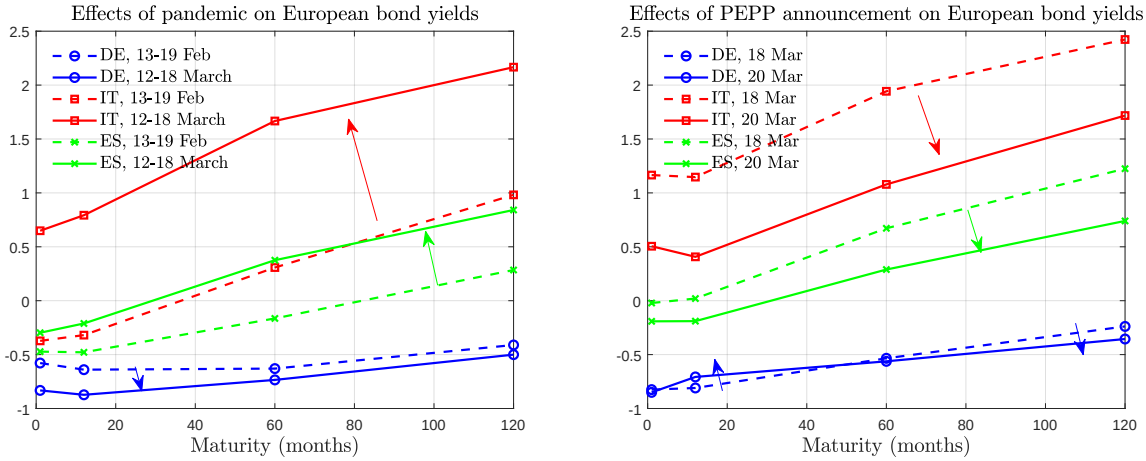

Notes. Data source: Datastream.
Left panel. Shifts in German, Spanish, and Italian zero-coupon yields (annual percentage points) from the weekly average of 13-19 Feb. 2020 (dashes), to that of 12-18 Mar. 2020 (solid).
Right panel. Shifts in German, Spanish, and Italian zero-coupon yields (annual percentage points) from 18 March 2020 (dashes, before PEPP announcement) to 20 March 2020 (solid, after).

risk on the debt of the safest issuers, such as the US Treasury, such an abstraction is less suitable for the euro area, where sovereign issuers that are viewed as safe coexist – and share a common monetary policy – with other issuers that face high and volatile credit risk premia. Sovereign credit risk offers a possible explanation for the nearly mirror-image dynamics of European yield curves in response to the pandemic outbreak and the PEPP announcement, if we view these not as two qualitatively different shocks, but as two impulses that each affect yields through changes, of opposite sign, in the net supply of defaultable bonds to private investors.

Motivated by these observations, this paper proposes a micro-founded model of the term structure of sovereign interest rates designed to address a heterogeneous monetary union such as the euro area. To do so, we extend the Vayanos and Vila (2021) term structure model to a multi-country setting with sovereign default risk. Concretely, we consider a monetary union consisting of two member states: Core, which issues default-free bonds, and Periphery, which is subject to default risk. The model is populated by arbitrageurs, who trade bonds across both countries and all maturities, and preferred-habitat investors, who demand bonds of a specific maturity from a specific jurisdiction.

Bond yields in the model are driven by one or more stochastic factors, including the short-term riskless rate.[1] Yields also depend on the *net* supply of bonds of each maturity and jurisdiction, by which we mean bond supply from the governments minus the bonds held by the common monetary authority. For analytical convenience, we treat the governments' bond supply and central bank bond demand as deterministic sequences; this may be interpreted as a situation in which the public sector commits to a particular time path for the net supply of bonds in the market.

We start by analyzing a model version with an exogenous default arrival probability, following Duffie and Singleton (1999), which is useful for two reasons. First, it shows how the affine solution of the Vayanos and Vila (2021) model generalizes in the presence of default risk. Second, it highlights key results that are independent of how one models the probability of sovereign default. In particular, our solution decomposes bond yields into four components: (i) an *expectations* term that represents the expected future path of the risk-free rate; (ii) a *term premium* representing the risk-averse compensation for bearing duration risk; (iii) an *expected default loss*, which captures the compensation that a risk-neutral investor would require for holding defaultable bonds; and (iv) a *credit risk premium* that represents the risk-averse compensation for absorbing default risk (over and above expected default losses). Thus, while many analyses of asset purchase programs emphasize the duration extraction channel, our model distinguishes this from a *default risk extraction channel* that operates through the credit risk premium rather than the term premium: risk-averse investors demand less compensation to hold a defaultable bond when there is less default risk outstanding in the market. Moreover, we show that the presence of default risk allows for shifts in the front end of the yield curve in response to shocks that cause the default probability to vary but have otherwise no effect on short-term riskless rates.

While imposing an exogenous default probability simplifies and clarifies the analysis, in reality large-scale asset purchase shocks like the PEPP announcement, or other shocks with fiscal implications, such as the pandemic outbreak, are likely to affect the default probability perceived by markets. Therefore, we next extend the model by linking the default probability to underlying policy choices. To do so, we assume that the peripheral bond market is subject to rollover crises in the spirit of Calvo (1988) and Cole and Kehoe (2000). When a rollover crisis arrives, the peripheral fiscal authority decides whether to

[1] We begin by presenting a one-factor model in Sec. 2. We then extend our model to a multi-factor framework with preferred-habitat demand shocks for our empirical analysis in Sec. 4.

continue servicing its debts or else to partially default by applying a haircut to bonds of all maturities. We show that, under certain conditions, the peripheral government's default probability at any given time *decreases* with the stream of bond redemptions to be paid to the central bank for the duration of the rollover crisis. This is because redemptions of bonds held by the central bank (or interest payments on those bonds) represent payments from the treasury to the central bank which may be rebated back to the treasury through central bank dividends. Therefore, by purchasing sovereign bonds, the central bank reduces the fiscal pressure that the peripheral government will face if a rollover crisis arrives, and thus reduces its incentives to default, a point made by Corsetti and Dedola (2016).[2] The implicit assumption is that the central bank's ability to finance bond purchases by expanding its monetary base can help reduce the fiscal pressure that the government can be expected to endure in an eventual rollover crisis. Crucially, all results obtained from the exogenous default probability case carry through to the endogenous case. However, endogenizing the default probability reinforces the yield curve impact of asset purchases, both because purchases decrease the expected default loss and – more importantly – because the default risk extraction channel is stronger when asset purchases *both* reduce the net supply of defaultable bonds *and* reduce the default risk on each bond.

We then calibrate our model to Germany and Italy. The calibration uses yield curve data from the period 1999-2022 that goes back to the establishment of the euro, and also from the two-day window around the ECB's initial PEPP announcement on March 18, 2020, which declared an aggregate purchase envelope of 750 billion euros. The surprise nature of this announcement, in an emergency meeting of the ECB Governing Council, makes it easy to map this episode into our model. Despite its parsimony, our model replicates well the average shape and volatility of both countries' yield curves in the full sample, as well as their asymmetric reaction at the time of the PEPP announcement, including the large downward shift of the Italian curve.

Armed with the yield decomposition explained above, we use the calibrated model to shed light on the transmission channels of the PEPP, and more generally on the determinants of the Italian and German yield curves during the euro period. We find that default risk extraction is the most significant channel – more relevant than duration

[2]We implicitly assume the existence of national central banks that conduct asset purchases on behalf of the union-wide central bank. This is broadly consistent with Eurosystem practice, where the large majority of purchases are actually conducted by national central banks, instead of the ECB.

extraction, i.e., the fall in term premia – driving the response of the Italian yield curve to the PEPP announcement, and the asymmetry of the responses of the German and Italian curves. Moreover, the downward shift in the Italian sovereign spread, across all maturities, is mainly explained by a lower credit risk premium, driven both by a small decline in the probability of peripheral default and by a reduction in the quantity of defaultable assets that the market was expected to hold from then on; in contrast, the decrease in the expected loss due to default, by itself, plays only a small role in reducing the sovereign spread.[3] More generally, we find that most of the average sovereign spread in the full sample is explained by credit risk premia –i.e. the risk-averse pricing of default risk– as opposed to expected default losses –i.e. the amount of default risk itself.[4]

These results are extremely robust to a wide range of alternative parameterizations. We find that credit risk premia always exceed expected default losses unless risk aversion or default haircuts take implausibly low values that are inconsistent with the observed level, slope, and responsiveness of yields.

Our quantitative, structural model also allows us to construct counterfactual scenarios to compare PEPP with other possible asset purchase designs. To ensure an adequate response to the asymmetric impact of the Covid-19 shock, PEPP was designed to be *flexible* in the distribution of purchases over time, across asset classes, and across euro area jurisdictions. This flexibility contrasted with the ECB's longer-standing Asset Purchase Programme (APP), which fixed the pace of purchases over time, and allocated purchases across member states by their "capital keys" – i.e., in proportion to the share of each Eurosystem national central bank in the ECB's capital. Our simulations show that PEPP's flexible design substantially enhanced its impact, and that flexibility in the timing of purchases (frontloading) and flexibility in the allocation across countries (deviations from capital key) complement and reinforce one another. The PEPP announcement caused a large reduction in Italian yields across the yield curve, with a maximal impact of roughly 85bp at intermediate maturities. Approximately one-sixth

[3]These results are in line with the empirical study of Corradin et al. (2021) for the same episode, which concludes that a reduction in default risk was the dominant channel through which the PEPP announcement affected Italian yields; likewise they are consistent with findings of Krishnamurthy et al. (2018) and Demir et al. (2021) regarding earlier asset purchase programs in Europe.

[4]In our model, when the default probability is small, as is the case in our calibration, the term premium on Core and Periphery bonds is approximately the same. Since the expectations component is the same in both countries, it follows that the spread between Periphery and Core bond yields equals approximately the sum of the Periphery's credit risk premium and expected default loss.

of this overall effect (up to 14 bp) can be attributed to the flexibility of PEPP, as compared with a counterfactual program under which a constant rate of purchases would be allocated across countries according to capital key. Moreover, flexibility matters for the response of *average* euro-area yields, because reallocation towards peripheral bonds has a large impact on peripheral yields but a negligible impact on those of core bonds.

Related literature. This paper links two different strands of literature. First, we contribute to the finance literature on term structure models. In liquid markets, arbitrage links bond returns tightly across maturities and issuers. Ang and Piazzesi (2003), building on Duffie and Kan (1996), derived an analytical solution for the yield curve in the absence of arbitrage opportunities under the assumption that all yields are affine functions of a set of autoregressive Gaussian factors. Vayanos and Vila (2021) showed that an affine term structure model (ATSM) of this type applies to a micro-founded setting featuring arbitrageurs with mean-variance utility functions, together with "preferred-habitat" investors whose supply or demand for bonds of specific maturities is linear in those bonds' yields. This market structure makes it possible to model a variety of complex bond market interactions and policy interventions. For example, Greenwood and Vayanos (2014) offered empirical support for the model's prediction that the price of risk increases as arbitrageurs hold larger maturity-weighted positions; therefore quantitative easing can reduce yields, even if the face value of debt outstanding is unchanged. Further applications include quantitative easing at the effective lower bound (Hamilton and Wu, 2012; King, 2019), repo market dynamics (He et al., 2020), and exchange rates (Greenwood et al., 2020; Gourinchas et al., 2022). The bond market structure of Vayanos and Vila (2021) has also been embedded into a New Keynesian model to analyze monetary policy in general equilibrium (Ray 2019). Motivated by the theoretical insights of Vayanos and Vila (2021), various papers have incorporated net supply factors into otherwise standard no-arbitrage ATSMs, including Li and Wei (2013) and Eser et al. (2019); the latter paper uses security-level data on sectoral bond holdings to construct a measure of duration risk in the hands of price-sensitive investors (akin to Vayanos and Vila's arbitrageurs) and to analyze the impact of the APP.

While they have been widely applied, much of the literature using ATSMs has studied US markets, under the assumption that Treasury securities are nominally riskless. Applications to fixed exchange rate environments – including monetary unions – or to commercial debt make it necessary to consider default risk. Hamilton and Wu (2012) construct an ATSM that includes one-period defaultable non-Treasury debt. A key

insight about defaultable bond prices comes from Duffie and Singleton (1999), who show that if the loss caused by default is a fixed fraction of the bond's value, then the pricing formulas for default-free and defaultable bonds are formally identical, with an adjustment to the discount factor to account for expected losses due to default. Borgy et al. (2012) price defaultable euro-area debt under the assumption that the Duffie and Singleton (1999) condition holds. Altavilla et al. (2021) modelled euro area debt under the assumption that default risk can be priced like any other Gaussian factor.

We contribute to this literature in several ways. We show how the non-Gaussian risk of default – specifically, partial default on multi-period debt – can be incorporated into a microfounded ATSM in the Vayanos-Vila tradition. Crucially, we show that default risk opens up a novel *default risk extraction channel* of large-scale asset purchases, which enables the model to generate large, parallel yield curve shifts like those in Figure 1. In addition, we adapt the model to analyze policy interactions in the context of a heterogeneous monetary union, such as the euro area. Finally, we model explicitly how central bank asset purchases affect the default probability by incorporating the possibility of rollover crises, showing how this reinforces the default risk extraction channel *vis-à-vis* the simpler case with exogenous default probability. This mechanism can be seen as an extension of the two-period economy of Corsetti and Dedola (2016) to a fully dynamic environment.

This paper also relates to the literature on monetary-fiscal interactions in the presence of sovereign risk.[5] In contrast to previous related work, we focus on how central bank asset purchases can reduce the probability of default, and how they affect the whole term structure of interest rates. Linking the ATSM literature to that on sovereign risk is fruitful, because it clarifies that duration extraction is neither the only channel, nor the primary channel, by which asset purchases transmit to yields in the European context. Instead, our model shows that default risk extraction is the predominant channel of asset purchases in the euro area, as the extraction of defaultable bonds from private hands and the associated reduction in the probability of sovereign default reinforce one another in shrinking the credit risk premium. The quantitative discipline of the ATSM framework is crucial here – arbitrage pricing implies that the actual expected loss from default is much smaller than the credit risk premium that the market demands to hold

[5]See Calvo (1988), Cole and Kehoe (2000), Aguiar et al. (2015), Reis (2013), Corsetti and Dedola (2016), Camous and Cooper (2019), Bacchetta et al. (2018), Nuño et al. (2022), Na et al. (2018), Arellano et al. (2020), or Bianchi and Mondragon (2022).

defaultable debt. The channel we identify is consistent with evidence of De Grauwe and Ji (2013) showing that sovereign spreads are less stable in the euro area than in other open economies with independent monetary policies, and findings of Broeders et al. (2021) showing that ECB asset purchases reduced the impact of bond market volatility on euro area sovereign spreads.

2 Bond market equilibrium with default risk

We begin by building a model of bond market equilibrium that incorporates an exogenous but time-varying probability of partial default. This simple version of our model shows how introducing default risk in a Vayanos-Vila framework that is entirely standard – apart from its two-country monetary union structure – modifies the bond market equilibrium and shapes the transmission of central bank asset purchases, without taking a stance on the modelling of sovereign default. Subsequently, we will extend the model to include a monetary/fiscal interactions block that endogenizes the default probability.

Time is continuous, with an infinite horizon. We consider a monetary union composed of two countries, Core and Periphery, with a single central bank. The key difference between the two governments is that Core issues risk-free debt whereas Periphery may default on its obligations. We denote Core variables with an asterisk, $'*'$. There exists a continuum of zero-coupon government bonds of different maturities. The time-t price of a bond with maturity τ is $P_t(\tau)$ for Peripheral bonds and $P_t^*(\tau)$ for Core bonds. The *yield* is the spot rate for maturity τ :

$$y_t(\tau) = -\frac{\log P_t(\tau)}{\tau}, \quad y_t^*(\tau) = -\frac{\log P_t^*(\tau)}{\tau} \ .$$

We assume that default follows a Poisson stochastic process, as in Duffie and Singleton (1999). Let ψ_t be the arrival rate of sovereign default by the government of Periphery. While it is easy to allow for default by both sovereigns, for clarity we focus on the case where the probability of Core default is zero. Peripheral default, when it occurs, consists of a restructuring in which the government reneges on fraction δ of each of its outstanding bonds. Default thus affects all maturities of Peripheral debt equally.

There exists a short-term (instantaneous) riskless interest rate which is exogenous

and characterized by an Ornstein–Uhlenbeck process,

$$dr_t = \kappa\left(\bar{r} - r_t\right) dt + \sigma dB_t, \tag{1}$$

where B_t is a Brownian motion and κ, $\bar{r}$ and σ are constants. The short-term riskless rate and the default shock itself are the only stochastic processes in this economy. The Peripheral default arrival rate ψ_t is deterministic but may depend on time.[6] Allowing for time variation in the default rate allows us to model the impact of changes in fiscal conditions and changes in asset purchases on the default probability (see Sec. 3).

Net bond supply. The public sector of the monetary union determines the net supply of bonds, consisting of the gross supply issued by the Peripheral and Core governments minus the bonds held by the common central bank. Let $f_t(\tau)$ be the stock of Peripheral sovereign debt of maturity τ outstanding at time t, and let $\iota_t(\tau)$ represent the rate of issuance of bonds of this type per unit of time. Then the law of motion of the stock of Peripheral debt is

$$\frac{\partial f_t\left(\tau\right)}{\partial t} = \iota_t\left(\tau\right) + \frac{\partial f_t\left(\tau\right)}{\partial \tau}, \tag{2}$$

which implies that the quantity of bonds of residual maturity τ outstanding at time t, $f_t\left(\tau\right)$, equals the current gross issuance of bonds of that maturity, $\iota_t\left(\tau\right) dt$, plus the stock of bonds of maturity $\tau + dt$ that was outstanding at time $t - dt$. The dynamics of the Core debt stock $f_t^*(\tau)$, given issuances $\iota_t^*(\tau)$, are formally identical to (2). Likewise, the central bank purchases $\iota_t^{CB}\left(\tau\right)$ bonds of maturity τ from Periphery per unit of time, resulting in a Peripheral portfolio $f_t^{CB}\left(\tau\right)$ that evolves as

$$\frac{\partial f_t^{CB}\left(\tau\right)}{\partial t} = \iota_t^{CB}\left(\tau\right) + \frac{\partial f_t^{CB}\left(\tau\right)}{\partial \tau}, \tag{3}$$

with analogous dynamics for its portfolio of Core bonds. We denote the net supplies of Periphery and Core bonds by

$$S_t\left(\tau\right) \equiv f_t\left(\tau\right) - f_t^{CB}\left(\tau\right), \quad S_t^*\left(\tau\right) \equiv f_t^*\left(\tau\right) - f_t^{CB*}\left(\tau\right),$$

respectively. For ease of exposition, but without loss of generality, we assume that net

[6] The assumption that ψ_t is deterministic is essential in order to obtain an affine solution, as we will see below.

bond supplies are deterministic but possibly time-varying functions.

Bond demand. We consider two classes of private agents that demand bonds. *Preferred-habitat investors* demand bonds of a specific jurisdiction and specific maturity, as an increasing function of the bonds' yield. Market participants with these characteristics may include pension funds or insurance companies whose liability streams require them to hold assets paying off at specific times in the distant future, or money-market mutual funds that must hold assets that provide liquidity at short horizons. *Arbitrageurs* are willing to hold bonds of any maturity and jurisdiction, and may also invest in the riskless short rate, but their positions are limited by their risk aversion. These players represent liquid, well-informed market participants, such as hedge funds, which nonetheless are unwilling to take arbitrarily large risks.

As in Vayanos and Vila (2021) we assume that preferred-habitat investors' demand for bonds of a given jurisdiction and maturity increases with the yield on those bonds:

$$\begin{aligned} Z_t(\tau) &= h(\tau) - \alpha(\tau)\,\mathbb{E}_t\left[\log P_t(\tau) + \tau\hat{\delta}dN_t\right] = h(\tau) + \tau\alpha(\tau)\left[y_t(\tau) - \hat{\delta}\psi_t\right] \quad (4) \\ Z_t^*(\tau) &= h^*(\tau) - \alpha^*(\tau)\log P_t^*(\tau) = h^*(\tau) + \tau\alpha^*(\tau)\, y_t^*(\tau) \end{aligned}$$

where $\alpha(\tau), \alpha^*(\tau) \geq 0$ and $h_t(\tau), h_t^*(\tau)$ are deterministic functions and dN_t is a Poisson process capturing the arrival of the default event. Note that the demand for peripheral bonds may depend on the probability of default. In particular, setting $\hat{\delta} = \delta$, the demand for peripheral bonds depends on their yield net of the expected default loss ($\psi_t\delta$). If instead we set $\hat{\delta} = 0$, then the demand for peripheral bonds, like that for core bonds, simply depends on their yield.[7]

The main focus of our analysis is the arbitrageurs, who maximize a mean-variance objective over instantaneous changes in wealth, as in Vayanos and Vila (2021),[8]

$$\max_{\{X_t(\tau), X_t^*(\tau)\}_{\tau\in(0,\infty)}} \mathbb{E}_t(dW_t) - \frac{\gamma}{2}\mathbb{V}ar_t(dW_t) \quad (5)$$

[7]Later, in Sec. 4, we enhance the quantitative realism of the model by allowing for stochastic shifts in the preferred habitat demand equation (4), as in Vayanos and Vila (2021).

[8]Some papers have considered portfolio problems in mean-variance settings where asset returns are generated by jump processes, including Rachev and Han (2000), Ortobelli et al. (2003), Kallsen (2000), and Emmer and Kluppelberg (2004), among others. In the quantitative evaluation of the model presented in Sec. 4, we have verified that the variance of wealth due to diffusion (interest rate) risk is of the same order of magnitude as that associated to Poisson (default) risk.

subject to the law of motion of wealth:

$$\begin{aligned} dW_t &= \left[W_t - \int_0^\infty \left(X_t(\tau) + X_t^*(\tau)\right) d\tau\right] r_t dt \\ &+ \int_0^\infty \left(X_t(\tau)\left(\frac{dP_t(\tau)}{P_t(\tau)} - \delta dN_t\right) + X_t^*(\tau)\frac{dP_t^*(\tau)}{P_t^*(\tau)}\right) d\tau, \end{aligned} \tag{6}$$

where $\gamma > 0$ is the representative arbitrageur's risk-aversion coefficient, and $X_t(\tau)$ and $X_t^*(\tau)$ are the nominal quantities of bonds of different maturities held in the arbitrageur's portfolio. The first term in (6) shows the income from investing in the short-term riskless rate, while the second term shows the capital gains from holding a portfolio of Peripheral bonds $X_t(\tau)$ and Core bonds $X_t^*(\tau)$, adjusted for the possible arrival of the default event. Note that arbitrageurs can operate in both markets (Core and Periphery), similar to Gourinchas et al. (2022).

Bond market clearing. Bond market clearing requires consistency between supply and demand for bonds of each maturity and jurisdiction:

$$S_t(\tau) = Z_t(\tau) + X_t(\tau), \quad S_t^*(\tau) = Z_t^*(\tau) + X_t^*(\tau) \ . \tag{7}$$

That is, net supply by the public sector equals demand by preferred-habitat investors plus that of arbitrageurs.

Bond pricing. We assume that after default, the Peripheral government issues new bonds to replace the defaulted bonds, thus returning to its initial deterministic path of gross bond supply.[9] Thus, default leaves the state of the bond market unchanged, so we seek to construct an equilibrium in which bond prices do not depend on previous default events.[10] We conjecture that there exist two pairs of deterministic functions $(A_t(\tau), C_t(\tau))$ and $(A_t^*(\tau), C_t^*(\tau))$ such that the price of bonds can be expressed in

[9]Perhaps surprisingly, it would be unrealistic to suppose that debt decreases when default occurs. On the contrary, Arellano et al. (2019) show that debt is more likely to *increase* following a restructuring. As in their paper, the model of monetary/fiscal interactions that we develop in Sec. 3 implies that default serves to alleviate short-term fiscal pressure, not to reduce the debt load permanently.

[10]Duffie and Singleton (1999) show that default risk is easier to price if default causes the bondholder to lose a fixed proportion of the market value of the bond. By assuming, first, that default amounts to reneging on the fixed quantity δ of each bond, and second, that default leaves the state of the bond market unchanged, we construct an equilibrium in which bondholders lose fraction δ of the market value of their holdings of Peripheral bonds. Hence we can price default risk as Duffie and Singleton (1999) do, reflected in the term δdN_t in (6).

log-affine form:

$$P_t(\tau) = e^{-[A_t(\tau)r_t + C_t(\tau)]},\ P_t^*(\tau) = e^{-[A_t^*(\tau)r_t + C_t^*(\tau)]}. \tag{8}$$

Applying Itô's lemma, the time-t instantaneous return on an undefaulted bond of maturity τ is

$$\frac{dP_t(\tau)}{P_t(\tau)} = \mu_t(\tau)\,dt - \sigma A_t(\tau)\,dB_t,\ \frac{dP_t^*(\tau)}{P_t^*(\tau)} = \mu_t^*(\tau)\,dt - \sigma A_t^*(\tau)\,dB_t, \tag{9}$$

where[11]

$$\mu_t(\tau) = \left(\frac{\partial A_t}{\partial \tau} - \frac{\partial A_t}{\partial t}\right) r_t + \left(\frac{\partial C_t}{\partial \tau} - \frac{\partial C_t}{\partial t}\right) - A_t(\tau)\,\kappa(\bar{r} - r_t) + \frac{1}{2}\sigma^2 \left[A_t(\tau)\right]^2, \tag{10}$$

and

$$\mu_t^*(\tau) = \left(\frac{\partial A_t^*}{\partial \tau} - \frac{\partial A_t^*}{\partial t}\right) r_t + \left(\frac{\partial C_t^*}{\partial \tau} - \frac{\partial C_t^*}{\partial t}\right) - A_t^*(\tau)\,\kappa(\bar{r} - r_t) + \frac{1}{2}\sigma^2 \left[A_t^*(\tau)\right]^2. \tag{11}$$

If we substitute bond returns (9) into the law of motion of wealth (6), we obtain

$$\begin{aligned} dW_t &= \left[W_t r_t + \int_0^\infty \left(X_t(\tau)\left(\mu_t(\tau) - r_t\right) + X_t^*(\tau)\left(\mu_t^*(\tau) - r_t\right)\right) d\tau\right] dt \\ &- \left[\int_0^\infty \left(X_t(\tau)\,A_t(\tau) + X_t^*(\tau)\,A_t^*(\tau)\right) d\tau\right] \sigma dB_t \\ &- \left[\int_0^\infty X_t(\tau)\,d\tau\right] \delta dN_t. \end{aligned} \tag{12}$$

Thus, wealth is affected by two different types of risk: a Brownian variation in bond prices (seen in the second line of the formula), together with a Poisson risk of losing a fraction δ of the investment in Peripheral bonds (third line). Using equation (12) in

[11] Note that τ is a state with dynamics $d\tau = -dt$, so Itô's lemma yields derivatives in τ as well as t.

(5), one can see that the problem of the arbitrageurs accounts for both these risks:

$$\begin{aligned}\max_{\{X_t(\tau),X_t^*(\tau)\}_{\tau\in(0,\infty)}} \quad & \int_0^\infty \left(X_t\left(\tau\right)\left(\mu_t\left(\tau\right)-r_t\right)+X_t^*\left(\tau\right)\left(\mu_t^*\left(\tau\right)-r_t\right)\right)d\tau \\ - \quad & \tfrac{\gamma\sigma^2}{2}\left[\int_0^\infty \left(X_t\left(\tau\right)A_t(\tau)+X_t^*\left(\tau\right)A_t^*(\tau)\right)d\tau\right]^2 \\ - \quad & \psi_t\delta\left[\int_0^\infty X_t\left(\tau\right)d\tau\right] \\ - \quad & \tfrac{\gamma\psi_t}{2}\delta^2\left[\int_0^\infty X_t\left(\tau\right)d\tau\right]^2.\end{aligned}$$

The first two terms represent the expectation and variance of the component associated with price variation, while the last two terms are derived from default risk, using $\mathbb{E}\left[\delta dN_t\right]=\delta\psi_t$ and $\mathbb{V}ar\left[\delta dN_t\right]=\delta^2\psi_t$.

The first-order conditions are

$$\mu_t\left(\tau\right) = r_t+A_t\left(\tau\right)\lambda_t+\psi_t\delta+\xi_t, \tag{13}$$

$$\mu_t^*\left(\tau\right) = r_t+A_t^*\left(\tau\right)\lambda_t, \tag{14}$$

where[12]

$$\lambda_t=\gamma\sigma^2\int_0^\infty\left(X_t\left(\tau\right)A_t(\tau)+X_t^*\left(\tau\right)A_t^*(\tau)\right)d\tau \tag{15}$$

is the *market price of (interest rate) risk* and

$$\xi_t=\gamma\psi_t\delta^2\int_0^\infty X_t\left(\tau\right)d\tau \tag{16}$$

is the compensation required by risk-averse arbitrageurs for *default risk*. Equation (14) shows that the expected growth rate of Core bond prices equals the short-term riskless rate of return, r_t, plus the compensation $A_t^*(\tau)\lambda_t$ for the instantaneous price risk on a bond of a given maturity τ. Analogous terms apply to the expected growth of Peripheral bond prices, given by (13), plus the compensation $\psi_t\delta$ for the rate of expected loss due to default, together with the instantaneous default risk premium ξ_t.

Constructing an affine solution. Market clearing (7) requires that the positions of arbitrageurs equal those of the public sector minus those of the preferred-habitat

[12] Our notation in this section follows Vayanos and Vila (2021), except that we have reversed the sign on the variables λ and h.

investors. Using this in equations (15) and (16), the risk prices λ_t and ξ_t must satisfy:

$$\lambda_t = \gamma\sigma^2 \int_0^\infty \left[\left(S_t(\tau) - Z_t(\tau) \right) A_t(\tau) + \left(S_t^*(\tau) - Z_t^*(\tau) \right) A_t^*(\tau) \right] d\tau, \tag{17}$$

$$\xi_t = \gamma\psi_t\delta^2 \int_0^\infty \left(S_t(\tau) - Z_t(\tau) \right) d\tau. \tag{18}$$

Equations (17)-(18) can be used to solve for the unknown coefficients $A_t(\tau)$, $A_t^*(\tau)$, $C_t(\tau)$, and $C_t^*(\tau)$ in the bond price functions (see Online Appendix B.1). The solution hinges on the observation that if ψ_t is a deterministic function of time, then the left- and right-hand sides of (18) can both be affine functions of r_t (since preferred-habitat demand Z is affine in r).[13] In this case, we can construct a (potentially) time-varying affine solution (8) for prices and yields, in which the risk prices λ_t and ξ_t are also affine:

$$\lambda_t = \Lambda_t r_t + \bar{\lambda}_t, \tag{19}$$

$$\xi_t = \Xi_t r_t + \bar{\xi}_t. \tag{20}$$

Online App. B.1 spells out the affine solution in detail, stating the formulas for the factor loadings Λ_t and Ξ_t and intercept terms $\bar{\lambda}_t$ and $\bar{\xi}_t$ consistent with (17)-(18).

2.1 Equilibrium yield curves and monetary policy transmission: analytical results

Our model's analytical solution provides insight into yield curve dynamics and the transmission of conventional and unconventional monetary policy. Here we discuss four main findings. First, we decompose yields to distinguish the familiar *expectations* and *duration extraction* transmission channels of asset purchase policy from our model's novel *default risk extraction channel*, which arises when debt is defaultable. Second, we show how, when the default arrival rate is small, the term premium in the yield curves of both Core and Periphery depends on the *aggregate* net bond supply in the monetary union, irrespective of its distribution across countries. Third, we show that default risk allows for heterogeneous fluctuations in short-term sovereign rates in a monetary union, including shifts in the short end of the Peripheral yield curve even when the

[13] If instead ψ_t is a stochastic process that depends on r_t, then there are nonlinear terms on the right-hand side of (18), so the affine solution fails.

short-term riskless rate does not change. Finally, we show that conventional interest rate policy transmits homogeneously across a monetary union, limiting its scope for stabilizing asymmetric fluctuations.

Decomposing bond yields. In the absence of default risk, equations (10)-(11) and (13)-(14) imply identical yield curves for Core and Periphery. But when Peripheral bonds are defaultable, this opens up a spread relative to Core bonds. Taking expectations on both sides of (9), then using (13) and the fact that $P_t(0) = 1$, we can decompose the yield on a Peripheral bond of maturity τ as follows.[14]

Proposition 1 (Bond yield decomposition) *Peripheral yields $y_t(\tau)$ can be written as*

$$\begin{aligned} y_t(\tau) &= \underbrace{\frac{1}{\tau}\mathbb{E}_t\int_0^\tau r_{t+s}ds}_{\text{Expected rates } y_t^{EX}(\tau)} + \underbrace{\frac{1}{\tau}\mathbb{E}_t\int_0^\tau\left\{A_{t+s}(\tau-s)\lambda_{t+s} - \frac{\sigma^2}{2}\left[A_{t+s}(\tau-s)\right]^2\right\}ds}_{\text{Term premium } y_t^{TP}(\tau)} \\ &+ \underbrace{\frac{1}{\tau}\mathbb{E}_t\int_0^\tau \delta\psi_{t+s}ds}_{\text{Expected default loss } y_t^{DL}(\tau)} + \underbrace{\frac{1}{\tau}\mathbb{E}_t\int_0^\tau \xi_{t+s}ds}_{\text{Credit risk premium } y_t^{CR}(\tau)} . \end{aligned} \tag{23}$$

For the proof, see Online App. B.2.1. Thus, Peripheral yields decompose into four affine components. The default-related components are zero for Core:

$$y_t(\tau) = y_t^{EX}(\tau) + y_t^{TP}(\tau) + y_t^{DL}(\tau) + y_t^{CR}(\tau), \tag{24}$$

$$y_t^*(\tau) = y_t^{EX*}(\tau) + y_t^{TP*}(\tau). \tag{25}$$

The first component, which is equalized across countries, $y_t^{EX}(\tau) = y_t^{EX*}(\tau)$, is the yield in a default-free economy where investors are risk neutral. This is often called the *expected rates term*, since it is the yield in a default-free economy where the "expectations hypothesis" is true: that is, the bond yield equals the expected value of the short rate over the life of the bond. The second component is the *term premium*, that is, the compensation required by a risk-averse arbitrageur for holding a bond with

[14] Equivalently, the bond price can be written as a product of log-affine factors:

$$P_t(\tau) = P_t^{EX}(\tau)P_t^{TP}(\tau)P_t^{DL}(\tau)P_t^{CR}(\tau) \tag{21}$$

$$P_t^*(\tau) = P_t^{EX*}(\tau)P_t^{TP*}(\tau) \tag{22}$$

where, for each $i \in \{EX, TP, DL, CR\}$, we have $P_t^i(\tau) = \exp\left(-\tau y_t^i(\tau)\right)$, and likewise for Core.

a risky price.[15] Since the price process of a defaultable bond differs from that of a default-free bond, the Core and Peripheral term premia, $y_t^{TP*}(\tau)$ and $y_t^{TP}(\tau)$, are not exactly equal. The third component, in the case of Peripheral bonds, is the *expected default loss* $y_t^{DL}(\tau)$, which requires compensation even for a risk-neutral investor. Fourth, the yield on Peripheral bonds also carries a *credit risk premium* $y_t^{CR}(\tau)$, which is the additional return required, beyond the expected default loss, in order for a risk-averse arbitrageur to be willing to hold a defaultable bond. Together, the two components $y_t^{DL}(\tau) + y_t^{CR}(\tau)$, plus the cross-country difference in term premia $y_t^{TP}(\tau) - y_t^{TP*}(\tau)$, constitute the (sovereign) spread between Peripheral and Core debt.

This decomposition highlights four different channels of monetary policy transmission. First, policy transmits through anticipated changes in the future path of interest rates (e.g. due to forward guidance). Second, it operates through *duration extraction*, by which central bank bond purchases reduce the market price of interest rate risk, as in the one-factor version of Vayanos and Vila (2021). Third, policy transmits through changes in the expected default loss, as central bank purchases may reduce the likelihood of sovereign default, as explained in Sec. 3 below. Finally, it transmits through *default risk extraction*, as we can see by using (18) to write the credit risk premium as

$$y_t^{CR}(\tau) = \frac{\gamma\delta^2}{\tau}\mathbb{E}_t \int_0^\tau \left[\psi_{t+s} \int_0^\infty \left(S_{t+s}(\tau) - Z_{t+s}(\tau)\right) d\tau\right] ds \ .$$

This shows that central bank bond purchases reduce credit risk premia, both by extracting defaultable debt $S_{t+s}(\tau)$ from the market, and – once it is allowed to depend on central bank purchases – by lowering the probability of default ψ_{t+s} on that debt.

Term premium and sovereign spread in a monetary union. While our decomposition highlights a new transmission channel going through credit risk, our model also delivers basic insights about the transmission of asset purchases via term premia in a monetary union. For simplicity, but without loss of generality, we focus on the model's ergodic distribution, in which the short rate r_t is stochastic, but there is no further time variation in the model's parameters. We suppress time subscripts wherever possible when analyzing the ergodic distribution. As shown in Online App.

[15] To simplify the decomposition, we include the Itô adjustment term $-\frac{\sigma^2}{2}\left[A_{t+s}(\tau - s)\right]^2$ in the term premium, since it is related to price variability. Note, though, that a term of this form also exists in the case where arbitrageurs are risk-neutral.

B.2.2, in this case the coefficients $A_t(\tau)$ and $A_t^*(\tau)$ are given by

$$A^*(\tau) = \frac{1-e^{-\hat{\kappa}\tau}}{\hat{\kappa}},\ A(\tau) = \frac{(1+\Xi)\left(1-e^{-\hat{\kappa}\tau}\right)}{\hat{\kappa}}, \tag{26}$$

where

$$\hat{\kappa} = \kappa - \Lambda = \kappa + \gamma\sigma^2 \int_0^\infty \left(\alpha(\tau) \left(\frac{(1+\Xi)\left(1-e^{-\hat{\kappa}\tau}\right)}{\hat{\kappa}} \right)^2 + \alpha^*(\tau) \left(\frac{1-e^{-\hat{\kappa}\tau}}{\hat{\kappa}} \right)^2 \right) d\tau,$$

is the risk-neutral counterpart of κ, and $\Xi = -\gamma\psi\delta^2 \int_0^\infty \alpha(\tau) A(\tau) d\tau < 0$ is the steady-state value of the loading of the default risk price ξ_t on the short rate (eq. 20). We then obtain the following result:

Proposition 2 (Term premia in a monetary union with low default risk) *Let the default arrival rate ψ be arbitrarily close to zero, $\psi \to 0$, so that $\Xi \to 0$. In this limiting case, $A(\tau) = A^*(\tau)$. Term premia are then equalized across the two countries:*

$$y_t^{TP}(\tau) = \frac{1}{\tau}\mathbb{E}_t \int_0^\tau \left\{ A(\tau - s)\lambda_{t+s} - \frac{\sigma^2}{2}\left[A_{t+s}(\tau - s)\right]^2 \right\} ds = y_t^{TP*}(\tau),$$

and the market price of duration risk depends on the aggregate net bond supply in the monetary union:

$$\lambda_t = \gamma\sigma^2 \int_0^\infty \underbrace{\left[\left(S(\tau) + S^*(\tau)\right) - \left(Z_t(\tau) + Z_t^*(\tau)\right)\right]}_{\textit{aggregate net bond supply}} A(\tau) d\tau.$$

A policy implication of this result is that, when default risk is arbitrarily small, asset purchases affect Core and Peripheral term premia symmetrically, and this effect depends only on the *aggregate* amount of purchases and not on how they are distributed across jurisdictions. This benchmark will be helpful in interpreting our subsequent numerical results, since our calibrated default arrival rate turns out to be fairly small.

Notice that if the term premia roughly coincide, then the sovereign spread is just the expected default loss plus the credit risk premium: $y_t^*(\tau) - y_t(\tau) = y_t^{DL}(\tau) + y_t^{CR}(\tau)$. In the ergodic distribution, both objects are independent of maturity, and hence the spread is constant across τ and equals $y_t^*(\tau) - y_t(\tau) = \psi\delta + \left(\Xi\bar{r} + \bar{\xi}\right)$.

What drives the short end of the yield curve? For a country without default

risk, the shortest maturity yield coincides with the short-term riskless rate:

$$\begin{aligned}\lim_{\tau\to 0} y_t^*(\tau) &= \lim_{\tau\to 0}\left[\frac{1}{\tau}\mathbb{E}_t\int_0^\tau r_{t+s}ds + \frac{1}{\tau}\mathbb{E}_t\int_0^\tau A_{t+s}^*(\tau-s)\lambda_{t+s} - \frac{\sigma^2}{2}\left[A_{t+s}^*(\tau-s)\right]^2 ds\right] \\ &= r_t + A_t^*(0)\lambda_t - \frac{\sigma^2}{2}\left[A_{t+s}^*(0)\right]^2 = r_t,\end{aligned}$$

where the second line applies L'Hôpital's rule and the Leibniz rule and the fact that $A_t^*(0) = 0$. Therefore, in the absence of default risk, changes in structural parameters can produce changes in the slope of the yield curve, but the short end of the curve is pinned down to equal the short-term rate.[16]

Hence, if we abstract from default, our model cannot reproduce yield curve shifts like those observed in Europe in the context of Covid-19 and the PEPP announcement (see Fig. 1 above). But once we allow for default risk, parallel shifts are possible, even in the absence of changes in the short-term riskless rate.

Proposition 3 (Default risk-related shifts in the Peripheral yield curve) *In a country with default risk, the yield curve in the ergodic distribution is the sum of a constant term that depends on default* $\left(\psi\delta + \bar{\xi}\right)$ *and a maturity-dependent affine term:*

$$\begin{aligned}y_t(\tau) &= \frac{A(\tau)r_t + C(\tau)}{\tau} \\ &= \left(\psi\delta + \bar{\xi}\right) + \frac{(1+\Xi)\left(1-e^{-\hat{\kappa}\tau}\right)}{\tau\hat{\kappa}}r_t + \frac{\int_0^\tau\left[A(u)\left(\kappa\bar{r}+\bar{\lambda}\right) - \frac{1}{2}\sigma^2\left[A(u)\right]^2\right]du}{\tau}.\end{aligned}$$

Therefore, the short-term Peripheral yield is given by

$$\lim_{\tau\to 0} y_t(\tau) = (1+\Xi)r_t + \left(\psi\delta + \bar{\xi}\right).$$

For proof details, see Online App. B.2.2. Note that the default-related term $\psi\delta + \bar{\xi}$ is independent of maturity τ, so this term produces a parallel shift in the yield curve when any of its components change. Hence, the possibility of default affects even the shortest yields, generating a spread between the shortest-maturity Peripheral yield and the risk-free short rate. The spread includes the expected default loss $\psi\delta$. The second

[16] This result generalizes beyond the one-factor model considered here. Even in a multi-factor context, an instantaneous bond without default risk satisfies $A^*(0) = 0$ and $C^*(0) = 0$, implying $y_t^*(0) = r_t$. See Vayanos and Vila (2021), Lemma 3.

term is the intercept $\bar{\xi}$ of the credit risk premium ξ from (20), which is

$$\bar{\xi} = \gamma\psi\delta^2 \int_0^\infty \left(S\left(\tau\right) - h\left(\tau\right) - \alpha\left(\tau\right) C\left(\tau\right)\right) d\tau. \tag{27}$$

Equation (27) shows that changes in the default arrival rate ψ, the haircut δ or the risk aversion parameter γ will, *ceteris paribus*, modify the credit risk premium and hence shift the Peripheral yield curve. Asset purchases will also shift Peripheral yields, including the shortest yields, by decreasing $\bar{\xi}$ through two channels. First, they extract default risk from arbitrageurs' balance sheets (reducing the quantity $S(\tau)$ that private markets must hold). Second, if asset purchases reduce the probability of default, this will amplify the decrease in $\bar{\xi}$. In the next section, we show how monetary and fiscal interactions like those in the euro area imply that central bank sovereign bond purchases reduce fiscal pressure, and thereby lower the probability of Peripheral default.

Conventional monetary policy transmission. Finally, we analyze how default risk shapes the transmission of conventional (interest rate) monetary policy across the monetary union. For the purpose of this particular discussion, we interpret r_t as representing the interest paid by the central bank on its deposit facility.[17] Concretely, as in Vayanos and Vila (2021), we may assume that arbitrageurs are actually commercial banks, with access to the central bank's deposit facility. With this interpretation, $\tau^{-1}A_t(\tau)$ represents the reaction of the Peripheral yield curve, on impact, to a monetary policy shock, and $A_t^{'}(\tau)$ represents the reaction of the instantaneous forward rate, $i_t\left(\tau\right) \equiv -\frac{\partial \log(P_t(\tau))}{\partial \tau}$. Therefore:

Proposition 4 (Response to short-term rates) *The yield curve and the instantaneous forward rate both react less to a monetary policy shock in Periphery, compared with Core:*

$$\frac{\partial y_t^*\left(\tau\right)}{\partial r_t} = \frac{1 - e^{-\hat{\kappa}\tau}}{\tau\hat{\kappa}} > \frac{\left(1+\Xi\right)\left(1 - e^{-\hat{\kappa}\tau}\right)}{\tau\hat{\kappa}} = \frac{\partial y_t\left(\tau\right)}{\partial r_t}.$$

$$\frac{\partial i_t^*\left(\tau\right)}{\partial r_t} = -\frac{\partial}{\partial r_t}\frac{\partial \log\left(P_t\left(\tau\right)\right)}{\partial \tau} = e^{-\hat{\kappa}\tau} > \left(1+\Xi\right) e^{-\hat{\kappa}\tau} = \frac{\partial i_t\left(\tau\right)}{\partial r_t}.$$

Since $\Xi < 0$ (see Online App. B.2.2), the reaction of Peripheral yields is damped

[17] This implies that the short-term Core yield, $\lim_{\tau\to 0} y_t^*\left(\tau\right)$, coincides with the deposit facility rate. Of course, this is not precisely true in the euro area data, where the yield on short-term core (e.g. German) bonds typically exhibits a non-negligible and time-varying spread vis-à-vis the ECB's deposit facility rate, reflecting institutional features that fall outside the scope of our analysis.

relative to that of Core yields. But in practice, the difference is small: if the default arrival rate ψ is sufficiently close to zero, then $\Xi \approx 0$, so the responses of the two yield curves are approximately equal. In the quantitative section below we will see that the data call for a fairly small ψ. Therefore, in our calibrated model, the responses of Core and Peripheral yields to conventional monetary shocks are virtually indistinguishable.

3 A simple model of default risk

Thus far, we have treated the default arrival rate ψ_t as an arbitrary exogenous sequence. In practice, however, policy shocks like the PEPP announcement or the pandemic outbreak are likely to endogeneously affect the probability of default perceived by the market. Therefore, we next build a minimalist model of monetary and fiscal interactions that endogenizes ψ_t in a way that will suffice for our analysis of the yield curve. We assume at this point that the governments and the monetary authorities commit to fixed time paths for their respective bond issuances and purchases of bonds, as long as no rollover crisis occurs.[18] The one key policy choice that we will endogenize is Periphery's decision whether to repay or default in case of a rollover crisis.

Budget constraint of the government. The flow budget constraint of the Peripheral government can be written as

$$\overbrace{d_t}^{\text{Primary deficit (det.)}} + \overbrace{f_t(0)}^{\text{Bond redemptions}} = \overbrace{\int_0^\infty P_t(\tau)\,\iota_t(\tau)\,d\tau}^{\text{Bond issuance}} + \overbrace{\Gamma_t}^{\text{CB remittances}} + \overbrace{\Pi_t}^{\text{Emergency taxation}}, \tag{28}$$

where d_t is the deterministic part of the primary deficit[19] and $f_t(0)$ the amount of debt maturing, which must be financed with new bond issuances $\iota_t(\tau)$, income from central bank remittances Γ_t, or through adjustments in taxation (or reduced spending) Π_t. Our assumption that bond issuances $\iota_t(\tau)$ are deterministic implies that redemptions $f_t(0)$ are deterministic too. Since the government takes Γ_t as given, Π_t represents the part of primary deficit that must be adjusted to ensure that the budget constraint (28) is satisfied at all times. In the context of a rollover crisis, we may think of Π_t as

[18] As will become clear later on, this assumption is introduced in order to preserve the affine yield solution derived in Sec. 2.

[19] This may include spending or revenue items that are "hard" to change in the short run, such as pensions, benefits, the government wage bill, etc.

representing emergency taxation or, equivalently, emergency spending cuts.

Rollover crisis. Mirroring Corsetti and Dedola (2016), we focus on self-fulfilling debt crises *à la* Calvo (1988) or Cole and Kehoe (2000). We assume that investors sometimes, with a certain probability, coordinate on a pessimistic equilibrium in which they stop purchasing Periphery's debt, thus forcing its government to stop bond issuance ($\iota_t(\tau) = 0$, for all τ).[20] The arrival of this rollover crisis is governed by a Poisson process with rate parameter η. This random event is unrelated to the amount of a country's debt or its fiscal position.

At the onset of the crisis, the government must decide whether to default on its debts or to keep on repaying bonds that mature. If it decides to repay, the duration of the crisis is stochastic, governed by a Poisson process with parameter ϕ, and the government will be forced to finance its deficits and debt repayments with the revenues it obtains from emergency taxation and/or seigniorage as long as the crisis persists. Emergency taxes represent a utility loss for the government, which it seeks to minimize. Under these assumptions, the government's *cost of repayment* conditional on a rollover crisis at time 0, denoted by V_0^R, incorporates the present discounted value of emergency taxation incurred during the crisis, valued at a subjective discount rate $\hat{r}$, plus the continuation cost $V_t\left[f_t(\cdot), f_t^{CB}(\cdot)\right]$ after the crisis ends:

$$V_0^R\left[f_0(\cdot), f_0^{CB}(\cdot)\right] = \mathbb{E}_0\left\{\int_0^\infty e^{-(\hat{r}+\phi)t}\left(\underbrace{\Pi_t}_{\text{Flow of emergency taxes}} + \phi\underbrace{V_t\left[f_t(\cdot), f_t^{CB}(\cdot)\right]}_{\text{Loss after the crisis}}\right)dt\right\}. \tag{29}$$

If instead the government decides to *default*, it restructures by repudiating a fixed fraction δ of each outstanding bond. This restructuring ends the rollover crisis, but imposes a stochastic fixed cost χ on the government, with *c.d.f.* $\Phi(\chi)$. Thus, the loss due to default is the post-crisis continuation cost plus the fixed cost:

$$V_0^D\left[f_0(\cdot), f_0^{CB}(\cdot)\right] = V_0\left[f_0(\cdot), f_0^{CB}(\cdot)\right] + \chi. \tag{30}$$

Note that (30) says that default leaves the fiscal position of the government unchanged, with the same debts it faced before the crisis. While this may seem counterintuitive,

[20] We assume that the central bank cannot purchase new sovereign bonds at issuance, consistently with actual restrictions on the ECB's asset purchase programs. Thus, the fact that private investors stop purchasing new bonds effectively prevents the Peripheral government from issuing new bonds.

we make this assumption for two reasons. First, it is empirically realistic: Arellano et al. (2019) show that debt is rarely decreased by a restructuring. Second, it simplifies our asset pricing analysis, keeping the outstanding bond supply fixed, allowing us to seek a bond price solution that is unchanged by default.[21] Thus, in our model, default serves only to relieve short-term fiscal pressure during a rollover crisis, not to improve the government's long-term fiscal standing.

Default decision. The government's decision to default at the beginning of a crisis will thus depend on $\min\left[V_0^R, V_0^D\right]$. The continuation cost is given by

$$V_0\left[f_0\left(\cdot\right), f_0^{CB}\left(\cdot\right)\right] = \mathbb{E}_0\left\{\int_0^\infty e^{-(\hat{r}+\eta)t} \underbrace{\eta \min\left[V_t^R, V_t^D\right]}_{\text{Loss at onset of next crisis}} dt\right\}. \tag{31}$$

Equations (29)-(31) jointly determine the loss functions V_t^R, V_t^D, and V_t. For simplicity, we focus on the limit where crises are low-probability events ($\eta \to 0$), which means that the continuation cost is approximately zero, $V_t \to 0$, so that $V_0^D \to \chi$. Intuitively, the country compares the fixed cost χ to the present value of the expected emergency-tax deadweight cost V_0^R. Then the probability of default, conditional on a rollover crisis at time 0, is the probability that the cost of repayment exceeds the fixed cost χ:

$$\mathbb{P}\left(\text{default at time } 0|\text{crisis}\right) = \mathbb{P}\left(V_0^R > V_0^D\right) \approx \mathbb{P}\left(V_0^R > \chi\right) = \Phi\left(V_0^R\right). \tag{32}$$

Equations (32), (29) and (28), and the fact that there are no issuances during the rollover crisis ($\iota_t\left(\tau\right) = 0$ for all τ), imply that the *unconditional* arrival rate of default is $\psi_t = \eta\Phi_t$, where

$$\Phi_t \equiv \mathbb{P}\left(\text{default at time } t|\text{crisis}\right) = \Phi\left(\int_0^\infty e^{-(\hat{r}+\phi)s}\left\{d_{t+s} + f_{t+s}(0) - \Gamma_{t+s}\right\} ds\right). \tag{33}$$

Therefore, conditional on a rollover crisis materializing at time t, the probability that the government chooses to default increases with the discounted stream of primary deficits and bond redemptions during the crisis (as they both imply higher liquidity needs), and decreases with the discounted stream of remittances from the central bank

[21] Our interpretation of (30) is that after default, the Peripheral government immediately issues bonds that return it to the previously anticipated path of debt. Bondholders lose a fraction δ of their holdings, while the proceeds from the sale of new bonds accrue to international organizations, such as the IMF, that may intervene in the case of a sovereign debt crisis.

during the crisis (a source of government income that reduces liquidity needs).

Remittances rule. To evaluate expression (33), we must specify the central bank's remittances rule during a rollover crisis. It is plausible to conjecture that, should a full-blown rollover crisis hit a national government, the central bank would follow a rule under which an *increased* flow of central bank purchases of that government's bonds would *not reduce* resources for that government for the duration of the crisis.[22] We call such a rule *sovereign-supportive*. Formally, we define a sovereign-supportive rule $\Gamma_t = \Gamma\left(\left\{f^{CB}_{t+u}(\tau)\right\}_{u\geq 0,\tau\geq 0}\right)$ as a rule that, in a rollover crisis, satisfies:

$$\frac{\partial}{\partial \varepsilon}\left[\int_0^\infty e^{-(\hat{r}+\phi)u}\Gamma\left(\left\{f^{CB}_{t+u}(\tau)+\varepsilon h_{t+u}(\tau)\right\}_{u\geq 0,\tau\geq 0}\right)du\right]\geq 0, \tag{34}$$

where $h_{t+u}(\tau)\geq 0$ is a non-negative perturbation to the time-$(t+u)$ central bank holdings of Periphery bonds with residual maturity τ. That is, under a sovereign-supportive remittance rule, a central bank's decision to increase its future holdings of peripheral debt would not decrease the discounted stream of dividend payments to the peripheral government in case of – and for the duration of – a rollover crisis. It trivially follows that, for any rule satisfying this property, increasing central bank purchases of peripheral bonds (weakly) *reduces* the endogenous default arrival rate.

Having established this general result, we still need to specify a particular crisis-time remittance rule to use in our numerical analysis. There is little guidance as to how Eurosystem national central banks (NCB) would adapt their dividend policy should their country's government be hit by a rollover crisis. In practice, NCB dividend payments are typically based on their accounting profits, whereby a fraction of these is paid out as dividends to the respective government and the rest is retained as capital.[23] Thus, it seems plausible that crisis-time dividends would continue to be based on profits.

However, with profit-based rule in our model, we would no longer be able to obtain an affine solution for bond yields. This is because the default probability in equation (33) would depend on bond prices and therefore would no longer be deterministic,

[22]The central bank is assumed to stick to its bond purchase commitments when the private bond market enters into a rollover crisis.

[23]That being said, dividend rules are *not* harmonized across the Eurosystem. Each NCB autonomously decides how much of its accounting profits to pay to its national government, with criteria that vary across NCBs and also change over time.

which as explained in Sec. 2 is esssential for obtaining an affine solution.[24] With this limitation in mind, we assume the following remittance rule,

$$\Gamma_t = \zeta f_t^{CB}(0) - \bar{\Gamma}, \tag{35}$$

such that the central bank rebates to the Peripheral government a fraction $\zeta \in [0,1]$ of the inflow from redemptions of Peripheral government bonds ($f_t^{CB}(0)$), minus a fixed amount $\bar{\Gamma}$ aimed at preemptively protecting the central bank's capital during the rollover crisis against a possible default.[25] Rule (35) is compatible with an affine solution for bond yields, as redemptions of central bank-held bonds are assumed to follow a deterministic path.[26] Also, it is "sovereign-supportive" as defined above.[27]

The parameter ζ allows us to consider a wide range of "generosity" in the Peripheral national central bank's dividend policy, should its government be hit by a rollover crisis. At one extreme, $\zeta = 1$ represents a case in which the national central bank pays off its entire inflow from Peripheral bond redemptions. This is (much) higher than the accounting profits earned by the central bank on those bonds –as one needs to deduct the cost of purchasing them.[28] Therefore, this can be seen as a very generous central

[24] Online App. A shows how to calculate the central bank's profits in our model, and explains why a remittance rule based on profits would render our affine solution inapplicable. In a nutshell: the interest income on the central bank's bond portfolio depends on the price paid for each bond. Moreover, profits depend on interest payments on reserves. Keeping track of the stock of reserves introduces another endogenous state variable, and the evolution of this stock also depends on bond prices.

[25] In the event of a default, we assume there is no discrimination between public and private bondholders. Therefore, upon default the central bank would take a hit to its capital, which depending on its pre-default value could become even negative. As discussed by Del Negro and Sims, 2015, among others, central banks can operate with negative capital, but within certain limits, related to their future stream of seigniorage. Γ can therefore be seen as reflecting these concerns about central bank capital during a rollover crisis. Of course, in the event of default and for sufficiently negative capital, the central bank may still need to be recapitalized ex post by the government, via negative dividends.

[26] Notice that central bank remittances to the Peripheral government depend on its porfolio of Peripheral bonds only, and not on its combined portfolio of Core and Peripheral bonds. This assumption is consistent with the fact that, in the Eurosystem, the large majority of sovereign bonds are held by the national central banks (NCBs) of the sovereigns that issued them, with only a small fraction of holdings being subject to "risk sharing" across NCBs.

[27] Under the given rule, $\Gamma\left(\left\{f_{t+u}^{CB}(\tau) + \varepsilon h_{t+u}(\tau)\right\}_{u\geq 0,\tau\geq 0}\right) = \zeta\left(f_{t+u}^{CB}(0) + \varepsilon h_{t+u}(0)\right) - \bar{\Gamma}$. Therefore, $\frac{\partial \Gamma}{\partial \varepsilon} = \{\zeta h_{t+u}(0)\}_{u\geq 0}$, and hence the condition (34) is just $\zeta \int_0^\infty e^{-(\hat{r}+\phi)u} h_{t+u}(0) du \geq 0$, which is true since the constant ζ and the perturbation h are both non-negative.

[28] The income earned on a zero-coupon bond is the difference between its payment at redemption (i.e. its face value) and the price paid for it. Thus, the total interest income from the central bank's

bank dividend policy during the rollover crisis.[29] At the other extreme, $\zeta = 0$ represents a case in which the national central bank stops all dividend payments to its government for the duration of the rollover crisis (over and above net transfers in the amount $-\bar{\Gamma}$), motivated e.g. by concerns about preserving its capital base. This case is particularly useful because it allows us to shut down the channel through which central bank asset purchases reduce the endogenous default probability.

Default rate. Under remittance rule (35), the default rate equals:

$$\psi_t = \eta\Phi\left(\int_0^\infty e^{-(\hat{r}+\phi)s}\left\{d_{t+s} + f_{t+s}(0) - \zeta f_{t+s}^{CB}(0) + \bar{\Gamma}\right\} ds\right). \tag{36}$$

Equation (36) shows that the central bank can affect the default probability through its asset purchase policy, as long as $\zeta > 0$. Bond purchases imply higher future redemption payments from the government to the central bank ($\{f_{t+s}^{CB}(0)\}_{s\geq 0}$) conditional on, and during, a rollover crisis. However, a fraction ζ of those repayments is rebated back to the government in the form of dividends, thus partly alleviating the liquidity stress on the government associated to total bond redemptions ($\{f_{t+s}(0)\}_{s\geq 0}$). This reduces the cost of emergency taxation during the crisis and hence makes the government less likely to choose default once the rollover crisis arrives. Underlying this mechanism is the central bank's (unique) ability to finance bond purchases by expanding its monetary base (see Online App. A.1 for an explicit modelling of the central bank's balance sheet and budget constraint). This ability, together with the fact that its budget constraint is linked to the government's through central bank dividends, explains why central bank asset purchases can reduce sovereign default risk in our model.

Equation (36) also shows that the three factors affecting the default probability (primary deficits, total bond redemptions, and redemptions of central bank-held bonds) do so through a single sufficient statistic, which we may call *fiscal pressure*, F_t:

$$F_t \equiv \int_0^\infty e^{-(\hat{r}+\phi)s}\left(d_{t+s} + f_{t+s}(0) - \zeta f_{t+s}^{CB}(0)\right) ds, \tag{37}$$

so that $\psi_t = \eta\Phi\left(F_t + \frac{\bar{\Gamma}}{\hat{r}+\phi}\right)$.

bond portfolio at a given point in time equals bond redemptions, $f_t^{CB}(0)$, *minus* the total amount paid for those bonds by the central bank. See Online App. A for further details.

[29] Of course, such a dividend policy would erode the central bank's capital position. Online App. A derives the dynamics of central bank capital under our remittance rule.

This framework makes several stark assumptions which, together, deliver tractability. On one hand, we focus on perfect-foresight scenarios for fiscal policy and central bank purchases, assuming that the government returns to its previous path of debt after default occurs. Moreover, our remittance rule (35) ensures that the default probability depends only on deficits and bond redemption flows. Together, these assumptions imply that fiscal pressure is foreseeable, so default is an event that arrives at a known, deterministic Poisson rate $\psi_t = \eta\Phi_t$. This means we can apply the framework of Duffie and Singleton (1999) to obtain an affine solution for the term structure and to decompose bond yields into components related to the dynamics of the risk-free rate and components related to default, as described in Sec. 2.1.[30] Unanticipated changes in fiscal conditions will shift the default probability, with potential to explain the yield curve dynamics seen over the course of the Covid-19 crisis. We next calibrate our model to perform a quantitative evaluation of the PEPP announcement, which then provides a basis for counterfactual analysis of alternative asset purchase policies.

4 Calibration

4.1 Quantitative model

To calibrate the model, we interpret the two countries in the union, Core and Periphery, as Germany (DE) and Italy (IT), respectively.[31] Since inflation and growth were relatively low in much of the euro period, especially in the effective lower bound (ELB) period, we calibrate the model in nominal terms, without adjusting for real GDP growth or inflation.

Multifactor model. For quantitative realism, we enhance the previous one-factor model with additional shocks. While a model where the risk-free rate r_t is the only

[30] As we saw earlier, our affine solution requires the default arrival rate to be deterministic.

[31] Taken literally, this means that arbitrageurs hold bonds of only one country with default risk, thus limiting the scope for diversification across issuers. One way to justify this implicit assumption would be a model extension with default contagion across several "peripheral" countries. Suppose investors expect that, if Italy defaults, then other periphery countries will default too; this perfect correlation across country-specific defaults would make diversification fruitless. Of course, in practice default is not *perfectly* correlated across euro area countries. But the very high correlation between, e.g., Italian and Spanish spreads suggests that market participants perceive a high probability that, if default happens, it will happen in both countries. Relatedly, we note that calibrating the two countries to Germany and France, on the one hand, and Italy and Spain, on the other, yields very similar results.

stochastic factor can fit the level of the yield curve and its responsiveness to the pandemic and the PEPP announcement, the implied yields are much less variable than those observed in the data.[32] To better fit the variance of yields, we now allow for two mean-zero factors, ε_t^h and ε_t^{h*}, that shift preferred-habitat demand for Periphery and Core bonds as follows:

$$\begin{aligned} Z_t(\tau) &= h(\tau) - \varsigma(\tau)\varepsilon_t^h + \tau\alpha(\tau)\left(y_t(\tau) - \hat{\delta}\psi_t\right), \\ Z_t^*(\tau) &= h^*(\tau) - \varsigma^*(\tau)\varepsilon_t^{h*} + \tau\alpha^*(\tau)y_t^*(\tau), \end{aligned} \tag{38}$$

where the functions $\varsigma(\tau), \varsigma^*(\tau) \geq 0$ represent the impacts of ε_t^h and ε_t^{h*} on demand for each maturity τ, respectively. We group the risk-free rate and the demand shifters into a vector of factors $q_t \equiv [r_t, \varepsilon_t^h, \varepsilon_t^{h*}]^\top$ that follows the process

$$dq_t = -K(q_t - \bar{r}\mathcal{E}_1)dt + \Sigma dB_t, \tag{39}$$

where K and Σ are 3×3 matrices, $\mathcal{E}_1 = (1,0,0)^\top$, and B_t is a 3×1 vector of independent Brownian motions.

We conjecture that there exist deterministic functions $(A_t(\tau), C_t(\tau))$ and $(A_t^*(\tau), C_t^*(\tau))$, where $A_t(\tau)$ and $A_t^*(\tau)$ are 3×1 vectors, such that bond prices are log-affine in q_t:

$$P_t(\tau) = e^{-\left[A_t(\tau)^\top q_t + C_t(\tau)\right]}, \; P_t^*(\tau) = e^{-\left[A_t^*(\tau)^\top q_t + C_t^*(\tau)\right]}. \tag{40}$$

This model can be solved by the same procedure as our earlier one-factor model. For details, see Online App. B.3.

Calibration strategy. To calibrate this multifactor model, we proceed in two steps. First, we calibrate a set of parameters that can be directly inferred from the data, including some monetary and fiscal variables that affect the bond market in a time-varying way. Using this information, we can construct a distance metric to evaluate the model's quantitative performance relative to yields data. Hence, in a second step, we calibrate the remaining parameters by minimizing this metric.

Numerical method. The numerical method is described in Online App. C.2.[33]

[32] The one-factor version of our model is analyzed in our earlier working paper, Costain et al. (2022).

[33] The actual numerical implementation is programmed both as a discrete-time system of difference equations, and as a finite-difference approximation to the original continuous time problem. Both implementations give the same results. Online App. C.3 describes the discrete-time method.

It requires first solving the stationary model under constant fiscal pressure, and then computing the transitional dynamics under alternative paths for fiscal pressure. Both cases can be characterized as systems of partial differential equations, which can be solved by the finite differences method.

As Hayashi (2018) has shown, in the Vayanos and Vila (2021) model there may be multiple equilibria. In this respect, we have tried different initial guesses when solving the stationary model, and our algorithm always converged to the same solution.

4.2 Observables

We extract data on one-month, one-year, five-year, ten-year, and twenty-year zero coupon yields on German and Italian sovereign bonds, and also the one-month euro overnight interest swap (OIS) rate from Datastream. We consider a sample from January 1999 to December 2022.

Short-term rates. We begin by calibrating the risk-free short rate process, r_t.[34] We interpret this rate as the yield on one-month zero-coupon German sovereign bonds. The German one-month rate is only available back to 2011; therefore we splice it to the corresponding one-month OIS rate for dates prior to 2011.[35] The spliced series has a mean of 122 basis points (bp) *per annum*, and its standard deviation is 179 bp. Running an AR(1) estimate on the monthly spliced series, we find that the monthly autocorrelation is 0.9948. We parameterize the Ornstein-Uhlenbeck process that governs the risk-free rate in our model for consistency with these statistics. In annualized terms, this implies $\bar{r} = 1.22\%$, $\kappa = 0.062$, and $\sigma = 63$ bp.

Fiscal variables and Eurosystem asset purchases. Solving our model also requires forecasts of fiscal variables and of Eurosystem asset purchases. We need forecasts both because the bond price solution from Sec. 2 depends on the current and future net bond supply held by arbitrageurs, and because the default arrival rate from Sec. 3 depends on the Peripheral government's current and future liquidity needs. We use forecasts from several different sources and vintages. We employ two-years-ahead

[34] The time unit in our numerical model is one month. However, in the main body of the text we report yields and describe the parameters in annualized terms, for ease of interpretation.

[35] Alternatively, we could calibrate the risk-free rate process directly to OIS rates over the whole sample. However, this would oblige us to model the differences between OIS rates and German rates. Therefore, to simplify our model of sovereign yields, we interpret short rates as sovereign rates too, as far as data availability permits.

public Eurosystem forecasts, and extend them using a Banco de España in-house debt sustainability analysis model to produce long time series on fiscal trends at annual frequency for Germany and Italy, including the total face value of sovereign debt, primary deficits, and interest charges.[36] We interpolate these data to monthly frequency for use in our simulations.

Regarding Eurosystem bond absorption under the APP, we construct ten-years-ahead projections of total Eurosystem holdings of German and Italian sovereign bonds, based on ECB announcements. Similarly, we derive a forecast for Eurosystem bond absorption under the PEPP, for forecast vintage March 2020, from the ECB's initial PEPP announcement at that time. Thus, subtracting predicted Eurosystem bond absorption from predicted bond supply, for each country, we can infer the total debt of each sovereign that must be absorbed by the private sector at any future time, looking forward from the date of any available forecast vintage.

Maturity distribution. The data discussed so far only address total quantitites of debt issued and absorbed in the model. To calculate yields, we must also specify how bonds are distributed across maturities. We make several assumptions to characterize debt maturity distributions in a tractable way. We assume a maximum maturity T of 20 years. From the ECB, we obtained data on the maturity distribution of Eurosystem holdings of German and Italian debt of up to 20 years' maturity, as of July 2021. We assume for simplicity that the maturity distribution of these holdings replicates the distribution of debt in the market.[37] Thus, we construct the density of these ECB holdings (middle panel of Fig. 2), at face value, across maturities τ, smoothing it by computing its moving average over windows of 25 months and then fitting a quadratic polynomial. We call this smoothed density function $g(\tau)$. The corresponding cumulative distribution of bond holdings is shown in the left panel of the figure. In our simulations, we suppose that the initial density of gross bonds outstanding is given by $g(\tau)$. Thus, given the initial debt levels D_0^* and D_0 of Germany and Italy, the initial bond supplies, as functions of maturity, are $f_0^*(\tau) = D_0^* g(\tau)$ and $f_0(\tau) = D_0 g(\tau)$, respectively. Similarly, we set the initial density of Eurosystem bond holdings (if nonzero) in proportion to $g(\tau)$ in both countries.

The time path of the distribution of net bond supply also depends on how issuances

[36] In particular, we employ an extension of the model introduced by Burriel et al. (2022).

[37] In practice, the maturity distribution of Eurosystem bond holdings broadly replicates that of the eligible universe, reflecting the "market neutrality" principle of Eurosystem asset purchases.

Figure 2: Cross-sectional asset distributions

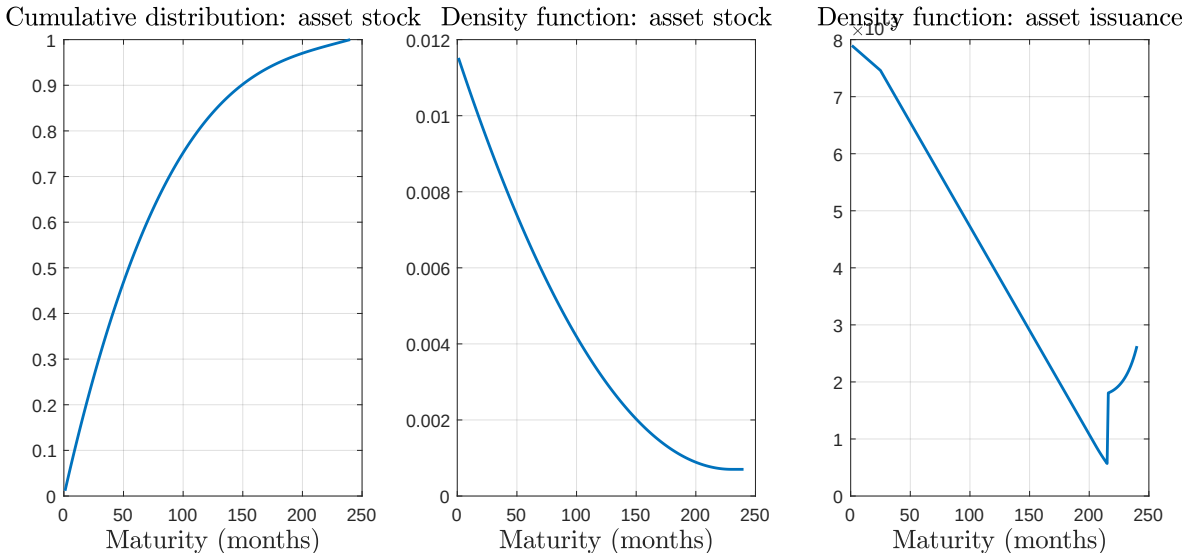

Data source: ECB data, smoothed by the authors..
Left panel: Cumulative distribution function, across maturities, of ECB holdings of German and Italian bonds, after smoothing.
Middle panel: Density, across maturities, of German and Italian bonds, approximated by a quadratic function. Called $g(\tau)$ in the text.
Right panel: Density of issuances, across maturities, that generates the PDF of the middle panel as the asset distribution in the long run. Called $\bar{\iota}(\tau)$ in the text.

and central bank purchases are distributed across maturities. We calculate the density $\bar{\iota}(\tau)$ of issuances across maturities that, if maintained at a constant rate, would generate the observed maturity distribution $g(\tau)$.[38] We assume that new bond issuances $\iota_t(\tau)$ are always distributed proportionally to $\bar{\iota}(\tau)$, which is shown in the right panel of Fig. 2. To reflect Eurosystem policy statements – which stated that purchases would reflect available supply – we assume that asset purchases are always distributed proportionally to $g(\tau)$.[39] Given these assumptions about the initial distributions and the distributions of issuances and purchases, together with forecasts of total face value at each point in time, we can trace forward the distributions $f^*_{t+s}(\tau)$, $f_{t+s}(\tau)$, $f^{CB,*}_{t+s}(\tau)$, and $f^{CB}_{t+s}(\tau)$

[38] The constant distribution of issuances $\iota(\tau)$ that generates maturity distribution $g(\tau)$ as a fixed point is simply $\iota(\tau) = -\frac{dg(\tau)}{d\tau}$. We have smoothed $\iota(\tau)$ with a moving window of 49 months, and rescaled it to obtain $\bar{\iota}(\tau) \equiv \frac{\iota(\tau)}{\int_0^T \iota(\tau)d\tau}$.

[39] The ECB refers to the principle of "market neutrality", that is, purchases should reflect the overall eligible market to ensure they do not distort the relative pricing of securities.

from the date t of any forecast vintage to any future horizon s.

Preferred-habitat demand. The average sovereign debt of Italy and Germany over the period 2013-2019, net of Eurosystem holdings, was 2,070 billion euros and 1,856 billion euros, respectively. To infer how much debt must be absorbed by arbitrageurs, we next calibrate preferred-habitat demand. Eser et al. (2019), Table 1, report that the fraction of net debt of the big-four euro area economies held by non-Eurosystem preferred-habitat investors was 41.4% in 2014, and 47.0% in 2018.[40] We consider the mean of these two figures – 44.2% of each country's net debt – , and calibrate the intercept terms $h(\tau)$ and $h^*(\tau)$ accordingly. That is, we scale the intercepts so that their sums across all maturities τ in steady state, $H \equiv \int_0^T h(\tau)d\tau = 927$ billion euros and $H^* \equiv \int_0^T h^*(\tau)d\tau = 820$ billion euros, equal 44.2% of Italy's and Germany's sovereign debt net of Eurosystem holdings in this period.

The impact of preferred-habitat investors also depends on how their demand is distributed across maturities. Lacking independent evidence on the distribution of preferred-habitat demand, we assume that each component of the demand functions $Z_t(\tau)$ and $Z_t^*(\tau)$ is proportional to $g(\tau)$. This assumption is not an unreasonable benchmark, since governments have an incentive to issue more of any given class of debt, relative to others, if there is more demand for that class of debt. Thus, for $\tau \leq T$, we set the intercepts to $h^*(\tau) = H^* g(\tau)$ and $h(\tau) = Hg(\tau)$, with zero demand for higher maturities. Analogously, we scale $\varsigma^*(\tau)$, $\varsigma(\tau)$, $\alpha^*(\tau)$, and $\alpha(\tau)$ in proportion to $g(\tau)$ as well (see Sec. 4.4 below). Under these assumptions, we can use market clearing (equations 7) to calculate the amounts that must be held by arbitrageurs at all times, across countries and maturities.

Default rates and haircuts. These assumptions also give us sufficient information to calculate the default rate. Knowing $f_{t+s}(\tau)$ and $f_{t+s}^{CB}(\tau)$ for each τ, we can calculate the net liquidity needs of the Italian government attributable to bond redemptions, $f_{t+s}(0) - \zeta f_{t+s}^{CB}(0)$. Also, the same fiscal forecasts from which we extracted the debt data allow us to calculate the Italian deficit d_{t+s} as the sum of its primary deficit and interest charges. Thus, given forecasts of a particular vintage t, we have all the monetary and fiscal information necessary to calculate fiscal pressure F_t from (37) and the default rate ψ_t from (36). Finally, we calibrate the default haircut to 25 percent,

[40] Eser et al. (2019) classify insurance companies and pension funds (ICPFs) and the official sector as preferred habitat investors.

$\delta = 0.25$, in light of international evidence.[41]

4.3 Constructing a distance criterion

The remaining parameters of our model are not directly observable. Therefore, we jointly calibrate them by minimizing a distance criterion that measures model fit. Our distance criterion assesses fit along two dimensions: (i) first and second moments of predicted yields on average, over the long run; ; and (ii) yield shifts in response to the PEPP announcement.

Long-run moments. For the first component of the distance criterion, we compare our full sample of yields (1999-2022) to the long-run distribution of yields in the model, when fiscal pressure is at its steady state value. Constant fiscal pressure implies that the default rate is also constant, $\psi_t = \underline{\psi}$, for some parameter $\underline{\psi}$ that will be included in the calibration. Using the analytical solution of the model's ergodic distribution, we calculate the sum of squared deviations between the model and the data for selected first and second moments:

- Mean yields on 1m, 1Y, 5Y, and 10Y DE bonds, and 1Y, 5Y, and 10Y IT bonds;
- The standard deviations of yields on 1m, 1Y, 5Y, and 10Y DE bonds, and 1Y, 5Y, and 10Y IT bonds;
- The correlations between 1Y and 10Y yields, for DE and IT bonds
- The cross-country correlation between 1Y yields, and the cross-country correlation between 10Y yields.

When calculating this sum of squared deviations, we express all yields and their standard deviations in annualized percentage points, and we express all correlations in percentage points. We abstract from 20-year bonds, and Italian 1-month bonds, since these are unavailable for the full sample; for German 1-month yields we use the spliced series of OIS and German rates described earlier.

PEPP announcement. The second component of the distance criterion measures the model's fit to the shift in yield curves that was observed after the PEPP announcement, in the context of the time-varying fiscal conditions that were then foreseen. The

[41] Cruces and Trebesch (2013) find haircuts on the order of 50% in evidence drawn mostly from emerging markets; for advanced economies we consider a smaller haircut more plausible.

PEPP was announced on March 18, 2020, with an initial purchase envelope of €750 bn.[42] The surprise nature of this announcement, in an emergency meeting of the ECB Governing Council, makes it easy to map this episode into our model.[43]

To evaluate the impact of the PEPP announcement, we use the ECB/Eurosystem projections of German and Italian gross debt around that announcement. For an initial time t that corresponds to March, 2020, we simulate a no-PEPP scenario, $\{f^{CB}_{t+s}(\tau), f^{CB*}_{t+s}(\tau)\}^{before}_{\tau\geq 0, s\geq 0}$, in which ECB bond holdings are determined by the earlier Asset Purchase Programme (including the expansion of APP on March 12, 2020), and a scenario $\{f^{CB}_{t+s}(\tau), f^{CB*}_{t+s}(\tau)\}^{after}_{\tau\geq 0, s\geq 0}$, in which the APP is complemented by PEPP purchases, as announced on March 18, 2020. We interpret the difference in yields between the two time-varying scenarios as the effect of the PEPP announcement. Both scenarios assume the same sequences $\{d_{t+s}, f_{t+s}(\tau), f^{*}_{t+s}(\tau)\}_{\tau\geq 0, s\geq 0}$ of deficits and gross bond supply, which are averages of fiscal forecasts from December, 2019 and June, 2020.[44]

Since the PEPP announcement permitted a flexible path of purchases, in contrast to the earlier APP, we must make some assumptions regarding arbitrageurs' expectations, in March 2020, about the eventual use of PEPP's margins of flexibility. Our scenario assumes that arbitrageurs anticipated PEPP purchases through June 2020 with perfect foresight – implying some frontloading, and some excess purchases of Italian debt, compared with Italy's capital key (the upper left panel of Fig. 7 graphs purchases in this scenario). We assume that from July to December, PEPP purchases were expected to accrue at a constant pace, up to the original PEPP envelope, while maintaining the

[42] The press release stated: "This new PEPP will have an overall envelope of €750 billion. Purchases will be conducted until the end of 2020 and will include all the asset categories eligible under the existing asset purchase programme (APP)." See https://www.ecb.europa.eu/press/pr/date/2020/html/ecb.pr200318_1~3949d6f266.en.html.

[43] We focus on the immediate effects of PEPP as it was originally announced in March, with an overall envelope of 750 billion euros to be spent over the course of 2020; these effects capture well the actual causal impact of the announcement, given its unexpected nature. Subsequent recalibrations of the PEPP purchase envelope (in June and December that year) were largely anticipated by the market, according to different surveys.

[44] To adequately capture expectations of future deficits and net bond supply in the early, pre-PEPP weeks of the pandemic crisis, we average across fiscal forecasts in the December, 2019 and June, 2020, ECB/Eurosystem projections. The June projections included an updated and quite pessimistic estimate of the impact of the pandemic, but were based partly on information that was not available to investors in mid-March. Thus, the average of the December and June fiscal projections provides a reasonable proxy of investors' expectations immediately ahead of the PEPP announcement.

deviations from capital key that were observed through June.[45]

We compare this model-generated shift in yield curves to the observed difference between the yields observed from 18 to 20 March, 2020, expressing all yields in annual percentage points. Hence the final component of our distance criterion is:

- The change in yields on 1m, 1Y, 5Y, 10Y, and 20Y DE and IT bonds from 18 to 20 March, 2020.

4.4 Minimizing the distance criterion

Functional forms. We now impose further functional form restrictions to reduce the number of free parameters we must estimate. First, we suppose that the distribution of the default cost, $\Phi(\chi)$, is uniform over an interval $[\underline{F}, \overline{F}]$ sufficiently wide to include all the fiscal scenarios we consider. Then, using equation (36), the default rate can be written as

$$\psi_t = \underline{\psi} + \theta \left(F_t - F_{ss} \right). \tag{41}$$

where $\theta \equiv \eta/(\overline{F} - \underline{F})$ equals the arrival rate η of a rollover crisis times the density $1/(\overline{F} - \underline{F})$ of the uniform distribution Φ, and $\underline{\psi}$ is an intercept term associated with the average fiscal pressure F_{ss}. Hence the default arrival rate has two parameters: its intercept, $\underline{\psi}$, described above, and its slope, θ.

Second, we assume that the impact of preferred-habitat demand shocks across different maturities τ is proportional both to $g(\tau)$, and to each country's steady-state debt stock, by setting $\varsigma^*(\tau) = \frac{H^*}{H^*+H} g(\tau)$ and $\varsigma(\tau) = \frac{H}{H^*+H} g(\tau)$. They also have the same autoregressive coefficient κ_h in the two countries. We also allow for correlation across the countries' bond demand shocks, but assume these are independent of the risk-free rate. Under these assumptions, the matrices K and Σ can be written as

$$K = \begin{bmatrix} \kappa & 0 & 0 \\ 0 & \kappa_h & 0 \\ 0 & 0 & \kappa_h \end{bmatrix}, \quad \Sigma = \begin{bmatrix} \sigma & 0 & 0 \\ 0 & \sigma_h & \chi_h \sigma_h \\ 0 & \chi_h \sigma_h & \sigma_h \end{bmatrix},$$

[45] Note that our simulation scenarios treat the PEPP envelope as a limit on the total face value of purchases. In reality, it limited the total market value of purchases. Assuming a limit on the face value instead simplifies our calculations, since it allows us to avoid a fixed point loop in bond prices and therefore to obtain an affine solution for yields.

where χ_h is the correlation between the Italian and German preferred-habitat demand innovations.

Finally, regarding the slope of preferred-habitat demand with respect to yield, we assume that it is also proportional to $g(\tau)$ over $[\bar{\tau}, T]$:

$$\tau\alpha(\tau) = \begin{cases} \alpha_h \varsigma(\tau), & \bar{\tau} \leq \tau \leq T, \\ 0, & \tau > T, \end{cases} \tag{42}$$

where $\bar{\tau}$ denotes one month, and T represents the maximum maturity of government debt, 20 years.[46] Likewise, for Core, we assume $\tau\alpha^*(\tau) = \alpha_h \varsigma^*(\tau)$ for $\bar{\tau} \leq \tau \leq T$, and $\tau\alpha^*(\tau) = 0$ at higher maturities.[47]

Parameters. This specification leaves us with nine model parameters to estimate, by minimizing the distance criterion defined in the previous subsection. Clearly, our distance metric overidentifies the nine parameters, as the number of moments (28) is much larger. The estimated parameter values are displayed in Table 1.[48] The estimated value of risk aversion γ is 0.0114. The long-run default rate is 75 bp *per annum*. The slope of the default rate θ is 1.9 bp per billion euros of additional fiscal pressure compared to the steady state. The effective discount rate in the fiscal pressure integral equals $\hat{r} + \phi = 35\%$ in annual terms.[49] The standard deviation of annual innovations to preferred-habitat (PH) demand is $\sigma_h = 87.6$ billion eur, with autoregressive coefficient $\kappa_h = 0.0048$ annually, implying that PH demand is highly volatile and persistent, almost Brownian motion. PH demand innovations are also highly correlated between IT and DE, with correlation coefficient 0.9997. Since $\int(\varsigma(\tau) + \varsigma^*(\tau))d\tau = 1$ by construction, an

[46] For values of τ less than one month, we define $\alpha(\tau) \equiv \alpha_h/\bar{\tau}$. From the perspective of our numerical results, this has no impact, since we do not perform simulations with a time step finer than one month. From an analytical point of view, it ensures that all integrals are bounded.

[47] Vayanos and Vila (2021) instead consider a specification where the slope with respect to yield is hump-shaped as a function of maturity: $\tau\alpha(\tau) = \tau\alpha \exp(-\delta_\alpha \tau)$, where α and δ_α are constants. Imposing this hump shape does not improve our model's fit to the data.

[48] Table 1 states the parameters in annualized terms. Table 4 in Online App. C.3 reports the parameters in the actual numerical model, which is programmed with a monthly time unit, but is quantitatively equivalent.

[49] This discount rate implies that our fiscal pressure measure (37) looks basically at a horizon of three to four years. This is plausible in our context, as it broadly coincides with the political cycle. Relatively high discount rates are not uncommon in the sovereign default literature; see for example Arellano (2008).

Table 1: Calibration

Parameters*	**Values**
γ: Risk aversion	0.0114
$\underline{\psi}$: Default rate intercept	75 bp
θ: Slope of default rate	1.9 bp / billion eur
$\hat{r} + \phi$: Discount rate in fiscal pressure	35 %.
κ_h: Coefficient of PH shocks	0.0048
σ_h: Coef. of volatility of PH shocks	87.6 billion eur
χ_h: Correlation between DE and IT PH shocks	0.9997
α_h: Slope of PH demand function	80 billion eur / p.p.
ζ: Remittance rule coefficient	1

interpretation of the PH demand coefficient α_h is that a 1pp across-the-board increase in yields causes an 80.0 billion eur rise in aggregate PH demand for IT and DE bonds. Finally, the estimated coefficient ζ in the remittance rule equals one, i.e., the distance minimization routine hits a corner solution at the upper bound we imposed on this parameter.

4.5 Model fit

Long sample. Our model reproduces many of the long-run patterns in the data, as Fig. 3 shows. The figure illustrates the fit of the model's ergodic distribution to first and second moments from our full sample period, 1999-2022.[50] The fit of the average yield curves is remarkably good for both countries. Furthermore, the standard deviation of yields in these long-run data is almost flat, independently of maturity. The calibrated model reproduces the volatility of short rates by construction, but also displays volatilities at long horizons that are similar to those at the short end, as is the case in the data. The upper panel of the figure also illustrates our yield decomposition. The left panel decomposes German yields into the expectations component $y_{ss}^{EX*}(\tau)$ and the term premium $y_{ss}^{TP*}(\tau)$.[51] The model slightly overpredicts the ten-year German term premium, which is 125 bp in the sample, versus 147 bp in the simulation. The model's overall

[50] The stars in Fig. 3 indicate the maturities that are included in the distance criterion to assess levels and standard deviations of yields.

[51] Notice that, under the assumed short-term rate process, the ergodic mean of the expectations component is constant across maturities at the level $y_{ss}^{EX*}(\tau) = \bar{r}$. Therefore, the ergodic mean of Core yields (net of $\bar{r}$) coincides with their model-implied term premium.

Figure 3: German and Italian yields: long-run behavior

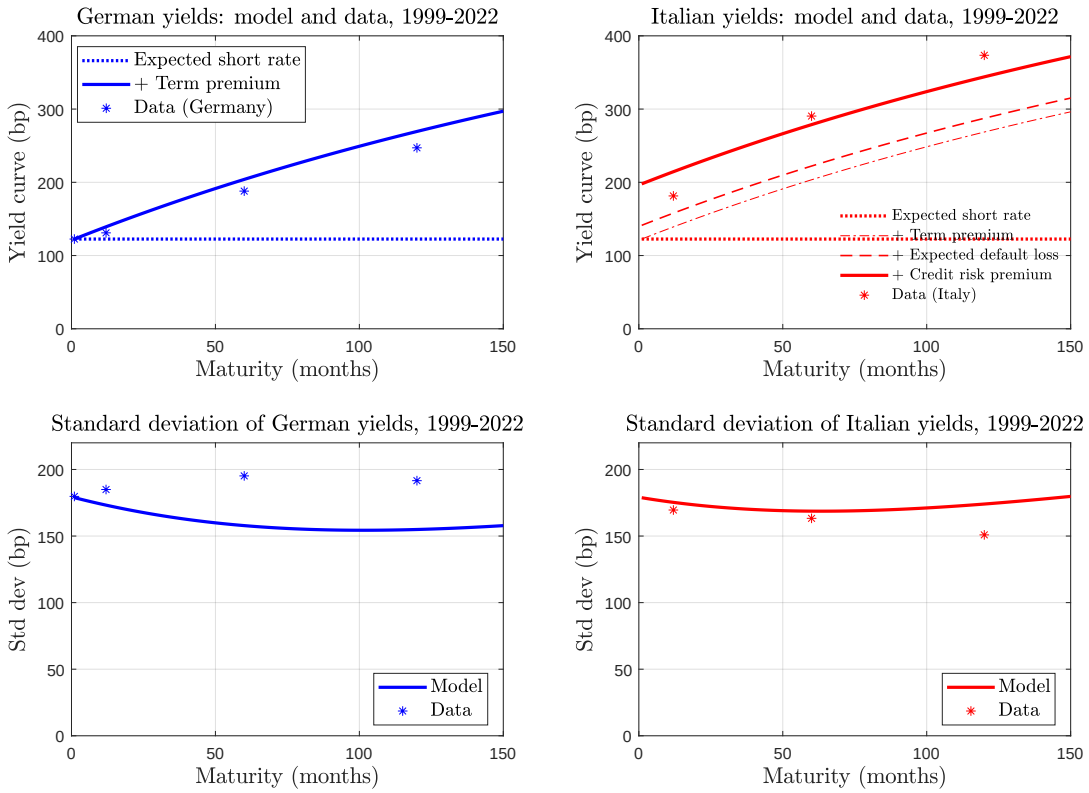

Data source: German and Italian yields (annualized, basis points) on zero-coupon 1m, 1Y, 5Y, and 10Y sovereign bonds from Datastream. German 1m yield is spliced to 1m OIS yield prior to 2011; Italian 1m yield unavailable.
Top row. *Stars*: average German (left) and Italian (right) sovereign yields, 1999-2022.
Lines: Decomposition of model-generated mean yields (solid), under the ergodic distribution, into expectations component (dotted) plus term premium (dash-dotted), plus expected default loss (dashed), plus credit risk premium.
Bottom row. *Stars*: standard deviations of German and Italian yields, 1999-2022.
Lines: model standard deviations of yields, under the ergodic distribution.

success in explaining the slopes of both countries' yield curves suggests that the degree of risk aversion γ is well calibrated, since this parameter strongly influences the term premium. As the right panel shows, the model-inferred Italian term premium $y_{ss}^{TP}(\tau)$ (dashed line) is almost identical to the German one, in line with Prop. 2, given that the ergodic default probability is relatively small. Hence, from Prop. 1, Italy-Germany sovereign spreads can be decomposed almost exactly into the other two components of the Italian yield curve: the expected loss due to default, $y_{ss}^{DL}(\tau) = \delta\underline{\psi}$ (the distance between the dash-dot and dashed lines), and the credit risk premium, $y_{ss}^{CR}(\tau) = \bar{\xi}$ (the

Table 2: Long-run moments: additional statistics

	Sharpe ratios*			
	1Y DE	10Y DE	1Y IT	10Y IT
Sharpe (data)	0.441	0.510	0.927	0.550
Sharpe (model)	0.590	0.601	0.275	0.272
	Long-short correlations		Cross-country correlations	
	DE1Y, DE10Y	IT1Y, IT10Y	DE1Y, IT1Y	DE10Y, IT10Y
Correlations (data)	0.9242	0.8568	0.9189	0.8289
Correlations (model)	0.8499	0.8666	0.9811	0.9869

Note. *The table reports the instantaneous Sharpe ratios $\mathbb{S}^*{}_t(\tau)$ and $\mathbb{S}_t(\tau)$, interpreting the time unit as one year, for $\tau = 1$ year and 10 years.

distance between the dashed and solid lines). Both objects are constant across maturities, as discussed in Sec. 2, and hence the spread is also constant across maturities at 75 bp. The spread decomposes into an expected default loss of 19 bp and a credit risk premium of 56 bp. That is, most (about 75%) of the Italian sovereign spread reflects, not the expected losses from default themselves, but how risk-averse investors price default risk (over and above expected default losses). Intuitively, Italy's fairly sizable sovereign spread in the euro period requires a substantial credit risk premium, given the rather moderate estimated level of default risk. Nonetheless, the bulk of Italian sovereign yields over the euro period is explained by expected future short rates and term premia, the more so the longer the maturity.

Table 2 reports additional statistics to further assess the goodness-of-fit to the sample data. We report one-year and ten-year German and Italian Sharpe ratios in the ergodic distribution of our model.[52] We also report correlations between 1-year and 10-year yields in each country, and cross-country correlations for 1-year bond yields and 10-year bond yields. The model predicts higher Sharpe ratios for Germany than for Italy, in contrast with the data. This discrepancy might be driven in part by a feature of the data that is absent in the model, namely the "convenience" of German bonds, which tends to lower their yields.

PEPP announcement. The other set of targets that define our distance criterion come from the impact of the 18 March 2020 PEPP announcement on German and Italian yields. As shown in Fig. 5, the fit of this episode is once again fairly good,

[52]The Sharpe ratios reported in the table are scaled for consistency with a time unit of one year. See Online App. C.3.5 for details on computing these ratios in the data and in the model.

despite the model's parsimony. We defer the detailed discussion of this event and how our time-varying solution explains it to Sec. 5.

Pandemic shifts. Finally, we evaluate how well the model explains the shift in yield curves that was observed during the Covid-19 pandemic outbreak in Europe. Specifically, we model the shift in yields from February to March, 2020, using data from the nearest available forecast vintages. As these observations have *not* been used in the distance criterion, this exercise serves as a useful out-of-sample test.

We model the main impact channel of the pandemic on euro area yield curves, going through governments' increased deficits and debt issuances to finance their pandemic responses.[53] Using fiscal forecasts from December 2019 (based again on Burriel et al., 2022), and Eurosystem portfolio projections from the same date, we construct monthly pre-outbreak forecasts of fiscal conditions, following the methods discussed earlier. In particular, we calculate the anticipated net supplies of German and Italian bonds, $f^*_{t+s}(\tau) - f^{CB,*}_{t+s}(\tau)$ and $f_{t+s}(\tau) - f^{CB}_{t+s}(\tau)$, for each s and τ, and the anticipated path of fiscal pressure $\{F_{t+s}\}_{s\geq 0}$ facing Italy, for each s, from the point of view of the pre-pandemic forecast date t.[54] To construct a post-outbreak forecast, we use the average of the December 2019 and the June 2020 forecast vintages.[55]

Just as we did to model the impact of PEPP, here again we calculate anticipated net bond supplies, and anticipated fiscal pressure on Italy, conditional on the post-outbreak forecast, and we calculate how yields change due to this update in fiscal forecasts. Fig. 4 compares the model-generated shift in yield curves to the difference between the average yields observed over the week of 13-19 February 2020, and the average yields observed over the week of 12-18 March 2020 (which is exactly four weeks later, and precedes the announcement of the PEPP).

The right panel of the figure shows that the change in fiscal expectations associated with the pandemic generates a large upward shift in Italian yields in our model (red curves), of the same order of magnitude as the shift observed in bond markets from February to March 2020 (red stars). The model overpredicts somewhat the market

[53] We also consider an initial shock to the short-term rate, in line with the observed fall in the yield of 1-month DE bonds from February to March, 2020.

[54] We drop the first three months of the series so that they can be interpreted as forecasts from March 2020 onwards, without knowledge of the pandemic.

[55] The post-outbreak scenario coincides, by definition, with the pre-PEPP scenario we described earlier, in Sec. 4.2.

Figure 4: Impact of the pandemic outbreak: German and Italian yields, Feb.-Mar. 2020

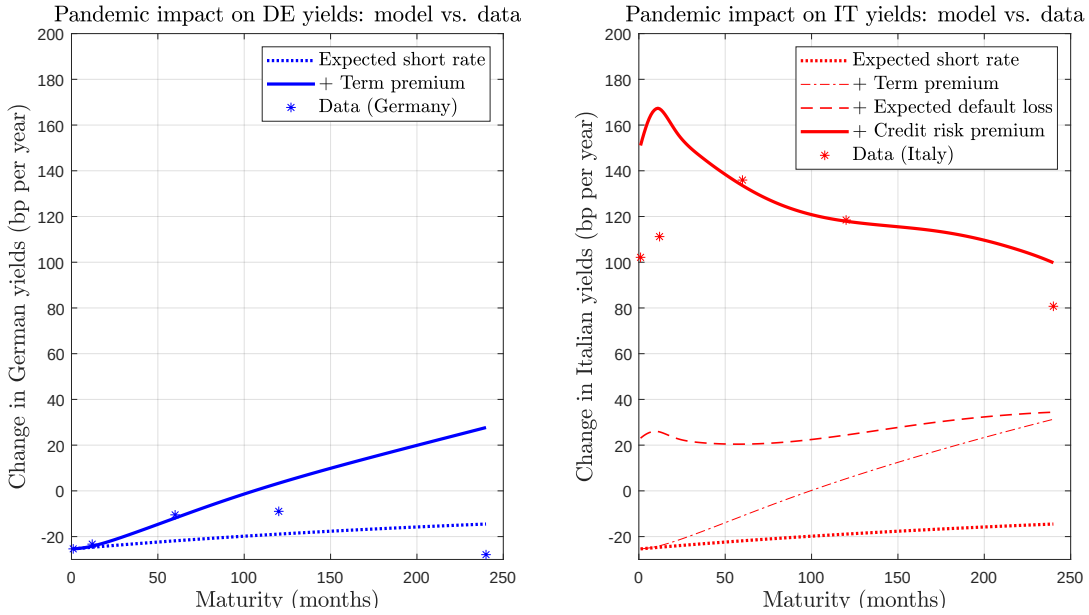

Data source: German and Italian yields (annualized, basis points) on zero-coupon 1m, 1Y, 5Y, 10Y, and 20Y sovereign bonds from Datastream.
Stars: Shift in weekly average German yields (left) and Italian yields (right) from week of 13-19 February 2020 to week of 12-18 March 2020.
Lines: Model-generated change in yields in response to revised fiscal expectations associated with the pandemic (solid), decomposed into expectations component (dotted), plus term premium (dash-dotted), plus expected default loss (dashed), plus credit risk premium.

reaction at the shortest maturities, and for 20-year bonds. Most importantly, our model generates an upward shift across all maturities of Italian yields, a feature that cannot be explained by a standard model without default. Our results show that, viewed through the lens of our model, the pandemic shock represented an increase in the expected default loss due to the new fiscal scenario, as well as an (even larger) increase in the the credit risk premium.

5 PEPP announcement and policy counterfactuals

As the pandemic took hold in Italy, Spain, and the rest of Europe, it became clear that a massive fiscal response would be needed, implying higher expected gross debt levels. Shortly thereafter, the PEPP announcement revealed that much of this new debt would be taken onto the Eurosystem's balance sheet. In standard (no default) models

of risk-averse arbitrageurs, these changes in net supply would steepen the yield curves as the pandemic spread, and flatten them when PEPP was announced, *via* changes in term premia. But in our model, their impact is reinforced by several additional effects related to default. On one hand, a reduction in the net supply of defaultable bonds $S_t(\tau)$ shrinks the credit risk premium $y_t^{CR}(\tau)$ that markets demand to hold those bonds. This effect operates even if the default probability is exogenous. On the other hand, with endogenous default, purchases increase future redemptions of central bank-held Periphery bonds, $f_{t+s}^{CB}(0)$, and hence reduce the default probability (both at t and at future times $t+s$). This lowers the expected default loss $y_t^{DL}(\tau)$ and also reinforces the fall in the credit risk premium.

5.1 The PEPP announcement

Benchmark case. The results of our benchmark PEPP simulation are shown in Fig. 5, where stars in the top panels indicate the observed change in yields between March 18 (pre-announcement) and March 20, 2020 (after the PEPP announcement).[56] The blue stars in the top left panel show that the PEPP announcement had a small, non-monotonic impact on German yields, which rose for one-year bonds and fell at five- to twenty-year maturities. In contrast, Italian yields fell dramatically (top right panel, red stars), with a hump-shaped decline that had its largest impact, of 86 bp, on five-year bonds. Hence, across all maturities, the announcement was associated with a large reduction in average eurozone bond yields, and a sharp drop in cross-country differentials.

Our simulation is based on the parameter estimate shown in Table 1, conditional on the purchase scenario illustrated in the top, left panel of Fig. 7. The model does a good job of reproducing the shifts in both countries' yield curves, and allows us to decompose the mechanisms behind the shifts The model predicts a small decline in the German term premium in response to the PEPP announcement, of roughly 10 bp for ten-year bonds and 11 bp for 20-year bonds.[57] Consistently with Prop. 2, the inferred effect on the Italian term premium is similar. However, the sovereign spread on Italian

[56] We take the change from March 18 to 20 as our measure of the impact of the PEPP announcement, because yields were still volatile across Europe on the 19th, but settled down from the 20th onwards.

[57] Since the model treats the riskless short rate as an exogenous factor, changing the path of purchases has no impact on the expectations component $y_t^{EX}(\tau)$.

Figure 5: Effects of PEPP announcement: baseline scenario ($\zeta = 1$).

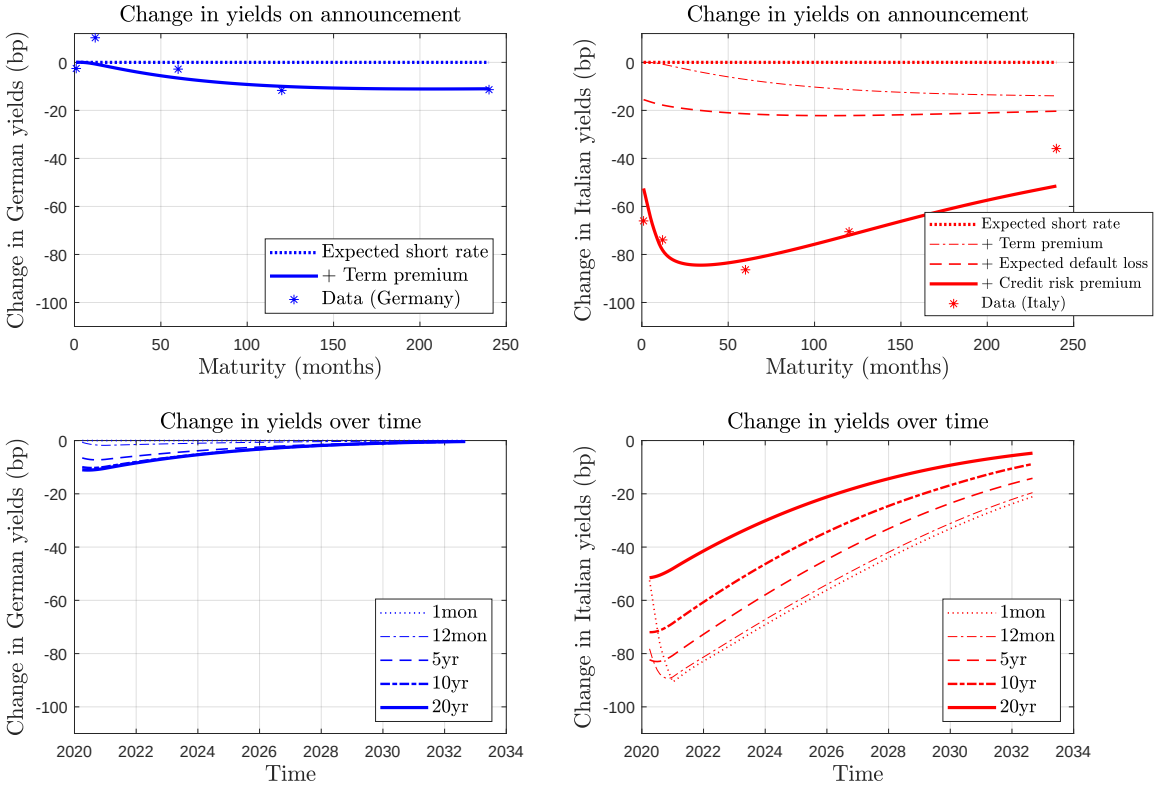

Data source: German and Italian yields (annualized, basis points) on zero-coupon 1m, 1Y, 5Y, 10Y, and 20Y sovereign bonds from Datastream.
Top row. *Stars*: Shift in German (left) and Italian (right) yields, 18 to 20 March, 2020.
Lines: Model-generated shift in yields upon PEPP announcement (solid), decomposed into expectations component (dotted) plus term premium (dash-dotted), plus expected default loss (dashed), plus credit risk premium.
Bottom row. Model-generated impulse response of 1m, 1Y, 5Y, 10Y and 20Y yields in response to PEPP announcement.

debt declines sharply, first of all because the increased absorption of credit risk makes the market much more willing to take part of this risk into its own hands. Moreover, the PEPP announcement reduces the default probability substantially, as can be seen inthe expected default loss component, with a maximum impact of 17 bp on Italian bonds of two years' maturity or less. The reduction in the default probability in turn reinforces the compression in credit risk premia. Thus, the model suggests that the extraction of defaultable bonds from the market, together with the resulting reduction in their default risk, jointly caused a large decrease in the credit risk premium $y_t^{CR}(\tau)$,

accounting for the lion's share of the response to the announcement.

Italian yields decline upon the announcement at all maturities, but the reduction is strongest for bonds of intermediate duration, which will be maturing when cumulative net purchases are still large. In contrast, one-month bonds mature before many purchases have taken place. At the opposite extreme, for 20-year bonds, most net redemptions will have occurred, and hence yields will be normalized again, by the time the bonds mature. Since yields are forward-looking, the future return to normality limits the change in longer yields on impact.

Beyond its powerful effect at announcement, the model also predicts that PEPP's impact should be persistent over time. The bottom panels of Fig. 5 illustrate the impulse responses of yields to the announcement, for selected maturities, assuming that the purchase program unfolds as expected under our baseline scenario. The small decrease in German yields (left panel) mostly affects long bonds, and decays smoothly. The much larger reduction in Italian yields (right panel) is very persistent, but differs across durations. The shortest yields fall steadily over the course of 2020, because the quantity of short bonds held increases over that period, accumulating new purchases with bonds purchased earlier at slightly greater maturity. The maximal impact on short yields, of over 90 basis points, occurs just as gross purchases cease. From this time onwards, the whole portfolio gradually matures, causing the effects on 20- and 10-year bonds to fade away smoothly over time. The decrease in 20-year yields from 2021 onwards (i.e., after the end of the net purchase phase envisioned in the March 2020 announcement) is only due to arbitrage across durations, not because the program still holds any bonds with a 20-year residual maturity. As the average maturity of the PEPP portfolio shortens, its impact on long yields fades away, followed by its impact on short yields. The final effects of the program disappear as the last bonds mature, 240 months after the end of gross purchases.

The low-remittances scenario. As explained in Sec. 4.4, our baseline calibration includes an estimated coefficient $\zeta = 1$ in the remittance rule (35). While the yield data seem to favor that parameterization, it is instructive to consider alternative calibrations for ζ, which gauges the strength with which asset purchases affect the Peripheral default probability. For clarity we consider the simple, polar-opposite case $\zeta = 0$, representing a scenario in which the central bank would *not* provide any income support during a rollover crisis (over and above net transfers in the amount $-\bar{\Gamma}$). This case clarifies the analysis by shutting down any impact of asset purchases on default risk.

Figure 6: Effects of PEPP announcement: low-remittances scenario ($\zeta = 0$).

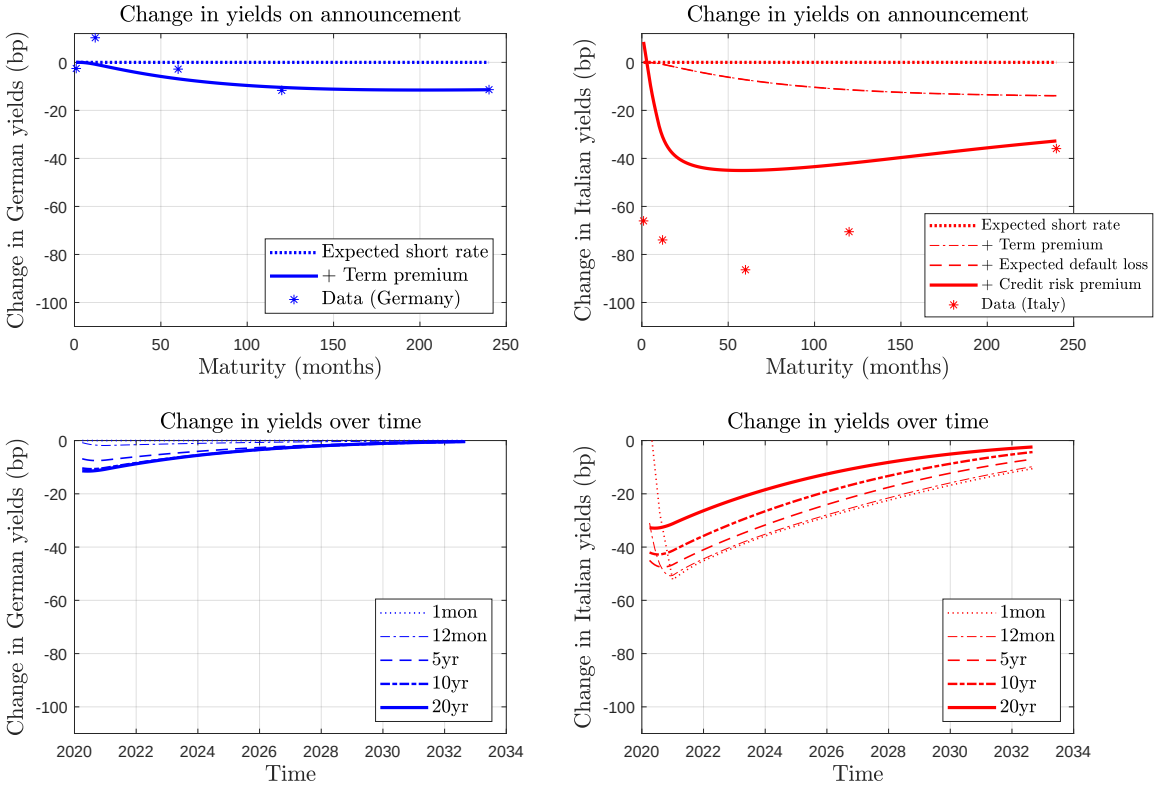

Data source: German and Italian yields (annualized, basis points) on zero-coupon 1m, 1Y, 5Y, 10Y, and 20Y sovereign bonds from Datastream.
Top row. *Stars*: Shift in German (left) and Italian (right) yields, 18 to 20 March, 2020.
Lines: Model-generated shift in yields upon PEPP announcement (solid), decomposed into expectations component (dotted) plus term premium (dash-dotted), plus expected default loss (dashed), plus credit risk premium.
Bottom row. Model-generated impulse response of 1m, 1Y, 5Y, and 10Y yields in response to PEPP announcement.

Fig. 6 displays the results in this case. The fit to the Italian yield curve movement worsens relative to the baseline calibration, as the expected default loss does not change and the impact on the credit risk premium is smaller in this case. Nonetheless, the overall response is still large, and qualitatively similar, except at the very shortest end. As it seems unlikely that central banks would fail to provide any income support to their treasuries during a rollover crisis, we can view this scenario as a lower bound on the impact of large-scale asset purchases in the euro area. It shows that credit risk extraction remains a relevant channel of impact on defaultable bonds even if purchases

have no effect on the default probability itself.

5.2 Counterfactuals: flexibility and effectiveness of purchases

Since our model matches the impact of PEPP well, across jurisdictions and maturities, it may also serve as a useful tool for evaluating how the PEPP's flexible design altered its impact, by comparing it to some counterfactual scenarios. Fig. 7 illustrates four of the scenarios we will compare, showing cumulative purchases at face value, in billions of euro, over months 3-12 (indicating March-December, 2020). All panels show German and Italian purchases as blue lines with circles, and red lines with squares, respectively; their sum is shown as a black line.

The top, left panel shows the baseline scenario that we used in Sec. 5.1 as a stand-in for expectations about the PEPP upon its announcement. The path of purchases up to the end of June represents actual PEPP purchases, which accumulated almost linearly over time, at a pace that, if continued, would have exhausted the envelope before the end of the year. As a fraction of the monthly total, Italian purchases exceeded Italy's capital key, while purchases of German bonds were close to capital key (purchases of French bonds were substantially below capital key). Since our scenario is intended to model the effects of the initial announcement, we abstract from the actual path of purchases after June (when a recalibration of the PEPP purchase envelope was announced), and instead suppose that purchases from July onwards would use up the remaining PEPP envelope at a constant pace, while maintaining the initial deviations in capital key.

APP-style purchases. We now compare our PEPP scenario to a counterfactual alternative based on the inflexible design principles of the longer-standing Asset Purchase Programme (APP). That program imposed a constant pace of purchases over a pre-specified period of time, and allocated purchases according to each eurozone state's capital key. Following these principles, we design a hypothetical "APP-style" purchase announcement whereby the ECB would have committed to the same overall envelope, but would have distributed the purchases linearly over time, allocating them in proportion to the German (26.4%) and Italian (17.0%) capital keys.[58] This comparison is illustrated in the top, right panel of Fig. 7. Dashed lines represent the APP-style scenario, while solid lines represent our benchmark PEPP scenario (the color coding is

[58] While the total PEPP envelope was 750 billion euros, we only analyze the part that was dedicated to sovereign bonds (608 billion), abstracting from private-sector and supranational purchases.

Figure 7: Baseline purchase scenario and counterfactual experiments.

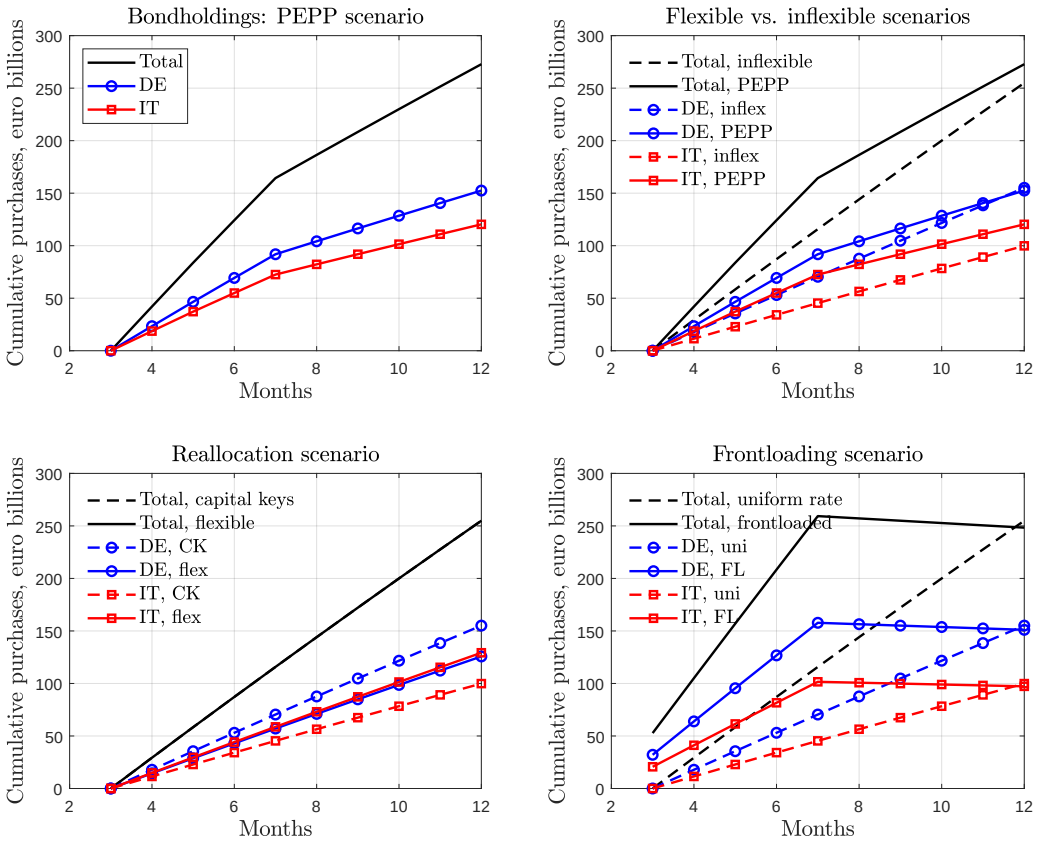

Top, left panel: Baseline model scenario for PEPP purchase expectations as of March 2020. Blue circles: DE; red squares: IT; black: aggregate face value. Effect on yields is shown in Figs. 5-6.
Top, right panel: Comparing baseline PEPP scenario vs. inflexible "APP-style" scenario with a constant pace of purchases and allocations equal to capital keys. Blue circles: DE; red squares: IT; black: aggregate face value. Effect on yields is shown in Fig. 8.
Bottom, left panel: Comparing "APP-style" scenario with a scenario that reallocates purchases by ±5%. Blue circles: DE; red squares: IT; black: aggregate face value. Effect on IT yields is shown as a blue dotted line in Fig. 9.
Bottom, right panel: Comparing "APP-style" scenario with a "frontloading" scenario that completes all purchases by July. Blue circles: DE; red squares: IT; black: aggregate face value.

the same as before). Clearly, our PEPP scenario imposes frontloading, with an initial pace of purchases faster than the APP design would permit. Simultaneously, the PEPP scenario allocates more purchases to Italy than the APP design would, while total purchases of German debt in the PEPP scenario are similar to those in the APP scenario

(close to capital key).[59]

Figure 8: Comparing impact of PEPP scenario with "inflexible" alternative

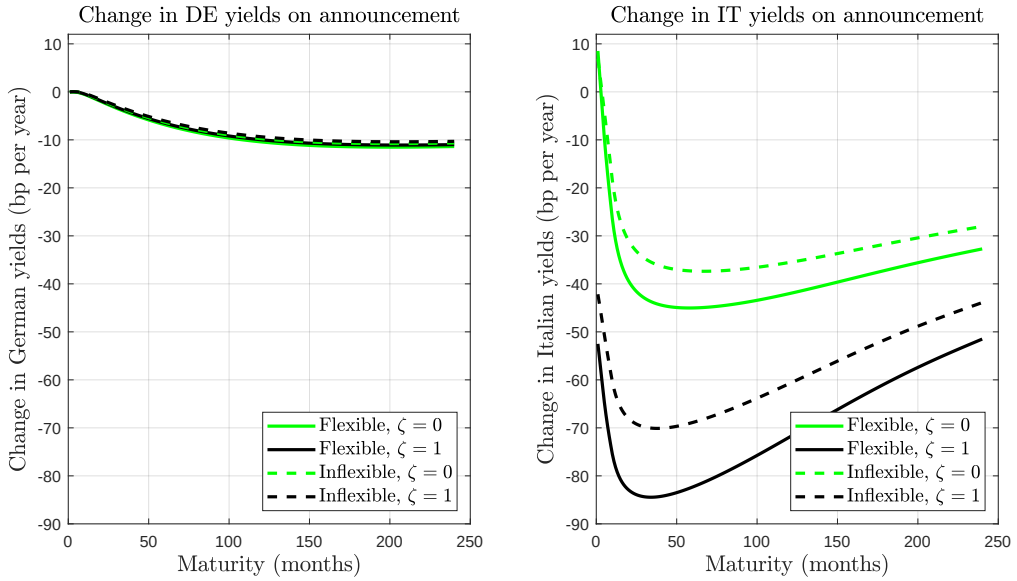

Left panel: model simulations of Germany. *Right panel*: model simulations of Italy.
Panels show the model-generated impact of the PEPP announcement (solid lines) and an "APP-style" scenario (dashed lines) that imposes a constant pace of purchases and allocations equal to capital keys, as illustrated in top, right panel of Fig. 7.
Black lines: full pass-through of bond redemption income ($\zeta = 1$) to the Peripheral treasury.
Green lines: zero pass-through ($\zeta = 0$).

Fig. 8 compares the effects of the purchases under the PEPP and APP designs, showing that the former reduces yields more than the latter, in both countries and at all maturities. The left panel refers to Germany, while the right panel refers to Italy. The PEPP design causes a tiny extra reduction in German yields, by 1 bp at longer maturities, compared to the APP-style program. The reduction in yields is much more significant in the Italian case, where PEPP shifts the yield curve by up to 14 additional basis points, exceeding 10 bp at almost all maturities, compared with the APP design. Most of the difference between the PEPP and APP designs is attributable to a decline in the credit risk premium (not shown). In the counterfactual low-remittances scenario ($\zeta = 0$) this difference in impact across program designs is reduced, but still significant.

[59]Hence total PEPP purchases (black solid line) end up slightly above the intended envelope (black dashed line) since our two-country simulation abstracts from the jurisdictions where purchases were lowest, relative to capital key.

Effects of flexibility in cross-country allocation and timing. Which aspect of the flexibility of PEPP is most important for its stronger impact on yields, as compared with an APP design? Our next experiments seek to disentangle the role of flexibility in the cross-country allocation of purchases from flexibility in their timing. On one hand, we construct a scenario of *cross-country reallocation* alone, illustrated in the bottom, left corner of Fig. 7. Taking the APP design as a starting point (solid lines), it considers the impact of reallocating purchases worth five percentage points of the overall PEPP envelope from Germany to Italy (dashed lines), leaving total purchases unchanged. On the other hand, we also construct a scenario of *frontloading alone*, illustrated in the bottom, right panel of Fig. 7. In the frontloading scenario (dashed lines), all purchases are realized in the first five months of the purchase program, unlike the APP scenario (solid lines), where the pace of purchases is constant through December 2020.[60]

Fig. 9 illustrates the effects of the two dimensions of flexibility, and their interaction. The blue dotted line in the left panel of Fig. 9 documents the effect of *cross-country reallocation* alone. The impact on Italian yields is striking. Reallocating 5% of the PEPP envelope causes a large, persistent decrease in Italian yields, of up to 19 bp. In contrast, the impact on German yields (not shown) is negligible, as we saw earlier in Fig. 8. These results again reflect Prop. 2, which showed that with low default risk, term premia are essentially driven by the overall quantity of purchases, not their jurisdictional distribution. Since the expectations term is unaffected by purchases in our model, we can furthermore conclude that if Italian default risk is low, then the German yield curve is determined by the total quantity of purchases, regardless of how those purchases are distributed. But for Italy, country-specific purchases are crucial for yields, because decreasing free-floating default risk makes the market more willing to hold this risk. Hence, from the point of view of reducing average euro area yields, reallocating purchases from Germany to Italy makes the purchase program more effective. In other words, flexibility in allocation across countries is an important factor in explaining the effectiveness of the PEPP design.

The green dashed line in the left panel of Fig. 9 sums the impact of the frontloading scenario with the impact of cross-country reallocation scenario (represented by the blue dotted line discussed above). Frontloading causes a tiny decrease, on impact, in the German yield curve (not shown). For Italy (left panel of Fig. 9) it causes a significant

[60] Thus, the degree frontloading in this exercise is substantially stronger than the mildly accelerated purchase pace seen in our baseline PEPP scenario.

Figure 9: Effects of flexibility in cross-country allocation and timing on Italian yields

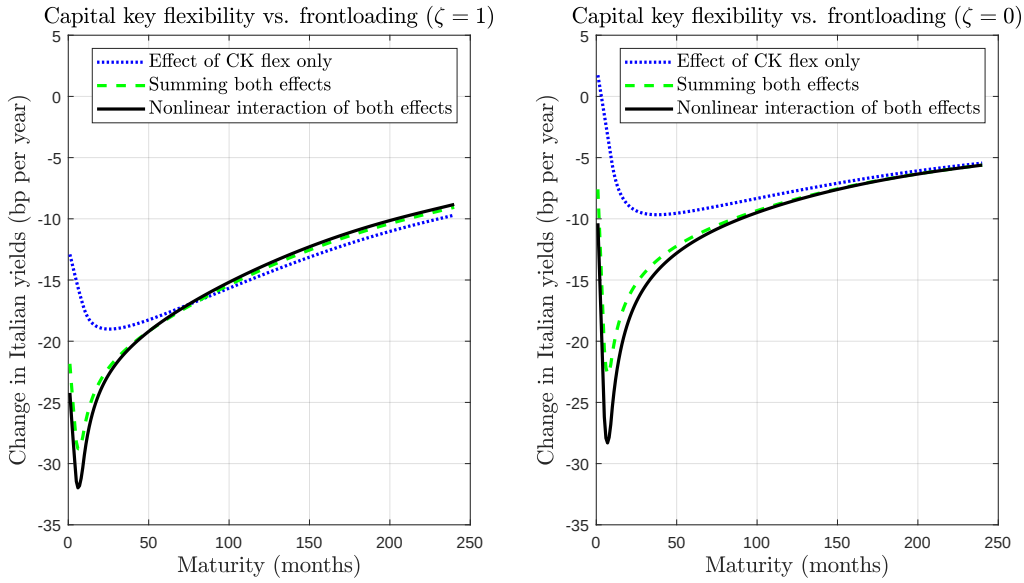

Left panel. Effects of flexibility on Italian yields, assuming high pass-through of bond redemptions to Italian treasury ($\zeta = 1$).
Right panel. Effects of flexibility on Italian yields, assuming low pass-through of bond redemptions to Italian treasury ($\zeta = 0$).
Blue dotted lines: effect of cross-country reallocation (reallocating 5% of the total PEPP envelope from Germany to Italy).
Green dashed lines: summing the effect of cross-country reallocation, plus the effect of frontloading all purchases to the first four months.
Black solid lines: simultaneous implementation of cross-country reallocation and frontloading.

decrease in short yields on impact, of more than 10 bp for six-month maturities, but at the same time, it increases yields on bonds of maturities greater than 6 years. Frontloading implies a faster pace of purchases early in the program, but by the same token it implies a slower pace later, and eventually causes the whole portfolio to mature earlier. Hence, the impact of frontloading over time is a sharp decrease in most yields at the beginning of the program, but a small increase later, when the portfolio matures.

Thus, reallocation can have a big impact on Italian yields, with negligible effects on German ones, while frontloading trades off a large decrease in short-term Italian yields against a small increase in longer Italian yields. But how do these policies interact? In contrast to the green dashed line, which simply sums the impacts of the two forms of flexibility, the black solid line in the left panel of Fig. 9 instead shows the joint, nonlinear effect of a policy that combines reallocation from Germany to Italy (as in the lower,

left panel of Fig. 7) with frontloading over time (as in the lower, right panel of Fig. 7). Hence, the difference between the black solid line and the green dashed line shows that reallocation and frontloading interact in a nonlinear way. Combining reallocation with frontloading decreases short yields by up to 32 basis points, while the impact of the two policies separately sums to only 29 basis points for the same maturities. We conclude that flexibility across jurisdictions and flexibility across time are complements, rather than substitutes: each aspect of flexibility contributes individually to the peak effectiveness of asset purchases, and more so jointly.

The right panel of Fig. 9 repeats this exercise for the counterfactual low-remittances scenario, $\zeta = 0$. While the overall impact is quite similar to the baseline, the impact of flexibility in capital allocation is diminished, as purchases have no effect on the default probability, whereas that of flexibility in timing is amplified.

5.3 Robustness

Our results indicate that the overall compensation for peripheral default risk in the euro area context is driven primarily by a credit risk premium component which is substantially larger than the expected loss due to default, and also reacts more to Eurosystem asset purchases. Table 3 explores the robustness of this conclusion to alternative parameterizations. The third column reports the contribution of the mean credit risk premium $\mathbb{E}y_t^{CR}(\tau)$ as a fraction of the total compensation for default risk, $\mathbb{E}\left(y_t^{CR}(\tau) + y_t^{DL}(\tau)\right)$, for bonds of maturity τ equal to 10 years, under the ergodic distribution. The fourth column does the same for the contribution of the credit risk premium to the *change* in the compensation for default risk, $\Delta y_t^{CR}(\tau) / \left(\Delta y_t^{CR}(\tau) + \Delta y_t^{DL}(\tau)\right)$, induced by the announcement of PEPP, in our model's time-varying solution conditional on the fiscal conditions of March 2020.

The main message from the table is that our key result is remarkably robust. Under most parameterizations considered, the credit risk premium accounts for roughly three-quarters of the total compensation for default risk, in levels, in the model's ergodic distribution. The credit risk premium is even more important in the context of the PEPP announcement, with a contribution over 80% in those same parameterizations.

The table also identifies extreme calibrations for which our main result disappears, in the sense that the contribution of the credit risk premium decreases relative to that of the expected default loss until the two are roughly balanced, either in the long run

Table 3: Robustness

Calibration	Model fit[a]	Credit risk prem. contribution[b]		Mean yields[c]		Standard deviation[c]		Sharpe ratio		PEPP impact[c]
		Long-run	PEPP	DE	IT	DE	IT	DE	IT	IT
Data	-	-	-	247	373	192	151	0.51	0.55	-71
Benchmark*	0.735	0.75	0.82	269	344	155	174	0.60	0.28	-72
Parameters calibrated directly from observables										
$\kappa \times 1.5$	1.111	0.75	0.82	245	321	134	154	0.55	0.27	-71
$\kappa \div 1.5$	0.786	0.75	0.82	289	363	171	190	0.64	0.27	-73
$\sigma \times 1.25$	2.989	0.75	0.82	340	413	203	223	0.72	0.27	-76
$\delta = 0.1$	2.889	0.55	0.69	271	288	156	158	0.61	0.13	-25
$\delta = 0.05$	3.796	0.38	0.53	272	278	156	156	0.61	0.11	-16
Parameters estimated by minimizing the distance criterion										
$\gamma \times 1.25$	1.353	0.79	0.84	303	391	166	193	0.74	0.34	-84
$\gamma \div 3$	5.596	0.51	0.64	173	211	135	137	0.21	0.094	-34
$\gamma \div 6$	8.538	0.34	0.49	146	175	133	134	0.11	0.048	-23
$\underline{\psi} \times 1.25$	0.837	0.75	0.82	269	362	155	179	0.60	0.30	-72
$\overline{\theta} \times 1.25$	0.815	0.75	0.81	269	344	155	174	0.60	0.27	-84
$(\hat{r} + \phi) \times 1.25$	0.777	0.75	0.82	269	344	155	174	0.60	0.27	-63
$\varsigma_h \times 1.25$	0.837	0.75	0.82	271	347	170	198	0.61	0.27	-74
$\kappa_h \times 1.25$	0.750	0.75	0.82	269	344	150	165	0.60	0.27	-72
$\chi_h \div 1.25$	0.748	0.75	0.82	269	343	150	165	0.60	0.27	-71
$\alpha \times 2$	1.080	0.73	0.79	246	313	145	160	0.52	0.25	-60
$\alpha \div 2$	0.854	0.76	0.84	284	363	161	183	0.65	0.29	-82
$\zeta = 0$	1.682	0.75	1.00	269	344	155	174	0.60	0.27	-42

Notes. *The benchmark calibration is described in Table 1. The following rows each describe the effect of changing one parameter by the stated amount, relative to its benchmark value.
[a]"Model fit" refers to the sum of squared deviations of the statistics, expressed in percentage points, listed in the bullet points in Sec. 4.3.
[b]"Credit risk contribution" means the contribution of the credit risk premium as a fraction of the 10-year sovereign spread, both in the long run and in response to the PEPP announcement.
[c]Annual yields on 10-year bonds, expressed in basis points.

or in response to the PEPP announcement. Reducing the risk aversion coefficient γ to 1/3 of its baseline value implies a nearly balanced (51%) contribution of the credit risk premium in the stochastic steady state, and reducing it to 1/6 of its baseline calibration implies that the two components of default risk compensation respond roughly equally to the PEPP announcement. Intuitively, it takes an extremely low degree of risk aversion to make the credit risk premium as small as the expected default loss.

Likewise, haircuts δ as low as 0.1 and 0.05 reduce the contribution of the credit

risk premium to roughly one-half in steady state, and in the impact of the PEPP announcement, respectively. This reflects the fact that, as shown in Sec. 2, expected default losses and credit risk premia are proportional to δ and δ^2, respectively, so reducing the haircut lowers the latter more quickly than it does the former.

However, these low-risk-aversion and low-haircut calibrations are empirically implausible, substantially worsening model fit (see the second column of the table). By shrinking the credit risk premium, low γ and low δ both decrease the level of Italian yields and their responsiveness to PEPP; in addition, low γ shrinks the term premium, reducing all yields. Hence, in the last three columns of the table, we see that the low-γ and low-δ calibrations both imply a far smaller reaction of Italian 10-year yields to the PEPP announcement (from 16 to 34 bp) than the observed one (71 bp). They also predict much lower average yield levels than in the data, especially on Italian bonds (from 175 to 288 bp, vs 373 bp in the data). In sum, while there are parameters that overturn our key results, such calibrations considerably worsen the model's ability to explain yield data, both in the full sample period and in the PEPP episode.

6 Conclusions

In this paper, we propose a micro-founded model of the term structure of sovereign interest rates in a heterogeneous monetary union. We extend the Vayanos and Vila (2021) affine term structure model to a two-country monetary union where one of the two sovereign issuers (Periphery) faces default risk, due to the possibility of rollover crises. In addition to the standard and well-documented *duration risk extraction channel* of asset purchase programs, our model features a *default risk extraction channel*, whereby announcements of central bank asset purchases reduce both the expected amount of defaultable bonds the market must absorb and the sovereign default probability itself, thus reducing the compensation risk-averse investors require to absorb default risk.

We apply our model to analyze the impact of the ECB's pandemic emergency purchase programme (PEPP), announced in March 2020 in a context of rising expected issuance of euro area sovereign debt as a consequence of the Covid-19 crisis. We calibrate the model to data on German and Italian yields, by targeting the average shape of both countries' sovereign yield curves and the change in Italian yields over the two days following the PEPP announcement. Under the inferred parameters, the sovereign credit risk premium is larger than the expected loss due to default. We show analyt-

ically that under this parameter configuration, the term premium and hence German yields depend approximately on aggregate asset purchases, regardless of their cross-country distribution. In contrast, the Italian yield curve depends strongly on how asset purchases are allocated across countries. Quantitatively, we conclude that default risk extraction is the most significant channel to explain the response of the Italian yield curve to the PEPP announcement, much more so than duration extraction.

We then perform counterfactual simulations to evaluate how important the PEPP's flexible design was for its impact. A key feature of the PEPP was flexibility in the distribution of purchases over time and across jurisdictions. We find that the flexible allocation of purchases permitted by the PEPP design substantially enhanced its impact. The PEPP announcement reduces Italian yields by up to 86 bp in our simulations, of which 14 bp can be attributed to the flexibility of PEPP, as compared with a hypothetical announcement with the same overall envelope but an APP-style design (a constant pace of purchases, allocated across countries according to the ECB's capital key). Overall, since the impact of asset purchase redistributions on German yields is negligible, average euro-area yields depend strongly on the cross-country allocation of purchases, through their effect on peripheral yields.

References

Aguiar, M., M. Amador, E. Farhi, and G. Gopinath (2015). Coordination and crisis in monetary unions. *Quarterly Journal of Economics 130*(4), 1727–1779. 5

Altavilla, C., G. Carboni, and R. Motto (2021). Asset purchase programs and financial markets: Lessons from the euro area. *International Journal of Central Banking 17*, 1–48. 1

Ang, A. and M. Piazzesi (2003). A no-arbitrage vector autoregression of term structure dynamics with macroeconomic and latent variables. *Journal of Monetary Economics 50*, 745–787. 1

Arellano, C. (2008). Default risk and income fluctuations in emerging economies. *American Economic Review 98*, 690–712. 49

Arellano, C., Y. Bai, and G. P. Mihalache (2020). Monetary policy and sovereign risk in emerging economies (NK-default). NBER Working Paper 26671. 5

Arellano, C., X. Mateos-Planas, and V. Ríos-Rull (2019). Partial default. NBER Working Paper 26076. 9, 3

Bacchetta, P., E. Perazzi, and E. van Wincoop (2018). Self-fulfilling debt crises: Can monetary policy really help? *Journal of International Economics 110*, 119–134. 5

Bianchi, J. and J. Mondragon (2022). Monetary independence and rollover crises. *Quarterly Journal of Economics 137*, 435–491. 5

Borgy, V., T. Laubach, J.-S. Mésonnier, and J.-P. Renne (2012). Fiscal sustainability, default risk, and euro area sovereign bond spreads. Banque de France DT350. 1

Broeders, D., L. de Haan, and J. W. van den End (2021). How QE changes the nature of sovereign risk. Manuscript, De Nederlandsche Bank. 1

Burriel, P., I. Kataryniuk, and J. J. Perez (2022, May). Computing the EU SURE interest savings using an extended debt sustainability assessment tool. Occasional Papers 2210, Bank of Spain. 36, 4.5

Calvo, G. (1988). Servicing the public debt: The role of expectations. *American Economic Review 78*(4), 647–661. 1, 5, 3

Camous, A. and R. Cooper (2019). "Whatever it takes" is all you need: Monetary policy and debt fragility. *American Economic Journal: Macroeconomics 11*(4), 38–81. 5

Cole, H. L. and T. J. Kehoe (2000). Self-fulfilling debt crises. *Review of Economic Studies 67*(January), 91–116. 1, 5, 3

Corradin, S., N. Grimm, and B. Schwaab (2021). Euro area sovereign bond risk premia during the Covid-19 pandemic. ECB Working Paper 2561. 3

Corsetti, G. and L. Dedola (2016). The mystery of the printing press: Monetary policy and self-fulfilling debt crises. *Journal of the European Economic Assocation 14*(6), 1329–1371. 1, 5, 3

Costain, J., G. Nuño, and C. Thomas (2022). The term structure of interest rates in a heterogeneous monetary union. Banco de España Working Paper 2223. 32

Cruces, J. and C. Trebesch (2013). Sovereign defaults: The price of haircuts. *American Economic Journal: Macroeconomics 5*, 85–117. 41

De Grauwe, P. and Y. Ji (2013). Self-fulfilling crises in the eurozone: An empirical test. *Journal of International Money and Finance 34*, 15–36. 1

Del Negro, M. and C. Sims (2015). When does a central bank's balance sheet require fiscal support? *Journal of Monetary Economics 73*, 1–19. 25, A

Demir, I., B. Eroglu, and S. Yildirim-Karaman (2021). Heterogeneous effects of unconventional monetary policy on the bond yields across the euro area. *Journal Money, Credit and Banking Forthcoming*. 3

Duffie, D. and R. Kan (1996). A yield-factor model of interest rates. *Mathematical Finance 6*(4), 379–406. 1

Duffie, D. and K. Singleton (1999). Modeling term structures of defaultable bonds. *Review of Financial Studies 12*(4), 687–720. 1, 2, 10, 3

Emmer, S. and C. Kluppelberg (2004, January). Optimal portfolios when stock prices follow an exponential Lévy process. *Finance and Stochastics 8*(1), 17–44. 8

Eser, F., W. Lemke, K. Nyholm, S. Radde, and A. Vladu (2019). Tracing the impact of the ECB'sasset purchase programme on the yield curve. ECB Working Paper 2293. 1, 4.2, 40

Gourinchas, P.-O., W. Ray, and D. Vayanos (2022). A preferred-habitat model of term premia, exchange rates, and monetary policy spillovers. NBER Working Paper 29875. 1, 2

Greenwood, R., S. Hanson, J. Stein, and A. Sunderam (2020). A quantity-driven theory of term premia and exchange rates. NBER Working Paper 27615. 1

Greenwood, R. and D. Vayanos (2014). Bond supply and excess bond returns. *Review of Financial Studies 27*(3), 663–713. 1, 1

Hamilton, J. and J. C. Wu (2012). The effectiveness of alternative monetary policy tools in a zero lower bound environment. *Journal of Money, Credit and Banking 44*(Supplement), 1–46. 1, 1, C.3, 68, 69

Hayashi, F. (2018). Computing equilibrium bond prices in the Vayanos-Vila model. *Research in Economics 72*(2), 181–195. 4.1

He, Z., S. Nagel, and Z. Song (2020). Treasury inconvenience yields during the Covid-19 crisis. Univ. of Chicago, Becker Friedman Institute Working Paper 2020-79. 1

Kallsen, J. (2000, August). Optimal portfolios for exponential Lévy processes. *Mathematical Methods of Operations Research 51*(3), 357–374. 8

King, T. B. (2019). Expectation and duration at the zero lower bound. *Journal of Financial Economics 134*(3), 736–760. 1

Krishnamurthy, A. (2022). Quantitative easing: What have we learned? Seminar presentation, Princeton Univ., 24 March. 1

Krishnamurthy, A., S. Nagel, and A. Vissing-Jorgensen (2018). ECB policies involving government bond purchases: Impact and channels. *Review of Finance 22*(1), 1–44. 3

Li, C. and M. Wei (2013). Term structure modeling with supply factors and the Federal Reserve's large-scale asset purchase programs. *International Journal of Central Banking 9*(1), 375–402. 1

Na, S., S. Schmitt-Grohe, M. Uribe, and V. Yue (2018). The twin Ds: Optimal default and devaluation. *American Economic Review 108*(7), 1773–1819. 5

Nuño, G., S. Hurtado, and C. Thomas (2022). Monetary policy and sovereign debt sustainability. *Journal of the European Economic Association Forthcoming*. 5

Ortobelli, S., I. Huber, S. Rachev, and E. Schwartz (2003). Portfolio choice theory with non-gaussian distributed returns. In: Handbook of Heavy Tailed Distributions in Finance (S. T. Rachev, ed.). 8

Rachev, S. and S. Han (2000, April). Portfolio management with stable distributions. *Mathematical Methods of Operations Research 51*(2), 341–352. 8

Ray, W. (2019). Monetary policy and the limits to arbitrage: Insights from a New Keynesian preferred habitat model. Manuscript, UC Berkeley. 1

Reis, R. (2013). The mystique surrounding the central bank's balance sheet, applied to the european crisis. *American Economic Review 103*(3), 135–140. 5, A

Vayanos, D. and J.-L. Vila (2021). A preferred habitat model of the term structure of interest rates. *Econometrica 89*, 77–112. 1, 2, 2, 7, 12, 2.1, 16, 2.1, 4.1, 47, 6, 65

Internet Appendix

A Appendix: Central bank accounting

The main text focuses on bond market equilibrium, without spelling out the broader financial context, including notably the role of the central bank. Here, we provide more context. Most importantly, we derive expressions for central bank profits and use them to explain why a remittance rule based on profits would render our affine solution method inapplicable.

Besides the arbitrageurs and preferred-habitat investors, financial market participants include commercial banks that can hold short-term riskless bonds and central bank reserves (indeed, some of the arbitrageurs may be commercial banks). Arbitrage then ensures that the short-term riskless rate (r_t) equals the interest rate on reserves.

The balance sheet of the common central bank consists of sovereign bonds on the assets side and bank reserves and capital on the liabilities side. We assume that the central bank maintains separate accounts associated with each national government in the monetary union, and determines seignorage transfers in relation to its holdings of each country's bonds. This structure roughly corresponds to the case of the Eurosystem, in which most bonds are held by the national central banks of the countries that issued those bonds, with only a small fraction of holdings subject to "risk sharing" across the national central banks.

In our model, the central bank's balance sheet affects the bond market equilibrium in two ways. First, central bank bond holdings reduce the net supply of bonds that must be absorbed by the private sector ($S_t(\tau), S_t^*(\tau)$). Second, under our assumed remittance rule (equation 35), redemptions of central bank-held bonds affect dividend payments to the government and therefore the default probability (equation 33). As an alternative to our redemptions-based rule, one could consider remittance rules based on the central bank's profit, which would be more consistent with actual practice. However, as explained in the main text, this would prevent us from obtaining an affine solution for bond yields, which is central for our entire analysis. Before elaborating on this limitation, we next show how to compute central bank profits in our framework. In doing so, we pay particular attention to the ECB/Eurosystem accounting principles for valuing securities held for monetary policy purposes (the only central bank asset in our

model), but we also show how one can simplify the algebra by relaxing such principles.

Central bank profits: some additional notation. For each bond in the central bank's portfolio at time t, let $\tilde{t} \in [t - \tau^{max}, t]$ denote the time when it was purchased and $\tilde{\tau}$ its residual maturity at the time of purchase. Residual maturity in the present is then $\tau = \tilde{\tau} - (t - \tilde{t})$, i.e. residual maturity at the purchase date minus the time elapsed since then. Let $P_{\tilde{t}}(\tilde{\tau})$ denote the purchase price. For a zero-coupon bond, the yield-to-maturity at the time of purchase, $y_{\tilde{t}}(\tilde{\tau})$, is determined by

$$P_{\tilde{t}}(\tilde{\tau}) = e^{-y_{\tilde{t}}(\tilde{\tau})\tilde{\tau}}. \tag{43}$$

Amortised cost accounting. All Eurosystem members (the ECB and the national central banks) are required to value their monetary policy portfolios *at amortised cost*. The value at amortised cost at time t of bond $(\tilde{\tau}, \tilde{t})$ is given by

$$V_t(\tilde{\tau}, \tilde{t}) = P_{\tilde{t}}(\tilde{\tau}) e^{y_{\tilde{t}}(\tilde{\tau})(t-\tilde{t})}. \tag{44}$$

Therefore, the initial value of the bond equals its purchase price: $V_{\tilde{t}}(\tilde{\tau}, \tilde{t}) = P_{\tilde{t}}(\tilde{\tau})$. After that, its value grows at the same rate as the bond's IRR, $y_{\tilde{t}}(\tilde{\tau})$, until converging at maturity to its face value: $V_{\tilde{t}+\tilde{\tau}}(\tilde{\tau}, \tilde{t}) = P_{\tilde{t}}(\tilde{\tau}) e^{y_{\tilde{t}}(\tilde{\tau})\tilde{\tau}} = 1$, where the second equality follows from (43). In turn, the *interest income* from the bond at time t is given by

$$I_t(\tilde{\tau}, \tilde{t}) = V_t(\tilde{\tau}, \tilde{t}) y_{\tilde{t}}(\tilde{\tau}), \tag{45}$$

i.e. the bond's current value (at amortized cost) times its yield at the time of purchase. Notice that, since the bond's value $V_t(\cdot)$ increases over time, so does its interest income.

Equation (45) represents how amortised cost accounting *periodifies* the bond's total income over the period in which it is held (to maturity) by the central bank. To see this, and to simplify the algebra –without any loss of generality–, normalize the time of purchase to $\tilde{t} = 0$, and let $P_0(\tilde{\tau}) \equiv P(\tilde{\tau})$, $y_0(\tilde{\tau}) \equiv y(\tilde{\tau})$, $V_t(\tilde{\tau}, 0) = P(\tilde{\tau}) e^{y(\tilde{\tau})t} \equiv V_t(\tilde{\tau})$, and $I_t(\tilde{\tau}, 0) = V_t(\tilde{\tau}) y(\tilde{\tau}) \equiv I_t(\tilde{\tau})$. Integrating equation (45) over the holding period then yields

$$\int_0^{\tilde{\tau}} I_t(\tilde{\tau}) dt = y(\tilde{\tau}) P(\tilde{\tau}) \int_0^{\tilde{\tau}} e^{y(\tilde{\tau})t} dt = y(\tilde{\tau}) P(\tilde{\tau}) \left[\frac{1}{y(\tilde{\tau})} e^{y(\tilde{\tau})t} \right]_0^{\tilde{\tau}} = P(\tilde{\tau}) \left[e^{y(\tilde{\tau})\tilde{\tau}} - 1 \right] = 1 - P(\tilde{\tau}),$$

where in the last equality we have used the fact that $P(\tilde{\tau}) e^{y(\tilde{\tau})\tilde{\tau}} = 1$. The last expression

in the above equation is precisely the total income on a zero-coupon bond: its face value (which we normalize to one) minus its price at the time of purchase.

Central bank profits. Let $f_t^{CB}(\tilde{\tau}, \tilde{t})$ denote the central bank's holdings at time t of bonds that were purchased at time $\tilde{t}$ with residual maturity $\tilde{\tau}$ at that time.[61] Then the total interest income from the bond portfolio at time t is given by

$$I_t^{tot} = \int_{t-\tau^{max}}^{t} \int_0^{\tau^{max}} I_t(\tilde{\tau}, \tilde{t}) f_t^{CB}(\tilde{\tau}, \tilde{t}) d\tilde{\tau} d\tilde{t}. \tag{46}$$

The central bank's profit flow at time t is finally given by total interest income minus interest payments on reserves,

$$\Pi_t^{cb} = I_t^{tot} - r_t D_t, \tag{47}$$

where D_t are central bank reserves and r_t is the interest rate on reserves. Finally, the law of motion of reserves is given by

$$\dot{D}_t = r_t D_t + \int_0^{\tau^{max}} P_t(\tau) \iota_t^{CB}(\tau) d\tau + \Gamma_t - f_t^{CB}(0), \tag{48}$$

i.e. reserves increase with interest payments on reserves, bond purchases ($\int P_t(\tau)\iota_t^{CB}(\tau)d\tau$) and dividend payments (Γ_t), and decrease with bond redemptions ($f_t^{CB}(0)$).

Profit-based remittance rules. As discussed in the main text, remittance rules based on the central bank's profits would render our affine solution methodology inapplicable. As shown in equation 33 in the paper, the default rate at a given point in time depends on the future stream of government primary deficits and of total bond redemptions –both assumed to be deterministic–[62], as well as on the future stream of dividends payments to the Treasury, $\{\Gamma_{t+s}\}_{s\geq 0}$. Under profit-based dividend rules, this last term would depend on past and future bond prices, thus making our affine solution technique inapplicable.

To see this in the simplest possible terms, assume that the central bank pays off

[61] We do not need to include the *current* (time-t) residual maturity as an argument of the portfolio distribution, as it is implied by the other arguments: $\tau = \tilde{\tau} - (t - \tilde{t})$.

[62] As explained in the paper, we assume that the central bank commits to a certain path of future bond purchases in *face value* terms (as opposed to in market value terms), precisely in order to be able to obtain an affine solution for bond yields. Under this assumption, the future stream of central bank-held bond redemptions is indeed deterministic and therefore does not depend on bond prices.

its entire accounting profit at all times: $\Gamma_{t+s} = \Pi^{cb}_{t+s} = I^{tot}_{t+s} - r_{t+s}D_{t+s}$ for all $s \geq 0$.[63] The default probability would then depend on the future stream of interest income and interest payments on reserves, both of which depend on past and future (from the point of the present, i.e. time t) bond prices. Indeed, from (46), (45) and (44), total interest income I^{tot}_t equals

$$I^{tot}_t = \int_{t-\tau^{max}}^{t} \int_0^{\tau^{max}} P_{\tilde{t}}(\tilde{\tau}) e^{y_{\tilde{t}}(\tilde{\tau})(t-\tilde{t})} y_{\tilde{t}}(\tilde{\tau}) f^{CB}_t(\tilde{\tau}, \tilde{t}) d\tilde{\tau} d\tilde{t}, \tag{49}$$

where yields depend on prices through $y_{\tilde{t}}(\tilde{\tau}) = -\log(P_{\tilde{t}}(\tilde{\tau}))/\tilde{\tau}$. Therefore, at any future time $t + s > t$, interest income I^{tot}_{t+s} would depend on the prices paid by the central bank on all bonds held in its portfolio at that time. As regards interest payments on reserves, from equation (48) the stock of reserves at any future time $t + s$ is given by

$$D_{t+s} = e^{\int_0^s r_{t+j} dj} D_t + \int_0^s e^{\int_u^s r_{t+j} dj} \left(\int_0^{\tau^{max}} P_{t+u}(\tau) \iota^{CB}_{t+u}(\tau) d\tau + \Gamma_{t+u} - f^{CB}_{t+u}(0) \right) du,$$

Therefore, future reserves –and hence future interest payments on reserves, $r_{t+s}D_{t+s}$– depend on future bond prices, both through the prices paid in future bond purchases ($\int_0^{\tau^{max}} P_{t+u}(\tau)\iota^{CB}_{t+u}(\tau)d\tau$) and through the very profit-based dividend rule ($\Gamma_{t+u} = \Pi^{cb}_{t+u}$).

Simplifying the algebra of central bank profits. As mentioned before, the total income earned on a zero-coupon bond from the time of purchase until its redemption is given by

$$1 - P_{\tilde{t}}(\tilde{\tau}), \tag{50}$$

i.e. its payment upon redemption minus the purchase price. While amortised cost accounting periodifies this income over the entire holding period, one could consider a simple accounting framework in which the central bank recognizes the bond's income only upon redemption. Under this assumption, one could aggregate expression (50) across those bonds that mature at time t (i.e. those with residual maturity $\tau = 0$) to obtain the following simple expression for total bond income,

$$\hat{I}^{tot}_t = \int_0^{\tau^{max}} (1 - P_{\tilde{t}}(\tilde{\tau})) \tilde{f}^{CB}_t(0, \tilde{t}) d\tilde{t} = f^{CB}_t(0) - \int_0^{\tau^{max}} P_{\tilde{t}}(\tilde{\tau}) \tilde{f}^{CB}_t(0, \tilde{t}) d\tilde{t}, \tag{51}$$

[63] In reality, Eurosystem central banks typically do not paid the entire accounting profit to their national treasuries, but instead retain part of it in order to accumulate capital buffers. How much is retained varies across NCBs, depending on the risks in each NCB's balance sheet and the methodology used for calculating risk provisions.

where $\tilde{f}_t^{CB}(0,\tilde{t})$ is the mass of central bank-held bonds maturing at time t that where purchased at time $\tilde{t}$ (when their residual maturity was $\tilde{\tau} = t - \tilde{t}$) and $f_t^{CB}(0) = \int_0^{\tau^{max}} \tilde{f}_t^{CB}(0,\tilde{t})d\tilde{t}$ are total time-t redemptions of central bank-held bonds. While far simpler than the expression for income under amortised-cost accounting (equation 46), expression (51) depends again on bond prices. Therefore, adopting a simpler accounting convention for central bank profits would not avoid the fact that profit-based remittance rules would continue to depend on bond prices and to prevent us from obtaining an affine solution.

Central bank capital in a rollover crisis. As mentioned in the main text, our assumed remittance rule implies that the central bank generally cannot avoid a reduction in its capital. To see this formally, we can use equation (35) in equation (48) to obtain the law of motion of central bank reserves in a rollover crisis,

$$\dot{D}_t = r_t D_t + \int P_t(\tau)\, \iota_t^{CB}(\tau)\, d\tau - \bar{\Gamma} - (1-\zeta)\, f_t^{CB}(0)\,. \tag{52}$$

We can define the national central bank's capital as

$$K_t \equiv \int_{t-\tau^{max}}^{t} \int_0^{\tau^{max}} V_t(\tilde{\tau},\tilde{t}) f_t^{CB}(\tilde{\tau},\tilde{t}) d\tilde{\tau} d\tilde{t} - D_t,$$

Capital then evolves as follows,

$$\begin{aligned}
\dot{K}_t &= \int_0^{\tau^{max}} \left[V_t(\tilde{\tau},\tilde{t}) f_t^{CB}(\tilde{\tau},\tilde{t}) - V_{t-\tau^{max}}(\tilde{\tau},\tilde{t}) f_{t-\tau^{max}}^{CB}(\tilde{\tau},\tilde{t})\right] d\tilde{\tau} d\tilde{t} \\
&+ \int_{t-\tau^{max}}^{t} \int_0^{\tau^{max}} \int \left(\frac{\partial V_t(\tilde{\tau},\tilde{t})}{\partial t} f_t^{CB}(\tilde{\tau},\tilde{t}) + V_t(\tilde{\tau},\tilde{t}) \frac{\partial f_t^{CB}(\tilde{\tau},\tilde{t})}{\partial t} \right) d\tilde{\tau} d\tilde{t} - \dot{D}_t.
\end{aligned}$$

During a rollover crisis, equation (52) implies

$$\begin{aligned}
\dot{K}_t &= \int_0^{\tau^{max}} \left[V_t(\tilde{\tau},\tilde{t}) f_t^{CB}(\tilde{\tau},\tilde{t}) - V_{t-\tau^{max}}(\tilde{\tau},\tilde{t}) f_{t-\tau^{max}}^{CB}(\tilde{\tau},\tilde{t})\right] d\tilde{\tau} d\tilde{t} \\
&+ \int_{t-\tau^{max}}^{t} \int_0^{\tau^{max}} \int \left(\frac{\partial V_t(\tilde{\tau},\tilde{t})}{\partial t} f_t^{CB}(\tilde{\tau},\tilde{t}) + V_t(\tilde{\tau},\tilde{t}) \frac{\partial f_t^{CB}(\tilde{\tau},\tilde{t})}{\partial t} \right) d\tilde{\tau} d\tilde{t} \\
&- r_t D_t - \int_0^{\tau^{max}} P_t(\tau) \iota_t^{CB}(\tau) d\tau + \bar{\Gamma} + (1-\zeta)\, f_t^{CB}(0)\,.
\end{aligned}$$

Capital can thus decrease during a crisis, potentially falling below zero. This will depend

on the maturity structure of the central bank assets, the path of interest payments on reserves, and the constant term $\bar{\Gamma}$. In particular, a sufficiently large capital retention term $\bar{\Gamma}$ can make the probability of a negative capital event arbitrarily small. In any case, as discussed by Del Negro and Sims (2015) and Reis (2013), a central bank can operate with low or even negative capital (within certain limits). Hence the small probability that the central bank could at some time face negative capital is inessential for our analysis.

B Model solution

B.1 Solving the one-factor model

Since preferred habitat demand is assumed to be an affine function of yield, equations (17) and (18) imply that the risk prices λ_t and ξ_t must be affine too. Hence, a solution requires $\lambda_t = \Lambda_t r_t + \bar{\lambda}_t$ and $\xi_t = \Xi_t r_t + \bar{\xi}_t$, where

$$\begin{aligned}
\Lambda_t &\equiv -\gamma\sigma^2 \int_0^\infty \left(\alpha(\tau)\left[A_t(\tau)\right]^2 + \alpha^*(\tau)\left[A_t^*(\tau)\right]^2\right) d\tau, \\
\bar{\lambda}_t &\equiv \gamma\sigma^2 \int_0^\infty \left[\left(S_t(\tau) - h_t(\tau) - \alpha(\tau) C_t(\tau) + \tau\alpha(\tau)\hat{\delta}\psi_t\right) A_t(\tau) + \left(S_t^*(\tau) - h_t^*(\tau) - \alpha^*(\tau) C_t^*(\tau)\right) A_t^*(\tau)\right] d\tau, \\
\Xi_t &\equiv -\gamma\psi_t\delta^2 \int_0^\infty \alpha(\tau) A_t(\tau)\, d\tau, \\
\bar{\xi}_t &\equiv \gamma\psi_t\delta^2 \int_0^\infty \left(S_t(\tau) - h_t(\tau) - \alpha(\tau) C_t(\tau) + \tau\alpha(\tau)\hat{\delta}\psi_t\right) d\tau.
\end{aligned}$$

With this notation, if we substitute $\mu_t(\tau)$ and $\mu_t^*(\tau)$ from (10)-(11) into (13)-(14), the first-order conditions on the arbitrageurs' portfolio weights are:

$$\begin{aligned}
0 \quad = \quad & -\left(\frac{\partial A_t}{\partial \tau} - \frac{\partial A_t}{\partial t}\right) r_t - \left(\frac{\partial C_t}{\partial \tau} - \frac{\partial C_t}{\partial t}\right) + A_t(\tau)\,\kappa\left(\bar{r} - r_t\right) - \frac{1}{2}\sigma^2\left[A_t(\tau)\right]^2 + r_t \\
+ \quad & A_t(\tau)\left(\Lambda_t r_t + \bar{\lambda}_t\right) + \psi_t\delta + \left(\Xi_t r_t + \bar{\xi}_t\right),
\end{aligned}$$

and

$$\begin{aligned}
0 \quad = \quad & -\left(\frac{\partial A_t^*}{\partial \tau} - \frac{\partial A_t^*}{\partial t}\right) r_t - \left(\frac{\partial C_t^*}{\partial \tau} - \frac{\partial C_t^*}{\partial t}\right) + A_t^*(\tau)\,\kappa\left(\bar{r} - r_t\right) - \frac{1}{2}\sigma^2\left[A_t^*(\tau)\right]^2 + r_t \\
+ \quad & A_t^*(\tau)\left(\Lambda_t r_t + \bar{\lambda}_t\right).
\end{aligned}$$

Separating the terms with and without r, we must have

$$
\begin{aligned}
0 &= -\frac{\partial A_t}{\partial \tau} + \frac{\partial A_t}{\partial t} - A_t(\tau)\kappa + 1 + \Lambda_t A_t(\tau) + \Xi_t, && (53)\\
0 &= -\frac{\partial C_t}{\partial \tau} + \frac{\partial C_t}{\partial t} + A_t(\tau)\kappa\bar{r} - \frac{1}{2}\sigma^2\left[A_t(\tau)\right]^2 + \bar{\lambda}_t A_t(\tau) + \psi_t\delta + \bar{\xi}_t, && (54)\\
0 &= -\frac{\partial A_t^*}{\partial \tau} + \frac{\partial A_t^*}{\partial t} - A_t^*(\tau)\kappa + 1 + \Lambda_t A_t^*(\tau), && (55)\\
0 &= -\frac{\partial C_t^*}{\partial \tau} + \frac{\partial C_t^*}{\partial t} + A_t^*(\tau)\kappa\bar{r} - \frac{1}{2}\sigma^2\left[A_t^*(\tau)\right]^2 + \bar{\lambda}_t A_t^*(\tau). && (56)
\end{aligned}
$$

This provides a system of PDEs to determine functions $(A_t(\tau), C_t(\tau))$ and $(A_t^*(\tau), C_t^*(\tau))$, verifying our guess that the bond price is an affine function of r_t.

B.2 Derivation of analytical results from Sec. 2.1

B.2.1 Proof of Prop. 1

We want to prove the decomposition: (1)

$$
\begin{aligned}
y_t(\tau) &= \underbrace{\frac{1}{\tau}\mathbb{E}_t\int_0^\tau r_{t+s}ds}_{\text{Expected rates } y_t^{EX}(\tau)} + \underbrace{\frac{1}{\tau}\mathbb{E}_t\int_0^\tau\left[A_{t+s}(\tau-s)\lambda_{t+s} - \frac{\sigma^2}{2}\left[A_{t+s}(\tau-s)\right]^2\right]ds}_{\text{Term premium } y_t^{TP}(\tau)}\\
&+ \underbrace{\frac{1}{\tau}\mathbb{E}_t\int_0^\tau \delta\psi_{t+s}ds}_{\text{Expected default loss } y_t^{DL}(\tau)} + \underbrace{\frac{1}{\tau}\mathbb{E}_t\int_0^\tau \xi_{t+s}ds}_{\text{Credit risk premium } y_t^{CR}(\tau)}.
\end{aligned}
$$

We can compute each of the terms of the decomposition recursively. We illustrate it in the case of the last term, the credit risk premium, but the proof is similar for the others. Note that we can express the credit risk premium as

$$
\tau y_t^{CR}(\tau) = \mathbb{E}_t\int_0^{\hat{\tau}}\xi_{t+s}ds + \mathbb{E}_t\int_{\hat{\tau}}^\tau \xi_{t+s}ds = \mathbb{E}_t\int_0^{\hat{\tau}}\xi_{t+s}ds + (\tau-\hat{\tau})\mathbb{E}_t\left[y_{t+\hat{\tau}}^{CR}(\tau-\hat{\tau})\right].
$$

This uses the fact that

$$
\mathbb{E}_t\int_{\hat{\tau}}^\tau \xi_{t+s}ds = \mathbb{E}_t\left(\mathbb{E}_{t+\hat{\tau}}\int_0^{\tau-\hat{\tau}}\xi_{t+\hat{\tau}+s}ds\right) = (\tau-\hat{\tau})\mathbb{E}_t\left[y_{t+\hat{\tau}}^{CR}(\tau-\hat{\tau})\right].
$$

Then, using the affine representation $\tau y_t^{CR}(\tau) = \left[A_t^{CR}(\tau) r_t + C_t^{CR}(\tau)\right]$, we can write

$$A_t^{CR}(\tau) r_t + C_t^{CR}(\tau) = \mathbb{E}_t \int_0^{\hat{\tau}} \xi_{t+s} ds + \mathbb{E}_t \left[A_{t+\hat{\tau}}^{CR}(\tau - \hat{\tau}) r_{t+\hat{\tau}} + C_{t+\hat{\tau}}^{CR}(\tau - \hat{\tau})\right].$$

If we take the derivative with respect to $\hat{\tau}$, we get

$$0 = \xi_{t+\hat{\tau}} + \mathbb{E}_t \left[- \left(\frac{\partial A_{t+\hat{\tau}}^{CR}}{\partial \tau} - \frac{\partial A_{t+\hat{\tau}}^{CR}}{\partial t} \right) r_{t+\hat{\tau}} + A_{t+\hat{\tau}}^{CR}(\tau - \hat{\tau}) \kappa (\bar{r} - r_{t+\hat{\tau}}) - \left(\frac{\partial C_{t+\hat{\tau}}^{CR}}{\partial \tau} - \frac{\partial C_{t+\hat{\tau}}^{CR}}{\partial t} \right) \right],$$

so we can then take the limit as $\hat{\tau} \to 0$ and separate terms:

$$\begin{aligned} 0 &= -\frac{\partial A_t^{CR}}{\partial \tau} + \frac{\partial A_t^{CR}}{\partial t} - \kappa A_t^{CR}(\tau) + \Xi_t, \\ 0 &= -\frac{\partial C_t^{CR}}{\partial \tau} + \frac{\partial C_t^{CR}}{\partial t} + A_t^{CR}(\tau)^\top \kappa \bar{r} + \bar{\xi}_{t+\hat{\tau}}. \end{aligned}$$

We can derive similar recursive representations for the other components. The expected future rates:

$$\begin{aligned} 0 &= -\frac{\partial A_t^{EX}}{\partial \tau} + \frac{\partial A_t^{EX}}{\partial t} - \kappa A_t^{EX}(\tau) + 1, \\ 0 &= -\frac{\partial C_t^{EX}}{\partial \tau} + \frac{\partial C_t^{EX}}{\partial t} + A_t^{EX}(\tau)^\top \kappa \bar{r}. \end{aligned}$$

The term premium:

$$\begin{aligned} 0 &= -\frac{\partial A_t^{TP}}{\partial \tau} + \frac{\partial A_t^{TP}}{\partial t} - \kappa A_t^{TP}(\tau) + \Lambda_t A_t(\tau), \\ 0 &= -\frac{\partial C_t^{TP}}{\partial \tau} + \frac{\partial C_t^{TP}}{\partial t} + A_t^{TP}(\tau) \kappa \bar{r} - \frac{\sigma^2}{2} \left[A_t(\tau)\right]^2 + A_t(\tau) \bar{\lambda}_t. \end{aligned}$$

And the expected default loss:

$$\begin{aligned} 0 &= -\frac{\partial A_t^{DL}}{\partial \tau} + \frac{\partial A_t^{DL}}{\partial t} - \kappa A_t^{DL}(\tau), \\ 0 &= -\frac{\partial C_t^{DL}}{\partial \tau} + \frac{\partial C_t^{DL}}{\partial t} + A_t^{DL}(\tau)^\top \kappa \bar{r} + \psi_t \delta. \end{aligned}$$

Defining $A_t(\tau) \equiv A_t^{CR}(\tau) + A_t^{EX}(\tau) + A_t^{TP}(\tau) + A_t^{DL}(\tau)$, and $C_t(\tau) \equiv C_t^{CR}(\tau) + C_t^{EX}(\tau) + C_t^{TP}(\tau) + C_t^{DL}(\tau)$, it is straightforward to verify these four pairs of equations sum up to the equations (53)-(54) that govern $A_t(\tau)$ and $C_t(\tau)$. Therefore solutions for

(53)-(54) sum up to a solution for $A_t(\tau)$ and $C_t(\tau)$.

B.2.2 Details of Props. 2-4

To derive the formulas on which Props. 2, 3, and 4 are based, we start with equations (53)-(56) from App. B.1. In steady state, the system simplifies to

$$\begin{aligned}
0 &= -\frac{\partial A}{\partial \tau} - A(\tau)\kappa + 1 + \Lambda A(\tau) + \Xi. && (57)\\
0 &= -\frac{\partial C}{\partial \tau} + A(\tau)\kappa\bar{r} - \frac{1}{2}\sigma^2 [A(\tau)]^2 + \bar{\lambda} A(\tau) + \psi\delta + \bar{\xi}. && (58)\\
0 &= -\frac{\partial A^*}{\partial \tau} - A^*(\tau)\kappa + 1 + \Lambda A^*(\tau) && (59)\\
0 &= -\frac{\partial C^*}{\partial \tau} + A^*(\tau)\kappa\bar{r} - \frac{1}{2}\sigma^2 [A^*(\tau)]^2 + \bar{\lambda} A^*(\tau), && (60)
\end{aligned}$$

where we have suppressed the time index as functions are time-invariant. Differential equations (57) and (59) can be solved as

$$A^*(\tau) = \frac{1 - e^{-\hat{\kappa}\tau}}{\hat{\kappa}},\ A(\tau) = \frac{(1+\Xi)\left(1 - e^{-\hat{\kappa}\tau}\right)}{\hat{\kappa}}, \quad (61)$$

where

$$\hat{\kappa} = \kappa - \Lambda = \kappa + \gamma\sigma^2 \int_0^\infty \left(\alpha(\tau) \left(\frac{(1+\Xi)\left(1 - e^{-\hat{\kappa}\tau}\right)}{\hat{\kappa}} \right)^2 + \alpha^*(\tau) \left(\frac{1 - e^{-\hat{\kappa}\tau}}{\hat{\kappa}} \right)^2 \right) d\tau.$$

Then, integrating equations (58) and (60), we get

$$\begin{aligned}
C^*(\tau) &= \int_0^\tau \left[A^*(u)\left(\kappa\bar{r} + \bar{\lambda}\right) - \frac{1}{2}\sigma^2 [A^*(u)]^2 \right] du,\\
C(\tau) &= \left(\psi\delta + \bar{\xi}\right)\tau + \int_0^\tau \left[A(u)\left(\kappa\bar{r} + \bar{\lambda}\right) - \frac{1}{2}\sigma^2 [A(u)]^2 \right] du.
\end{aligned}$$

Next, we analyze the limit as maturity converges to zero:

$$\begin{aligned}
\lim_{\tau\to 0} y_t(\tau) &= \left(\psi\delta + \bar{\xi}\right) + \lim_{\tau\to 0} \left[\frac{(1+\Xi)\left(1 - e^{-\hat{\kappa}\tau}\right)}{\hat{\kappa}} r_t + A(\tau)\left(\kappa\bar{r} + \bar{\lambda}\right) - \frac{1}{2}\sigma^2 [A(\tau)]^2 \right]\\
&= (1+\Xi) r_t + \left(\psi\delta + \bar{\xi}\right).
\end{aligned}$$

Here we have used L'Hôpital's rule to obtain

$$\lim_{\tau\to 0}\frac{(1+\Xi)\left(1-e^{-\hat{\kappa}\tau}\right)}{\hat{\kappa}\tau}=\lim_{\tau\to 0}\frac{(1+\Xi)\,\hat{\kappa}e^{-\hat{\kappa}\tau}}{\hat{\kappa}}=(1+\Xi),$$

and the fact that $A(0)=0$ to derive

$$\lim_{\tau\to 0}\frac{\int_0^\tau\left[A(u)\left(\kappa\bar{r}+\bar{\lambda}\right)-\frac{1}{2}\sigma^2\left[A(u)\right]^2\right]du}{\tau} \;=\; \lim_{\tau\to 0}A(\tau)\left(\kappa\bar{r}+\bar{\lambda}\right)-\tfrac{1}{2}\sigma^2\left[A(\tau)\right]^2 \;=\; 0.$$

B.3 Solving the model with demand risk

For the model extension with demand risk factors, we again conjecture deterministic functions $(A_t(\tau), C_t(\tau))$ and $(A_t^*(\tau), C_t^*(\tau))$, where $A_t(\tau)=\left(A_t^r(\tau), A_t^h(\tau), A_t^{h*}(\tau)\right)^\top$ and $A_t^*(\tau)=\left(A_t^{*r}(\tau), A_t^{*h}(\tau), A_t^{*h*}(\tau)\right)^\top$, such that bond prices can be expressed in log-affine form:

$$P_t(\tau)=e^{-\left[A_t(\tau)^\top q_t+C_t(\tau)\right]},\; P_t^*(\tau)=e^{-\left[A_t^*(\tau)^\top q_t+C_t^*(\tau)\right]}. \tag{62}$$

Applying Itô's lemma, the time-t instantaneous return on an undefaulted bond of maturity τ is

$$\frac{dP_t(\tau)}{P_t(\tau)}=\mu_t(\tau)\,dt-A_t(\tau)^\top\Sigma dB_t,\;\frac{dP_t^*(\tau)}{P_t^*(\tau)}=\mu_t^*(\tau)\,dt-A_t^*(\tau)^\top\Sigma dB_t, \tag{63}$$

where[64]

$$\mu_t(\tau)=\left(\frac{\partial A_t}{\partial\tau}-\frac{\partial A_t}{\partial t}\right)^\top q_t+\left(\frac{\partial C_t}{\partial\tau}-\frac{\partial C_t}{\partial t}\right)-A_t(\tau)^\top K\left(\bar{r}\mathcal{E}_1-q_t\right)+\frac{1}{2}A_t(\tau)^\top\Sigma\Sigma^\top A(\tau), \tag{64}$$

and

$$\mu_t^*(\tau)=\left(\frac{\partial A_t^*}{\partial\tau}-\frac{\partial A_t^*}{\partial t}\right)^\top q_t+\left(\frac{\partial C_t^*}{\partial\tau}-\frac{\partial C_t^*}{\partial t}\right)-A_t^*(\tau)^\top K\left(\bar{r}\mathcal{E}_1-q_t\right)+\frac{1}{2}A_t^*(\tau)^\top\Sigma\Sigma^\top A^*(\tau). \tag{65}$$

[64] Note that τ is a state with dynamics $d\tau=-dt$, so Itô's lemma yields derivatives in τ as well as t.

The first-order conditions on the arbitrageurs' portfolio weights are

$$\mu_t(\tau) = r_t + A_t(\tau)^\top \lambda_t + \psi_t \delta + \xi_t, \tag{66}$$

$$\mu_t^*(\tau) = r_t + A_t^*(\tau)^\top \lambda_t, \tag{67}$$

where

$$\lambda_t = \gamma \Sigma \Sigma^\top \int_0^\infty \left(X_t(\tau) A_t(\tau) + X_t^*(\tau) A_t^*(\tau) \right) d\tau \tag{68}$$

and

$$\xi_t = \gamma \psi_t \delta^2 \int_0^\infty X_t(\tau) \, d\tau, \tag{69}$$

where λ_t is a 3x1 vector and ξ_t is a scalar.

Since preferred habitat demand is assumed to be affine in the factors q_t, plugging the market clearing conditions into (68) and (69) implies that $\lambda_t = \Lambda_t^\top q_t + \bar{\lambda}_t$ and $\xi_t = \Xi_t^\top q_t + \bar{\xi}_t$ must also be affine functions, with the following weights:

$$\Lambda_t^\top \equiv \gamma \Sigma \Sigma^\top \int_0^\infty \left(\varsigma(\tau) A_t(\tau) \mathcal{E}_2^\top - \alpha(\tau) A_t(\tau) A_t(\tau)^\top + \varsigma^*(\tau) A_t^*(\tau) \mathcal{E}_3^\top - \alpha^*(\tau) A_t^*(\tau) A_t^*(\tau)^\top \right) d\tau,$$

$$\bar{\lambda}_t \equiv \gamma \Sigma \Sigma^\top \int_0^\infty \left[\left(S_t(\tau) - h_t(\tau) - \alpha(\tau) C_t(\tau) + \tau \alpha(\tau) \hat{\delta} \psi_t \right) A_t(\tau) + \left(S_t^*(\tau) - h_t^*(\tau) - \alpha^*(\tau) C_t^*(\tau) \right) A_t^*(\tau) \right] d\tau,$$

$$\Xi_t^\top \equiv \gamma \psi_t \delta^2 \int_0^\infty \left[\varsigma(\tau) \mathcal{E}_2^\top - \alpha(\tau) A_t(\tau)^\top \right] d\tau,$$

$$\bar{\xi}_t \equiv \gamma \psi_t \delta^2 \int_0^\infty \left(S_t(\tau) - h_t(\tau) - \alpha(\tau) C_t(\tau) + \tau \alpha(\tau) \hat{\delta} \psi_t \right) d\tau,$$

where $\mathcal{E}_2 = (0,1,0)^\top$ and $\mathcal{E}_3 = (0,0,1)^\top$. Notice that Λ_t is a 3x3 matrix, $\bar{\lambda}_t$ and Ξ_t are 3x1 vectors, and $\bar{\xi}_t$ is a scalar. Using this notation, the first-order conditions become:

$$\begin{aligned} 0 &= -\left(\frac{\partial A_t}{\partial \tau} - \frac{\partial A_t}{\partial t} \right)^\top q_t - \left(\frac{\partial C_t}{\partial \tau} - \frac{\partial C_t}{\partial t} \right) + A(\tau)^\top K (\bar{r} \mathcal{E}_1 - q_t) - \frac{1}{2} A_t(\tau)^\top \Sigma \Sigma^\top A_t(\tau) \\ &+ \mathcal{E}_1^\top q_t + A_t(\tau)^\top \left(\Lambda_t^\top q_t + \bar{\lambda}_t \right) + \psi_t \delta + \left(\Xi_t^\top q_t + \bar{\xi}_t \right), \end{aligned}$$

and

$$\begin{aligned} 0 &= -\left(\frac{\partial A_t^*}{\partial \tau} - \frac{\partial A_t^*}{\partial t} \right)^\top q_t - \left(\frac{\partial C_t^*}{\partial \tau} - \frac{\partial C_t^*}{\partial t} \right) + A_t^*(\tau)^\top K (\bar{r} \mathcal{E}_1 - q_t) - \frac{1}{2} A_t^*(\tau)^\top \Sigma \Sigma^\top A_t^*(\tau) \\ &+ \mathcal{E}_1^\top q_t + A_t^*(\tau)^\top \left(\Lambda_t^\top q_t + \bar{\lambda}_t \right). \end{aligned}$$

Transposing these equations and separating the terms with and without q, we must

have

$$0 = -\frac{\partial A_t}{\partial \tau} + \frac{\partial A_t}{\partial t} - K^\top A_t(\tau) + \Lambda_t A_t(\tau) + \mathcal{E}_1 + \Xi_t. \tag{70}$$

$$0 = -\frac{\partial C_t}{\partial \tau} + \frac{\partial C_t}{\partial t} + A_t(\tau)^\top K\mathcal{E}_1\bar{r} + A_t(\tau)^\top \bar{\lambda}_t - \frac{1}{2}A_t(\tau)^\top \Sigma\Sigma^\top A_t(\tau) + \psi_t\delta + \bar{\xi}_t. \tag{71}$$

$$0 = -\frac{\partial A_t^*}{\partial \tau} + \frac{\partial A_t^*}{\partial t} - K^\top A_t^*(\tau) + \Lambda_t A_t^*(\tau) + \mathcal{E}_1 \tag{72}$$

$$0 = -\frac{\partial C_t^*}{\partial \tau} + \frac{\partial C_t^*}{\partial t} + A_t^*(\tau)^\top K\mathcal{E}_1\bar{r} + A_t^*(\tau)^\top \bar{\lambda}_t - \frac{1}{2}A_t^*(\tau)^\top \Sigma\Sigma^\top A_t^*(\tau). \tag{73}$$

This system of PDEs suffices to determine the functions $(A_t(\tau), C_t(\tau))$ and $(A_t^*(\tau), C_t^*(\tau))$, verifying our guess that the bond price is an affine function of q_t.[65]

B.4 Model-generated moments

The yields for maturity τ in the periphery and core are

$$y_t(\tau) = \tau^{-1}\left(A_t^r(\tau) r_t + A_t^h(\tau)\varepsilon_t^h + A_t^{h*}(\tau)\varepsilon_t^{h*} + C_t(\tau)\right),$$

$$y_t^*(\tau) = \tau^{-1}\left(A_t^{*r}(\tau) r_t + A_t^{*h}(\tau)\varepsilon_t^h + A_t^{*h*}(\tau)\varepsilon_t^{h*} + C_t^*(\tau)\right).$$

Assuming that the demand risk factors are independent from the short-term rate, the volatility of the yields is

$$\sqrt{\mathbb{V}\mathrm{ar}\left(y_t(\tau)\right)} = \frac{\sqrt{A_t^r(\tau)^2\frac{\sigma_r^2}{2\kappa_r} + A_t^h(\tau)^2\frac{\sigma_\varepsilon^2}{2\kappa_\varepsilon} + A_t^{h*}(\tau)^2\frac{\sigma_{\varepsilon*}^2}{2\kappa_{\varepsilon*}} + 2A_t^h(\tau)A_t^{h*}(\tau)\mathbb{C}\mathrm{ov}\left(\varepsilon_t^h, \varepsilon_t^{h*}\right)}}{\tau},$$

$$\sqrt{\mathbb{V}\mathrm{ar}\left(y_t^*(\tau)\right)} = \frac{\sqrt{A_t^{*r}(\tau)^2\frac{\sigma_r^2}{2\kappa_r} + A_t^{*h}(\tau)^2\frac{\sigma_\varepsilon^2}{2\kappa_\varepsilon} + A_t^{*h*}(\tau)^2\frac{\sigma_{\varepsilon*}^2}{2\kappa_{\varepsilon*}} + 2A_t^{*h}(\tau)A_t^{*h*}(\tau)\mathbb{C}\mathrm{ov}\left(\varepsilon_t^h, \varepsilon_t^{h*}\right)}}{\tau}.$$

C Appendix: Computing the solution

C.1 Parameters

The parameters of our numerical model are reported in Table 4. The model is programmed with a monthly time unit (the units have been converted to annualized terms,

[65] Equations (70) and (72) correspond to equation (36) of Vayanos and Vila (2021), while equations (71) and (73) correspond to their (38).

in Table 1 of the main text, to better clarify their meaning). This is convenient because it allows us to verify our results by running either a continuous-time method (App. C.2) or a discrete-time method (App. C.3.2), without requiring any parameter transformations; the calibration stated in Table 4 applies to both algorithms.

Table 4: Calibration

Parameters*	**Values**
Parameters calibrated directly from observables	
$\bar{r}$: Mean of monthly risk-free rate r_t	0.0102
κ: Monthly autoregressive coefficient of r_t	0.0052
σ : Standard deviation of innovations to r_t	0.000153
Parameters estimated by minimizing the distance criterion	
γ: Risk aversion	0.0114
$\underline{\psi}$: Default probability intercept	0.000625
θ: Slope of default rate	1.59×10^{-5}
$\hat{r}+\phi$: Discount rate in fiscal pressure aggregate	0.0296
κ_h: Monthly autoregressive coefficient of PH shocks	0.00040
ς_h: Coef. of volatility of PH shocks	25.3
χ_h: Correlation between DE and IT PH shocks	0.9997
α_h: Slope of PH demand function	9.60×10^4
ζ: Pass-through in redemptions	1
* Parameters are expressed in terms of a monthly time unit. The unit of value is billions of euros.	

C.2 Numerical algorithm: continuous time

C.2.1 Finite-difference computation of the long-run solution

The long-run solution of our model must satisfy the system of ODEs (57)-(60). These can be solved by a finite difference method.[66] To do so, we consider a grid of maturities $(\tau_1, .., \tau_I)$ with $\tau_0 = 0$ and constant step size $\Delta\tau$, so that $\tau_i \equiv \tau(i) = i\Delta\tau$. Define

$$\begin{aligned} A_i &= A(\tau_i), A_i^* = A^*(\tau_i), C_i = C(\tau_i), C_i^* = C^*(\tau_i), \\ S_i &= S(\tau_i), S_i^* = S^*(\tau_i), \alpha_i = \alpha(\tau_i), \alpha_i^* = \alpha^*(\tau_i), \\ h &= h(\tau_i), h_i^* = h^*(\tau_i). \end{aligned}$$

[66] We have defined and computed both continuous-time and discrete-time versions of the model. The discrete time version is described in the next section. Numerical simulations of both versions give the same results.

The boundary conditions are $A_0 = A(0) = 0$ and $C_0 = C(0) = 0$ because an instantaneous bond trades at par. We begin with a guess of A_i^n, A_i^{n*}, with $n = 0$. For instance, we can begin with $A_i^n = A_i^{n*} = \tau_i$ and $C_i^n = C_i^{n*} = 0$. Then, considering a backward finite-difference approximation $\frac{\partial A^{n+1}(\tau(i))}{\partial \tau} \approx \frac{A_i^{n+1} - A_{i-1}^{n+1}}{\Delta\tau}$, and likewise for the other unknown functions, we approximate the ODEs as:

$$\begin{aligned}
\frac{A_i^{n+1} - A_{i-1}^{n+1}}{\Delta\tau} &= A_i^{n+1}\left(\Lambda^n - \kappa\right) + 1 + \Xi^n, \\
\frac{C_i^{n+1} - C_{i-1}^{n+1}}{\Delta\tau} &= A_i^{n+1}\left(\bar{\lambda}^n + \kappa\bar{r}\right) - \frac{1}{2}\sigma^2\left[A_i^{n+1}\right]^2 + \psi_{ss}\delta + \bar{\xi}^n, \\
\frac{A_i^{(n+1)*} - A_{i-1}^{(n+1)*}}{\Delta\tau} &= A_i^{(n+1)*}\left(\Lambda^n - \kappa\right) + 1, \\
\frac{C_i^{(n+1)*} - C_{i-1}^{(n+1)*}}{\Delta\tau} &= A_i^{(n+1)*}\left(\bar{\lambda}^n + \kappa\bar{r}\right) - \frac{1}{2}\sigma^2\left[A_i^{(n+1)*}\right]^2,
\end{aligned}$$

where

$$\begin{aligned}
\Lambda^n &= -\gamma\sigma^2\sum_{i=1}^{I}\left(\alpha_i\left[A_i^n\right]^2 + \alpha_i^*\left[A_i^{n*}\right]^2\right)\Delta\tau, \\
\bar{\lambda}^n &= \gamma\sigma^2\sum_{i=1}^{I}\left[\left(S_i - h_i - \alpha_i C_i^n + i\alpha_i\hat{\delta}\psi_{ss}\right)A_i^n + \left(S_i^* - h_i^* - \alpha_i^* C_i^{n*}\right)A_i^{n*}\right]\Delta\tau, \\
\Xi^n &= -\gamma\psi_{ss}\delta^2\sum_{i=1}^{I}\alpha_i A_i^n\Delta\tau. \\
\xi^n &= \gamma\psi_{ss}\delta^2\sum_{i=1}^{I}\left[\left(S_i - h_i - \alpha_i C_i^n + i\alpha_i\hat{\delta}\psi_{ss}\right)\right]\Delta\tau.
\end{aligned}$$

In matrix form, this amounts to

$$\overbrace{\begin{bmatrix}
\frac{1}{\Delta\tau} - \Lambda^n + \kappa & 0 & 0 & \cdots & 0 \\
-\frac{1}{\Delta\tau} & \frac{1}{\Delta\tau} - \Lambda^n + \kappa & 0 & \cdots & 0 \\
\vdots & -\frac{1}{\Delta\tau} & \frac{1}{\Delta\tau} - \Lambda^n + \kappa & \cdots & \vdots \\
0 & 0 & \cdots & \ddots & 0 \\
0 & 0 & \cdots & -\frac{1}{\Delta\tau} & \frac{1}{\Delta\tau} - \Lambda^n + \kappa
\end{bmatrix}}^{\mathbf{F^n}}
\overbrace{\begin{bmatrix} A_1^{n+1} \\ A_2^{n+1} \\ \vdots \\ A_{I-1}^{n+1} \\ A_I^{n+1} \end{bmatrix}}^{\mathbf{A^{n+1}}}
= \overbrace{\begin{bmatrix} 1 + \Xi^n \\ 1 + \Xi^n \\ \vdots \\ 1 + \Xi^n \\ 1 + \Xi^n \end{bmatrix}}^{\mathbf{f^n}}, \tag{74}$$

$$\begin{bmatrix} \frac{1}{\Delta\tau}-\Lambda^n+\kappa & 0 & 0 & \cdots & 0 \\ -\frac{1}{\Delta\tau} & \frac{1}{\Delta\tau}-\Lambda^n+\kappa & 0 & \cdots & 0 \\ \vdots & -\frac{1}{\Delta\tau} & \frac{1}{\Delta\tau}-\Lambda^n+\kappa & \cdots & \vdots \\ 0 & 0 & \cdots & \ddots & 0 \\ 0 & 0 & \cdots & -\frac{1}{\Delta\tau} & \frac{1}{\Delta\tau}-\Lambda^n+\kappa \end{bmatrix} \overbrace{\begin{bmatrix} A_1^{(n+1)*} \\ A_2^{(n+1)*} \\ \vdots \\ A_{I-1}^{(n+1)*} \\ A_I^{(n+1)*} \end{bmatrix}}^{\mathbf{A^{(n+1)*}}} = \overbrace{\begin{bmatrix} 1 \\ 1 \\ \vdots \\ 1 \\ 1 \end{bmatrix}}^{\mathbf{f^*}}, \tag{75}$$

$$\overbrace{\begin{bmatrix} \frac{1}{\Delta\tau} & 0 & 0 & \cdots & 0 \\ -\frac{1}{\Delta\tau} & \frac{1}{\Delta\tau} & 0 & \cdots & 0 \\ \vdots & -\frac{1}{\Delta\tau} & \frac{1}{\Delta\tau} & \cdots & \vdots \\ 0 & 0 & \cdots & \ddots & 0 \\ 0 & 0 & \cdots & -\frac{1}{\Delta\tau} & \frac{1}{\Delta\tau} \end{bmatrix}}^{\mathbf{G}} \overbrace{\begin{bmatrix} C_1^{n+1} \\ C_2^{n+1} \\ \vdots \\ C_{I-1}^{n+1} \\ C_I^{n+1} \end{bmatrix}}^{\mathbf{C^{n+1}}} = \overbrace{\begin{bmatrix} A_1^{n+1}\left(\bar{\lambda}^n+\kappa\bar{r}\right)-\frac{1}{2}\sigma^2\left[A_1^{n+1}\right]^2+\psi_{ss}\delta+\bar{\xi}^n \\ A_2^{n+1}\left(\bar{\lambda}^n+\kappa\bar{r}\right)-\frac{1}{2}\sigma^2\left[A_2^{n+1}\right]^2+\psi_{ss}\delta+\bar{\xi}^n \\ \vdots \\ A_{I-1}^{n+1}\left(\bar{\lambda}^n+\kappa\bar{r}\right)-\frac{1}{2}\sigma^2\left[A_{I-1}^{n+1}\right]^2+\psi_{ss}\delta+\bar{\xi}^n \\ A_I^{n+1}\left(\bar{\lambda}^n+\kappa\bar{r}\right)-\frac{1}{2}\sigma^2\left[A_I^{n+1}\right]^2+\psi_{ss}\delta+\bar{\xi}^n \end{bmatrix}}^{\mathbf{g^{n+1}}}, \tag{76}$$

$$\begin{bmatrix} \frac{1}{\Delta\tau} & 0 & 0 & \cdots & 0 \\ -\frac{1}{\Delta\tau} & \frac{1}{\Delta\tau} & 0 & \cdots & 0 \\ \vdots & -\frac{1}{\Delta\tau} & \frac{1}{\Delta\tau} & \cdots & \vdots \\ 0 & 0 & \cdots & \ddots & 0 \\ 0 & 0 & \cdots & -\frac{1}{\Delta\tau} & \frac{1}{\Delta\tau} \end{bmatrix} \overbrace{\begin{bmatrix} C_1^{(n+1)*} \\ C_2^{(n+1)*} \\ \vdots \\ C_{I-1}^{(n+1)*} \\ C_I^{(n+1)*} \end{bmatrix}}^{\mathbf{C^{(n+1)*}}} = \overbrace{\begin{bmatrix} A_1^{(n+1)*}\left(\bar{\lambda}^n+\kappa\bar{r}\right)-\frac{1}{2}\sigma^2\left[A_1^{(n+1)*}\right]^2 \\ A_2^{(n+1)*}\left(\bar{\lambda}^n+\kappa\bar{r}\right)-\frac{1}{2}\sigma^2\left[A_2^{(n+1)*}\right]^2 \\ \vdots \\ A_{I-1}^{(n+1)*}\left(\bar{\lambda}^n+\kappa\bar{r}\right)-\frac{1}{2}\sigma^2\left[A_{I-1}^{(n+1)*}\right]^2 \\ A_I^{(n+1)*}\left(\bar{\lambda}^n+\kappa\bar{r}\right)-\frac{1}{2}\sigma^2\left[A_I^{(n+1)*}\right]^2 \end{bmatrix}}^{\mathbf{g^{(n+1)*}}}, \tag{77}$$

where we have already applied the boundary conditions.

The idea is to solve equations (74) and (75) iteratively from the initial guess, updating Λ^n and Ξ^n and at each step, and then calculate $\bar{\lambda}^n$ and $\bar{\xi}^n$ in order to solve (76) and (77) in a single step.

C.2.2 Finite-difference computation of the long-run solution: multifactor case

The long-run solution of our model must satisfy the system of ODEs (70)-(73).The boundary conditions are $A_0 = A(0) = (0,0,0)^\top$ and $C_0 = C(0) = 0$ because an instantaneous bond trades at par. We begin by guessing the 3x1 vectors A_i^n, A_i^{n*} and the scalars C_i^n, C_i^{n*} at iteration step $n = 0$. For instance, we can begin with $A_i^n =$

$A_i^{n*} = (\tau_i, \tau_i, \tau_i)^\top$ and $C_i^n = C_i^{n*} = 0$. Then, considering a backward finite-difference approximation $\frac{\partial A^{n+1}(\tau(i))}{\partial \tau} \approx \frac{A_i^{n+1} - A_{i-1}^{n+1}}{\Delta\tau}$, and likewise for the other unknown functions, we approximate the ODEs as:

$$
\begin{aligned}
\frac{A_i^{n+1} - A_{i-1}^{n+1}}{\Delta\tau} &= \left(\Lambda^n - K^\top\right) A_i^{n+1} + \mathcal{E}_1 + \Xi^n, \\
\frac{C_i^{n+1} - C_{i-1}^{n+1}}{\Delta\tau} &= \left(A_i^{n+1}\right)^\top \left(\bar{\lambda}^n + K\mathcal{E}_1\bar{r}\right) - \frac{1}{2}\left(A_i^{n+1}\right)^\top \Sigma\Sigma^\top A_i^{n+1} + \psi_{ss}\delta + \bar{\xi}^n, \\
\frac{A_i^{(n+1)*} - A_{i-1}^{(n+1)*}}{\Delta\tau} &= \left(\Lambda^n - K^\top\right) A_i^{(n+1)*} + \mathcal{E}_1, \\
\frac{C_i^{(n+1)*} - C_{i-1}^{(n+1)*}}{\Delta\tau} &= \left(A_i^{(n+1)*}\right)^\top \left(\bar{\lambda}^n + K\mathcal{E}_1\bar{r}\right) - \frac{1}{2}\left(A_i^{(n+1)*}\right)^\top \Sigma\Sigma^\top A_i^{(n+1)*},
\end{aligned}
$$

where

$$
\begin{aligned}
\Lambda^n &= \gamma \sum_{i=1}^{I} \left(\varsigma_i \mathcal{E}_2 \left(A_i^n\right)^\top - \alpha_i A_i^n \left(A_i^n\right)^\top + \varsigma_i^* \mathcal{E}_3 \left(A_i^{n*}\right)^\top - \alpha_i^* A_i^{n*} \left(A_i^{n*}\right)^\top\right) \Sigma\Sigma^\top \Delta\tau, \\
\bar{\lambda}^n &= \gamma\Sigma\Sigma^\top \sum_{i=1}^{I} \left[\left(S_i - h_i - \alpha_i C_i^n + i\alpha_i\hat{\delta}\psi_{ss}\right) A_i^n + \left(S_i^* - h_i^* - \alpha_i^* C^{n*}\right) A_i^{n*}\right] \Delta\tau, \\
\Xi^n &= \gamma\psi_{ss}\delta^2 \sum_{i=1}^{I} \left(\varsigma_i \mathcal{E}_2 - \alpha_i \left(A_i^n\right)\right) \Delta\tau. \\
\xi^n &= \gamma\psi_{ss}\delta^2 \sum_{i=1}^{I} \left[\left(S_i - h_i - \alpha_i C_i^n + i\alpha_i\hat{\delta}\psi_{ss}\right)\right] \Delta\tau.
\end{aligned}
$$

In matrix form, with I_3 to indicate the 3x3 identity matrix, this amounts to

$$
\overbrace{\begin{bmatrix}
\frac{1}{\Delta\tau} I_3 - \Lambda^n + K^\top & 0 & 0 & \cdots & 0 \\
-\frac{1}{\Delta\tau} I_3 & \frac{1}{\Delta\tau} I_3 - \Lambda^n + K^\top & 0 & \cdots & 0 \\
\vdots & -\frac{1}{\Delta\tau} I_3 & \frac{1}{\Delta\tau} I_3 - \Lambda^n + K^\top & \cdots & \vdots \\
0 & 0 & \cdots & \ddots & 0 \\
0 & 0 & \cdots & -\frac{1}{\Delta\tau} I_3 & \frac{1}{\Delta\tau} I_3 - \Lambda^n + K^\top
\end{bmatrix}}^{\mathbf{F^n}}
\overbrace{\begin{bmatrix} A_1^{n+1} \\ A_2^{n+1} \\ \vdots \\ A_{I-1}^{n+1} \\ A_I^{n+1} \end{bmatrix}}^{\mathbf{A^{n+1}}}
= \overbrace{\begin{bmatrix} \mathcal{E}_1 + \Xi^n \\ \mathcal{E}_1 + \Xi^n \\ \vdots \\ \mathcal{E}_1 + \Xi^n \\ \mathcal{E}_1 + \Xi^n \end{bmatrix}}^{\mathbf{f^n}},
\tag{78}
$$

$$\overbrace{\begin{bmatrix} \frac{1}{\Delta\tau}I_3 - \Lambda^n + K^\top & 0 & 0 & \cdots & 0 \\ -\frac{1}{\Delta\tau}I_3 & \frac{1}{\Delta\tau}I_3 - \Lambda^n + K^\top & 0 & \cdots & 0 \\ \vdots & -\frac{1}{\Delta\tau}I_3 & \frac{1}{\Delta\tau}I_3 - \Lambda^n + K^\top & \cdots & \vdots \\ 0 & 0 & \cdots & \ddots & 0 \\ 0 & 0 & \cdots & -\frac{1}{\Delta\tau}I_3 & \frac{1}{\Delta\tau}I_3 - \Lambda^n + \kappa \end{bmatrix}}^{\mathbf{F^n}} \overbrace{\begin{bmatrix} A_1^{(n+1)*} \\ A_2^{(n+1)*} \\ \vdots \\ A_{I-1}^{(n+1)*} \\ A_I^{(n+1)*} \end{bmatrix}}^{\mathbf{A^{(n+1)*}}} = \overbrace{\begin{bmatrix} \mathcal{E}_1 \\ \mathcal{E}_1 \\ \vdots \\ \mathcal{E}_1 \\ \mathcal{E}_1 \end{bmatrix}}^{\mathbf{f^*}}, \tag{79}$$

$$\overbrace{\begin{bmatrix} \frac{1}{\Delta\tau} & 0 & 0 & \cdots & 0 \\ -\frac{1}{\Delta\tau} & \frac{1}{\Delta\tau} & 0 & \cdots & 0 \\ \vdots & -\frac{1}{\Delta\tau} & \frac{1}{\Delta\tau} & \cdots & \vdots \\ 0 & 0 & \cdots & \ddots & 0 \\ 0 & 0 & \cdots & -\frac{1}{\Delta\tau} & \frac{1}{\Delta\tau} \end{bmatrix}}^{\mathbf{G}} \overbrace{\begin{bmatrix} C_1^{n+1} \\ C_2^{n+1} \\ \vdots \\ C_{I-1}^{n+1} \\ C_I^{n+1} \end{bmatrix}}^{\mathbf{C^{n+1}}} = \overbrace{\begin{bmatrix} \left(A_1^{n+1}\right)^\top \left(\bar{\lambda}^n + K\mathcal{E}_1\bar{r}\right) - \frac{1}{2}\left(A_1^{n+1}\right)^\top \Sigma\Sigma^\top A_1^{n+1} + \psi_{ss}\delta + \bar{\xi}^n \\ \left(A_2^{n+1}\right)^\top \left(\bar{\lambda}^n + K\mathcal{E}_1\bar{r}\right) - \frac{1}{2}\left(A_2^{n+1}\right)^\top \Sigma\Sigma^\top A_2^{n+1} + \psi_{ss}\delta + \bar{\xi}^n \\ \vdots \\ \left(A_{I-1}^{n+1}\right)^\top \left(\bar{\lambda}^n + K\mathcal{E}_1\bar{r}\right) - \frac{1}{2}\left(A_{I-1}^{n+1}\right)^\top \Sigma\Sigma^\top A_{I-1}^{n+1} + \psi_{ss}\delta + \bar{\xi}^n \\ \left(A_I^{n+1}\right)^\top \left(\bar{\lambda}^n + K\mathcal{E}_1\bar{r}\right) - \frac{1}{2}\left(A_I^{n+1}\right)^\top \Sigma\Sigma^\top A_I^{n+1} + \psi_{ss}\delta + \bar{\xi}^n \end{bmatrix}}^{\mathbf{g^{n+1}}}, \tag{80}$$

$$\begin{bmatrix} \frac{1}{\Delta\tau} & 0 & 0 & \cdots & 0 \\ -\frac{1}{\Delta\tau} & \frac{1}{\Delta\tau} & 0 & \cdots & 0 \\ \vdots & -\frac{1}{\Delta\tau} & \frac{1}{\Delta\tau} & \cdots & \vdots \\ 0 & 0 & \cdots & \ddots & 0 \\ 0 & 0 & \cdots & -\frac{1}{\Delta\tau} & \frac{1}{\Delta\tau} \end{bmatrix} \overbrace{\begin{bmatrix} C_1^{(n+1)*} \\ C_2^{(n+1)*} \\ \vdots \\ C_{I-1}^{(n+1)*} \\ C_I^{(n+1)*} \end{bmatrix}}^{\mathbf{C^{(n+1)*}}} = \overbrace{\begin{bmatrix} \left(A_1^{(n+1)*}\right)^\top \left(\bar{\lambda}^n + K\mathcal{E}_1\bar{r}\right) - \frac{1}{2}\left(A_1^{(n+1)*}\right)^\top \Sigma\Sigma^\top A_1^{(n+1)*} \\ \left(A_2^{(n+1)*}\right)^\top \left(\bar{\lambda}^n + K\mathcal{E}_1\bar{r}\right) - \frac{1}{2}\left(A_2^{(n+1)*}\right)^\top \Sigma\Sigma^\top A_2^{(n+1)*} \\ \vdots \\ \left(A_{I-1}^{(n+1)*}\right)^\top \left(\bar{\lambda}^n + K\mathcal{E}_1\bar{r}\right) - \frac{1}{2}\left(A_{I-1}^{(n+1)*}\right)^\top \Sigma\Sigma^\top A_{I-1}^{(n+1)*} \\ \left(A_I^{(n+1)*}\right)^\top \left(\bar{\lambda}^n + K\mathcal{E}_1\bar{r}\right) - \frac{1}{2}\left(A_I^{(n+1)*}\right)^\top \Sigma\Sigma^\top A_I^{(n+1)*} \end{bmatrix}}^{\mathbf{g^{(n+1)*}}}, \tag{81}$$

where we have already applied the boundary conditions. In these equations, $\mathbf{A^{n+1}}$ and $\mathbf{A^{(n+1)*}}$ are vectors of length $3I$, while $\mathbf{C^{n+1}}$ and $\mathbf{C^{(n+1)*}}$ are vectors of length I, while $\mathbf{F^n}$ and $\mathbf{G}$ are matrices of size $3I \times 3I$ and $I \times I$, respectively.

The idea is to solve equations (78) and (79) iteratively from the initial guess, updating Λ^n and Ξ^n and at each step, and then calculate $\bar{\lambda}^n$ and $\bar{\xi}^n$ in order to solve (80) and (81) in a single step.

C.2.3 Computation of the dynamics

To compute the dynamics, consider a distant terminal time T at which the model has converged to the long-run solution. We solve the PDEs (53)-(56) backwards from time T with time steps of size $\Delta t \equiv \Delta\tau$, so that backwards induction step n refers to calendar time $t(n) \equiv T - n\Delta\tau$. Using the fact that $A_i^{n+1} - A_i^n \approx -\frac{\partial A^n(\tau(i))}{\partial t}\Delta\tau$, the PDEs can

be discretized as follows::

$$\begin{aligned}
\frac{\mathbf{A}^{n+1}-\mathbf{A}^{n}}{\Delta\tau}+\mathbf{F}^{n}\mathbf{A}^{n} &= \mathbf{f}^{n},\\
\frac{\mathbf{A}^{(n+1)*}-\mathbf{A}^{n*}}{\Delta\tau}+\mathbf{F}^{n}\mathbf{A}^{n*} &= \mathbf{f}^{*},\\
\frac{\mathbf{C}^{n+1}-\mathbf{C}^{n}}{\Delta\tau}+\mathbf{G}\mathbf{C}^{n} &= \mathbf{g}^{n},\\
\frac{\mathbf{C}^{(n+1)*}-\mathbf{C}^{n*}}{\Delta\tau}+\mathbf{G}\mathbf{C}^{n*} &= \mathbf{g}^{n*}.
\end{aligned}$$

Matrices $\mathbf{F}^{n}$, $\mathbf{G}$, $\mathbf{f}^{n}$, $\mathbf{f}^{*}$, $\mathbf{g}^{n}$, and $\mathbf{g}^{n*}$ are defined as before, except that we calculate Λ_t, Ξ_t, $\bar{\lambda}_t$, and $\bar{\xi}_t$ under time-varying conditions. In particular, we evaluate them conditional on the net bond supply $S_t(\tau)$ and default rate ψ_t at time $t = t(n)$.[67]

C.3 Discrete time representation

Here we present the discrete-time counterpart of the model, along the lines of Hamilton and Wu (2012) .

C.3.1 Single-factor case

It is straightforward to derive and compute a discrete-time framework that is equivalent to our continuous-time model. In discrete time, we write the price of a bond with a maturity of i periods, issued by jurisdiction $j \in \{P, C\}$ ("Periphery" or "Core"), as $P_{i,t}^{j} = \exp\left(p_{i,t}^{j}\right) = \exp\left(-A_{i,t}^{j} r_t - C_{i,t}^{j}\right)$. Let the rate on reserves follow $r_{t+1} = \rho r_t + (1-\rho)\bar{r} + \sigma\varepsilon_{t+1}$, where $\varepsilon_{t+1} \sim N(0,1)$. If arbitrageurs maximize a mean-variance utility function over the increase of their wealth, then if the time period is sufficiently short, their optimization problem can be approximated as follows:[68]

$$\begin{aligned}
\max_{\{X_{i,t}^{j}\}} \quad & \left(W_t - \textstyle\sum_{i=1}^{I}\sum_{j\in\{P,C\}} X_{i,t}^{j}\right) r_t \\
+ \quad & \textstyle\sum_{i=1}^{I}\sum_{j\in\{P,C\}} X_{i,t}^{j}\left(-C_{i-1,t+1}^{j} - A_{i-1,t+1}^{j}\left((1-\rho)\bar{r} + \rho r_t\right) + C_{i,t}^{j} + A_{i,t}^{j} r_t + \frac{\sigma^2}{2}\left(A_{i-1,t+1}^{j}\right)^2 - \delta\psi_t^{j}\right) \\
- \quad & \frac{\gamma\sigma^2}{2}\left[\textstyle\sum_{i=2}^{I}\sum_{j\in\{P,C\}} X_{i,t}^{j} A_{i-1,t+1}^{j}\right]^2 - \frac{\gamma\psi_t^{P}}{2}\delta^2\left[\textstyle\sum_{i=1}^{I} X_{i,t}^{P}\right]^2 .
\end{aligned}$$

[67] Inspecting the definitions of the matrices in (74)-(77), we can see that this algorithm calculates equilibrium objects at time $t(n) - \Delta\tau$ using the risk prices $\lambda_{t(n)}$ and $\xi_{t(n)}$ from time $t(n)$. It would therefore be incorrect to apply this algorithm with a large time step $\Delta\tau$, but in the limit as $\Delta\tau \to 0$, it gives the correct solution of the continuous-time PDE.

[68] See Hamilton and Wu (2012) for details.

where $\psi_t^C = 0$ denotes the Core default probability, and $\psi_t^P = \psi_t$ is the Peripheral default probability, given by (36). Hence, the first-order condition on the investment $X_{i,t}^j$ in bonds of maturity i from jurisdiction j is

$$r_t \;=\; -\left(C_{i-1,t+1}^j + A_{i-1,t+1}^j\left((1-\rho)\bar{r} + \rho r_t\right)\right) + \left(C_{i,t}^j + A_{i,t}^j r_t\right) + \frac{\sigma^2}{2}\left(A_{i-1,t+1}^j\right)^2 - \delta\psi_t^j - A_{i-1,t+1}^j\lambda_t - \xi_t^j,$$

where

$$\lambda_t = \gamma\sigma^2 \sum_{i=2}^{I} \sum_{j\in\{P,C\}} X_{i,t}^j A_{i-1,t+1}^j,$$

$$\xi_t^j = \gamma\psi_t^j\delta^2 \sum_{i=1}^{I} X_{i,t}^j \ .$$

Note that since $A_{0,t}^j = C_{0,t}^j = 0$, the first-order conditions for holdings of one-period bonds are simply

$$r_t = y_{1,t}^C = C_{1,t}^C + A_{1,t}^C r_t \ , \ r_t = C_{1,t}^P + A_{1,t}^P r_t - \delta\psi_t - \xi_t \ ,$$

which implies $A_{1,t}^C = 1$, $A_{1,t}^P = 1 + \Xi_t^j$, $C_{1,t}^C = 0$, and $C_{1,t}^P = \delta\psi_t + \bar{\xi}_t$. The FOC for longer bonds can be interpreted as

$$p_{i,t}^j \;=\; -r_t + E_t p_{i-1,t+1}^j + \frac{1}{2} Var_t p_{i-1,t+1}^j - A_{i-1,t+1}^j\lambda_t - \delta\psi_t^j - \xi_t^j,$$

or equivalently

$$P_{i,t}^j \;=\; \exp\left(-r_t - A_{i-1,t+1}^j\lambda_t - \delta\psi_t^j - \xi_t^j\right) E_t P_{i-1,t+1}^j.$$

We now apply the market clearing condition $X_{i,t}^j = S_{i,t}^j - Z_{i,t}^j$, where preferred-habitat demand is $Z_{i,t}^j = h_{i,t}^j + i\alpha_i^j\left(y_{i,t}^j - \hat{\delta}\psi_t^j\right)$ and we write the risk compensation terms in affine form as $\lambda_t = \Lambda_t r_t + \bar{\lambda}_t$ and $\xi_t^P = \Xi_t^P r_t + \bar{\xi}_t^P$, with $\xi_t^C = \Xi_t^C = \bar{\xi}_t^C = 0$. Then, the first-order conditions imply the following restrictions on the affine pricing coefficients:

$$A_{i,t}^j \;=\; 1 + A_{i-1,t+1}^j\left(\rho + \Lambda_t\right) + \Xi_t^j, \tag{82}$$

$$C_{i,t}^j \;=\; C_{i-1,t+1}^j - \frac{1}{2}\left(\sigma A_{i-1,t+1}^j\right)^2 + A_{i-1,t+1}^j\left((1-\rho)\,\bar{r} + \bar{\lambda}_t\right) + \delta\psi_t^j + \bar{\xi}_t^j, \tag{83}$$

where

$$\Lambda_t = -\gamma\sigma^2 \sum_{i=2}^{I} \sum_{j\in\{P,C\}} A^j_{i-1,t+1} \left(\alpha^j_i A^j_{i,t}\right), \tag{84}$$

$$\bar{\lambda}_t = \gamma\sigma^2 \sum_{i=2}^{I} \sum_{j\in\{P,C\}} A^j_{i-1,t+1} \left(S^j_{i,t} - h^j_{i,t} - \alpha^j_i C^j_{i,t} + i\alpha^j_i \hat{\delta}\psi^j_t\right), \tag{85}$$

$$\Xi^P_t = -\gamma\delta^2\psi^P_t \sum_{i=1}^{I} \left(\alpha^P_i A^P_{i,t}\right), \tag{86}$$

$$\bar{\xi}^P_t = \gamma\delta^2\psi^P_t \sum_{i=1}^{I} \left(S^P_{i,t} - h^P_{i,t} - \alpha^P_i C^P_{i,t} + i\alpha^P_i \hat{\delta}\psi^P_t\right). \tag{87}$$

These difference equations can be solved by backwards induction, starting from a distant time T at which we assume that the pricing functions are known, bearing in mind that $A^j_{0,t} = C^j_{0,t} = 0$ for all j and t. To ensure a correct solution of the discrete-time model, we can apply a fixed-point calculation at each time step:

1. Guess $A^j_{i,t} = A^j_{i,t+1}$ and $C^j_{i,t} = C^j_{i,t+1}$.
2. Calculate Λ_t, Ξ^P_t, $\bar{\lambda}_t$, and $\bar{\xi}^P_t$ from (84)-(87).
3. Update $A^j_{i,t} = A^j_{i,t+1}$ and $C^j_{i,t} = C^j_{i,t+1}$ using (82)-(83).
4. Iterate to convergence.

Once the time t equilibrium has been calculated, we can step backwards to calculate the time $t-1$ equilibrium by the same method.

C.3.2 Discrete time representation: multi-factor case

It is straightforward to derive and compute a discrete-time framework that is equivalent to our continuous-time model. In discrete time, we write the price of a bond with a maturity of i periods, issued by jurisdiction $j \in \{P, C\}$ ("Periphery" or "Core"), as $P^j_{i,t} = \exp\left(p^j_{i,t}\right) = \exp\left(-\left(A^j_{i,t}\right)^\top q_t - C^j_{i,t}\right)$. Let the factors follow $q_{t+1} = (I_3 - K)q_t + K\mathcal{E}_1\bar{r} + \Sigma\varepsilon_{t+1}$, where $\varepsilon_{t+1} \sim N(0, I_3)$. If arbitrageurs maximize a mean-variance utility function over the increase of their wealth, then if the time period is sufficiently short,

their optimization problem can be approximated as follows:[69]

$$\begin{aligned}\max_{\{X^j_{i,t}\}} \quad & \left(W_t - \sum_{i=1}^I \sum_{j\in\{P,C\}} X^j_{i,t}\right) r_t + \sum_{i=1}^I \sum_{j\in\{P,C\}} X^j_{i,t}\left(-C^j_{i-1,t+1} - \left(A^j_{i-1,t+1}\right)^\top (K\mathcal{E}_1\bar{r} + (I_3 - K)q_t)\right) \\ & + \sum_{i=1}^I \sum_{j\in\{P,C\}} X^j_{i,t}\left(C^j_{i,t} + \left(A^j_{i,t}\right)^\top q_t + \tfrac{1}{2}\left(A^j_{i-1,t+1}\right)^\top \Sigma\Sigma^\top A^j_{i-1,t+1} - \delta\psi^j_t\right) \\ & - \tfrac{\gamma}{2}\sum_{i,k=2}^I \sum_{j,l\in\{P,C\}} X^j_{i,t}X^l_{k,t}\left(A^j_{i-1,t+1}\right)^\top \Sigma\Sigma^\top A^l_{k-1,t+1} - \tfrac{\gamma\psi^P_t}{2}\delta^2\left[\sum_{i=1}^I X^P_{i,t}\right]^2.\end{aligned}$$

where $\psi^C_t = 0$ denotes the Core default probability, and $\psi^P_t = \psi_t$ is the Peripheral default probability, given by (36). Here we have used the fact that the variance of the portfolio value, conditional on no default, is

$$\mathbb{V}\mathrm{ar}_t \sum_{i=2}^I \sum_{j\in\{P,C\}} X^j_{i,t}P^j_{i-1,t+1} = E_t\left[\sum_{i=2}^I \sum_{j\in\{P,C\}} X^j_{i,t}\left(A^j_{i-1,t+1}\right)^\top \Sigma\varepsilon_{t+1}\right]^2 = \sum_{i,k=2}^I \sum_{j,l\in\{P,C\}} X^j_{i,t}X^l_{k,t}\left(A^j_{i-1,t+1}\right)^\top \Sigma\Sigma^\top A^l_{k-1,t+1}$$

Hence, the first-order condition on the investment $X^j_{i,t}$ in bonds of maturity i from jurisdiction j is

$$\begin{aligned} r_t = \mathcal{E}_1^\top q_t &= -\left(C^j_{i-1,t+1} + \left(A^j_{i-1,t+1}\right)^\top (K\mathcal{E}_1\bar{r} + (I_3 - K)q_t)\right) + \left(C^j_{i,t} + \left(A^j_{i,t}\right)^\top q_t\right) \\ &+ \frac{1}{2}\left(A^j_{i-1,t+1}\right)^\top \Sigma\Sigma^\top A^j_{i-1,t+1} - \delta\psi^j_t - \left(A^j_{i-1,t+1}\right)^\top \lambda_t - \xi^j_t,\end{aligned}$$

where

$$\lambda_t = \gamma\Sigma\Sigma^\top \sum_{i=2}^I \sum_{j\in\{P,C\}} X^j_{i,t}A^j_{i-1,t+1},$$

$$\xi^j_t = \gamma\psi^j_t\delta^2 \sum_{i=1}^I X^j_{i,t}\ .$$

Note that since $A^j_{0,t} = C^j_{0,t} = 0$, the first-order conditions for holdings of one-period bonds are simply

$$r_t = y^C_{1,t} = C^C_{1,t} + \left(A^C_{1,t}\right)^\top q_t\ ,\ r_t = C^P_{1,t} + \left(A^P_{1,t}\right)^\top q_t - \delta\psi_t - \xi_t\ ,$$

[69] See Hamilton and Wu (2012) for details.

which implies $A^C_{1,t} = \mathcal{E}_1$, $A^P_{1,t} = \mathcal{E}_1 + \Xi_t$, $C^C_{1,t} = 0$, and $C^P_{1,t} = \delta\psi_t + \bar{\xi}_t$. The FOC for longer bonds can be interpreted as

$$p^j_{i,t} = -r_t + E_t p^j_{i-1,t+1} + \frac{1}{2} Var_t p^j_{i-1,t+1} - \left(A^j_{i-1,t+1}\right)^\top \lambda_t - \delta\psi^j_t - \xi^j_t,$$

or equivalently

$$P^j_{i,t} = \exp\left(-r_t - \left(A^j_{i-1,t+1}\right)^\top \lambda_t - \delta\psi^j_t - \xi^j_t\right) E_t P^j_{i-1,t+1}.$$

We now apply the market clearing condition $X^j_{i,t} = S^j_{i,t} - Z^j_{i,t}$, where preferred-habitat demand is $Z^j_{i,t} = h^j_{i,t} - \varsigma^j_i \varepsilon^j_{i,t} + i\alpha^j_i \left(y^j_{i,t} - \hat{\delta}\psi^j_t\right)$, and we write the risk compensation terms in affine form as $\lambda_t = \Lambda^\top_t q_t + \bar{\lambda}_t$ and $\xi^P_t = \left(\Xi^P_t\right)^\top r_t + \bar{\xi}^P_t$, with $\xi^C_t = \Xi^C_t = \bar{\xi}^C_t = 0$. Then, the first-order conditions imply the following restrictions on the affine pricing coefficients:

$$A^j_{i,t} = \mathcal{E}_1 + \left(\Lambda_t + \left(I_3 - K^\top\right)\right) A^j_{i-1,t+1} + \Xi^j_t, \tag{88}$$

$$C^j_{i,t} = C^j_{i-1,t+1} - \frac{1}{2}\left(A^j_{i-1,t+1}\right)^\top \Sigma\Sigma^\top A^j_{i-1,t+1} + \left(A^j_{i-1,t+1}\right)^\top \left(K\mathcal{E}_1\bar{r} + \bar{\lambda}_t\right) + \delta\psi^j_t + \bar{\xi}^j_t \tag{89}$$

where

$$\Lambda^\top_t = \gamma\Sigma\Sigma^\top \sum_{i=2}^{I} \left[A^P_{i-1,t+1}\left(\varsigma^P_i \mathcal{E}^\top_2 - \alpha^P_i \left(A^P_{i,t}\right)^\top\right) + A^C_{i-1,t+1}\left(\varsigma^C_i \mathcal{E}^\top_3 - \alpha^C_i \left(A^C_{i,t}\right)^\top\right)\right], \tag{90}$$

$$\bar{\lambda}_t = \gamma\Sigma\Sigma^\top \sum_{i=2}^{I} \sum_{j\in\{P,C\}} A^j_{i-1,t+1}\left(S^j_{i,t} - h^j_{i,t} - \alpha^j_i C^j_{i,t} + i\alpha^j_i \hat{\delta}\psi^j_t\right), \tag{91}$$

$$\left(\Xi^P_t\right)^\top = \gamma\delta^2\psi^P_t \sum_{i=1}^{I}\left(\varsigma^P_i \mathcal{E}^\top_2 - \alpha^P_i \left(A^P_{i,t}\right)^\top\right), \tag{92}$$

$$\bar{\xi}^P_t = \gamma\delta^2\psi^P_t \sum_{i=1}^{I}\left(S^P_{i,t} - h^P_{i,t} - \alpha^P_i C^P_{i,t} + i\alpha^P_i \hat{\delta}\psi^P_t\right). \tag{93}$$

These difference equations can be solved by backwards induction, starting from a distant time T at which we assume that the pricing functions are known, bearing in mind that $A^j_{0,t} = C^j_{0,t} = 0$ for all j and t. To ensure a correct solution of the discrete-time model, we can apply a fixed-point calculation at each time step:

1. Guess $A^j_{i,t} = A^j_{i,t+1}$ and $C^j_{i,t} = C^j_{i,t+1}$.

2. Calculate Λ_t, Ξ_t^P, $\bar{\lambda}_t$, and $\bar{\xi}_t^P$ from (90)-(93).

3. Update $A_{i,t}^j = A_{i,t+1}^j$ and $C_{i,t}^j = C_{i,t+1}^j$ using (88)-(89).

4. Iterate to convergence.

Once the time t equilibrium has been calculated, we can step backwards to calculate the time $t-1$ equilibrium by the same method.

C.3.3 Decomposing prices and yields

The decomposition of the discrete-time version of the model can be computed by a method analogous to the one spelled out in App. B.2.1 for the continuous-time model. The overall yield can be decomposed into four affine terms:

$$\begin{aligned}\tau y_{i,t}^j(q) &= \left(A_{i,t}^j\right)^\top q + C_{i,t}^j \\ &= \left(A_{i,t}^{j,EX}\right)^\top q + C_{i,t}^{j,EX} + \left(A_{i,t}^{j,DL}\right)^\top q + C_{i,t}^{j,DL} + \left(A_{i,t}^{j,TP}\right)^\top q + C_{i,t}^{j,TP} + \left(A_{i,t}^{j,CR}\right)^\top q + C_{i,t}^{j,CR}.\end{aligned}$$

The individual components can each be computed recursively:

$$\begin{aligned} A_{i,t}^{j,EX} &= \mathcal{E}_1 + \left(I_3 - K_t^\top\right) A_{i-1,t+1}^{j,EX}, && (94)\\ C_{i,t}^{j,EX} &= C_{i-1,t+1}^{j,EX} + \left(A_{i-1,t+1}^{j,EX}\right)^\top K_t \mathcal{E}_1 \bar{r}_t. && (95)\end{aligned}$$

$$\begin{aligned} A_{i,t}^{j,DL} &= \left(I_3 - K_t^\top\right) A_{i-1,t+1}^{j,DL}, && (96)\\ C_{i,t}^{j,DL} &= C_{i-1,t+1}^{j,DL} + \left(A_{i-1,t+1}^{j,DL}\right)^\top K_t \mathcal{E}_1 \bar{r}_t + \delta \psi_t^j. && (97)\end{aligned}$$

$$\begin{aligned} A_{i,t}^{j,CR} &= \left(I_3 - K_t^\top\right) A_{i-1,t+1}^{j,CR} + \Xi_t^j, && (98)\\ C_{i,t}^{j,CR} &= C_{i-1,t+1}^{j,CR} + \left(A_{i-1,t+1}^{j,CR}\right)^\top K_t \mathcal{E}_1 \bar{r}_t + \bar{\xi}_t^j. && (99)\end{aligned}$$

$$\begin{aligned} A_{i,t}^{j,TP} &= \left(I_3 - K_t^\top\right) A_{i-1,t+1}^{j,TP} + \Lambda_t A_{i-1,t+1}^j, && (100)\\ C_{i,t}^{j,TP} &= C_{i-1,t+1}^{j,TP} + \left(A_{i-1,t+1}^{j,TP}\right)^\top K_t \mathcal{E}_1 \bar{r}_t - \frac{1}{2}\left(A_{i-1,t+1}^j\right)^\top \Sigma_t \Sigma_t^\top A_{i-1,t+1}^j + \left(A_{i-1,t+1}^j\right)^\top \bar{\lambda}_t && (101)\end{aligned}$$

These equations can all be solved backwards from the terminal conditions $A_{0,t}^{j,k} = \overrightarrow{0}$, and $C_{0,t}^{j,k} = 0$, for $k \in \{EX, DL, CR, TP\}$. We can see that the default loss and credit risk components are zero for Core, and in addition $A_{i,t}^{P,DL} = 0$ for Periphery.

It is straightforward to verify that equations (94)-(101) sum up to the equations (88)-(89) that govern $A_{i,t}^{j}$ and $C_{i,t}^{j}$. Therefore solutions to (94)-(101) sum up to a solution for $A_{i,t}^{j}$ and $C_{i,t}^{j}$.

C.3.4 Model generated moments

The one-period innovation to the factors is

$$q_{t+1} - E_t q_{t+1} \overset{iid}{\sim} N\left(0, \Sigma\Sigma^\top\right),$$

and the n-period innovation to the factors is

$$q_{t+n} - E_t q_{t+n} = \sum_{s=1}^{n} (I_3 - K)^{n-s} \Sigma \varepsilon_{t+s}.$$

Therefore, we can write the covariance between the factors at horizons n and m as

$$\begin{aligned}
\mathbb{C}\mathrm{ov}_t\left(q_{t+n}, q_{t+m}\right) &= E_t\left(\left(q_{t+n} - E_t q_{t+n}\right)\left(q_{t+m} - E_t q_{t+m}\right)^\top\right) \\
&= E_t\left(\left(\sum_{s=1}^{n} (I_3 - K)^{n-s} \Sigma \varepsilon_{t+s}\right)\left(\sum_{\tau=1}^{m} \varepsilon_{t+\tau}^\top \Sigma^\top (I_3 - K)^{m-\tau}\right)\right) \\
&= E_t\left(\sum_{s=1}^{\min(n,m)} (I_3 - K)^{n-s} \Sigma \varepsilon_{t+s} \varepsilon_{t+s}^\top \Sigma^\top (I_3 - K)^{m-s}\right) \\
&= \sum_{s=1}^{\min(n,m)} (I_3 - K)^{n-s} \Sigma\Sigma^\top (I_3 - K)^{m-s}.
\end{aligned}$$

The second line of the derivation makes use of the fact that $I_3 - K$ is a symmetric matrix, and the third and fourth lines use the fact that $E_t\left(\varepsilon_{t+s}\varepsilon_{t+\tau}^\top\right) = I_3$ if $s = \tau$, and is zero otherwise. Considering the case $n = m$, we can calculate the conditional variance of q_{t+n} and the unconditional variance of q_t as follows:

$$\mathbb{V}\mathrm{ar}_t\left(q_{t+n}\right) = \sum_{s=0}^{n-1}(I_3 - K)^s \Sigma\Sigma^\top (I_3 - K)^s,$$

$$\mathbb{V}\mathrm{ar}\left(q_t\right) = \sum_{s=0}^{\infty}(I_3 - K)^s \Sigma\Sigma^\top (I_3 - K)^s.$$

The shock to the yield $y^j_{i,t+1}$ is a linear transformation of the shock to q_{t+1}:

$$y^j_{i,t+1} - E_t y^j_{i,t+1} = \frac{1}{i}\left(A^j_{i,t+1}\right)^\top \left(q_{t+1} - E_t q_{t+1}\right).$$

Therefore, using the formulas for the variances of the factors, and considering a stationary situation in which the factor loadings A are independent of time, we can calculate the unconditional covariance of the yield $y^j_{i,t}$ with the yield $y^k_{l,t}$ as

$$\mathbb{C}\mathrm{ov}\left(y^j_{i,t}, y^k_{l,t}\right) = \frac{1}{il}\left(A^j_i\right)^\top \mathbb{V}\mathrm{ar}\left(q_t\right) A^k_l.$$

Similarly, taking the time unit to be one month, the covariance between the one-year changes in the yields $y^j_{i,t}$ and $y^k_{l,t}$ is

$$\mathbb{C}\mathrm{ov}_t\left(y^j_{i,t+12}, y^k_{l,t+12}\right) = \frac{1}{il}\left(A^j_i\right)^\top \mathbb{V}\mathrm{ar}_t\left(q_{t+12}\right) A^k_l.$$

C.3.5 Computing Sharpe ratios

To define Sharpe ratios in our context, note that excess returns are affected both by variations in bond prices and by default events. Therefore, the instantaneous Sharpe ratios for Core and Periphery in the continuous-time model can be defined as $\mathbb{S}^*_t(\tau)$ and $\mathbb{S}_t(\tau)$ in the following equations:

$$\mathbb{S}^*_t(\tau)dt^{1/2} \equiv \mathbb{E}_t\left(\frac{dP^*_t(\tau)}{P^*_t(\tau)} - r_t dt\right) / \left(\mathbb{V}ar_t\left(\frac{dP^*_t(\tau)}{P^*_t(\tau)}\right)\right)^{1/2}, \tag{102}$$

$$\mathbb{S}_t(\tau)dt^{1/2} \equiv \mathbb{E}_t\left(\frac{dP_t(\tau)}{P_t(\tau)} - \delta dN_t - r_t dt\right) / \left(\mathbb{V}ar_t\left(\frac{dP_t(\tau)}{P_t(\tau)} - \delta dN_t\right)\right)^{1/2}. \tag{103}$$

We report empirical and model counterparts to $\mathbb{S}_t^*(\tau)$ and $\mathbb{S}_t(\tau)$ in Tables 2 and 3, scaled for consistency with an annual time unit.

We compute the empirical Sharpe ratios from monthly yield series in Datastream for 1999-2022, as follows. We divide the monthly series of zero-coupon yields, in percentage points, by 1200 to construct samples of monthly logarithmic yields $\hat{y}_{i,t}^j$ for j =DE or IT, and for i =12, 24, 60, 108 or 120 months. We interpolate yields on 119-month bonds linearly using 9-year German yields and 5-year Italian yields together with 10-year yields, and we extrapolate yields on 11-month bonds linearly using 2-year and 1-year yields. We then construct samples of monthly excess returns $\hat{rx}_{i,t+1}^j = i\hat{y}_{i,t}^j - (i-1)\hat{y}_{i-1,t+1}^j - \hat{r}_t$, where $\hat{r}_t$ is the risk-free rate. Here we use the same spliced series of German 1-month yields and 1-month OIS that we used for the model calibration, dividing by 1200 to express it as a monthly logarithmic yield (also from Datastream; see Sec. 4.2).

We can then compute a monthly sample Sharpe ratio $\hat{S}_i^j$ as follows:

$$\hat{S}_i^j = \frac{\hat{\mathbb{E}}\left(\hat{rx}_{i,t+1}^j\right) + \frac{1}{2}\hat{\mathbb{V}ar}\left(\hat{rx}_{i,t+1}^j\right)}{\left(\hat{\mathbb{V}ar}\left(\hat{rx}_{i,t+1}^j\right)\right)^{1/2}},$$

where $\hat{\mathbb{E}}$ and $\hat{\mathbb{V}ar}$ denote the sample mean and variance. Since the numerator of this ratio scales in proportion to the time period, while the denominator scales in proportion to the square root of the time period, we multiply by $\sqrt{12}$ to produce the annualized empirical Sharpe ratios that are reported in the tables.

To compute the model counterparts of (102)-(103), the numerators can be calculated as

$$\begin{aligned}
\mathbb{E}_t\left(\frac{dP_t^*(\tau)}{P_t^*(\tau)} - r_t dt\right) &= \left(\mu_t^*(\tau) - r_t\right) dt \;=\; A_t^*(\tau)^\top \lambda_t dt, \\
\mathbb{E}_t\left(\frac{dP_t(\tau)}{P_t(\tau)} - \delta dN_t - r_t dt\right) &= \left(\mu_t(\tau) - \psi_t\delta - r_t\right) dt \;=\; \left(A_t(\tau)^\top \lambda_t + \xi_t\right) dt.
\end{aligned}$$

The variances in the denominators can be calculated as

$$\begin{aligned}
\mathbb{V}ar_t\left(\frac{dP_t^*(\tau)}{P_t^*(\tau)}\right) &= A_t^*(\tau)^\top \Sigma\Sigma^\top A_t^*(\tau) dt, \\
\mathbb{V}ar_t\left(\frac{dP_t(\tau)}{P_t(\tau)} - \delta dN_t\right) &= \left(A_t(\tau)^\top \Sigma\Sigma^\top A_t(\tau) + \psi_t\delta^2\right) dt.
\end{aligned}$$

We evaluate these formulas using the objects constructed in the finite difference approximation to the long-run solution of the continuous-time model, as described in Sec. C.2.2, setting the time unit and the finite time step to one month, to construct a monthly model Sharpe ratio.[70] We multiply by $\sqrt{12}$ to produce the annualized model Sharpe ratios that are reported in the tables.

[70] Alternatively, we can evaluate the formulas using the discrete time solution. The only difference is that factor loadings of maturity i, A_i^j, are replaced by the maturity $i-1$ loadings, A_{i-1}^j.